Endothelial specific inactivation of FAK-Y397 and FAK-Y861 phosphorylation in tumour growth and angiogenesis *in vivo*

Natalia Bodrug

Thesis submitted for Degree of
Doctor of Philosophy
University of London
September 2016

Adhesion and Angiogenesis Laboratory
Centre for Tumour Biology
Barts Cancer Institute
School of Medicine and Dentistry
Queen Mary University of London
Charterhouse Square
London EC1M 6BQ
United Kingdom

STATEMENT OF ORIGINALITY

I, Natalia Bodrug, confirm that the research included in this thesis is my own work and that where it has been carried out in collaboration with, or supported by others, that this is duly acknowledged below and my contributions indicated.

I attest that I have exercised reasonable care to ensure that the work is original, and does not to the best of my knowledge break any UK laws, infringe any third party's copyright or any other Intellectual property right, or contain any confidential material.

I accept that the College has the right to use plagiarism detection software to check the electronic version of the thesis.

I confirm that this thesis has not been previously submitted for the award of a degree by this or any other university.

The copyright of this thesis rests with the author and no quotations from it or information derived from it may be published without the prior written consent of the author.

Signature:

Date

ABSTRACT

Tumour angiogenesis is a hallmark of cancer. Focal adhesion kinase (FAK) is a non-receptor tyrosine kinase involved in endothelial cells (ECs) survival, proliferation and migration. FAK has several tyrosine phosphorylation sites thought to be involved in FAK function but the requirement of phosphorylation of these residues *in vivo* is unknown. We have generated mice where endogenous FAK is deleted simultaneously with the expression of non-phosphorylatable FAK-Y397F or FAK-Y861F mutated or wild type forms of FAK in adult endothelium in order to test this.

My data show that EC-FAK-Y397F^{KI} mice present with decreased tumour angiogenesis (in sygeneic B16F0, CMT19T and LLC) but impaired B16F0 and CMT19T tumour growth only, with increased tumour hypoxia. FAK-Y397F tumour endothelium is not perfusion, leakage or vascular maturation defective. This mutation affects VEGF-, PlGF- and bFGF-driven angiogenesis *in vivo* and VEGF+Ang2 administration is able to partially rescue this phenotype *ex vivo*.

In contrast, endothelial FAK-Y861F mutation leads to an initial delay in B16F0 tumour angiogenesis, that subsequently resolves, and does not affect B16F0 tumour growth. LLC and CMT19T tumour growth and angiogenesis are not affected by the endothelial FAK-Y861F mutation; neither are tumour blood vessel perfusion, leakage, vascular maturation or tumour hypoxia. VEGF-, PlGF- and bFGF-driven angiogenesis *in vivo* and *ex vivo* was not affected by the endothelial FAK-Y861F mutation, whereas increased *in vivo* angiogenesis was triggered by Ang2 administration.

Lastly, to understand whether cytokine profiles that might affect angiocrine signalling are affected differentially in FAK-Y397F vs FAK-Y861F endothelial cells, I show that CCL1 and CCL2 are increased in FAK-Y397F but IL-13, IL-1F3, CCL4, IL-1F1, CCL2 and others are increased in FAK-Y861F endothelial cells.

Overall my data indicates that endothelial-specific FAK mutations on two phosphorylation sites has different effects on tumour angiogenesis, tumour growth, growth factor stimulated angiogenesis *in vivo* and *ex-vivo* and cytokine production.

TABLE OF CONTENTS

STATEMENT OF ORIGINALITY **2**

ABSTRACT **3**

TABLE OF CONTENTS **5**

LIST OF FIGURES **8**

LIST OF TABLES **12**

CHAPTER I: INTRODUCTION **13**

1. ANGIOGENESIS 13
   - *1.1. Vasculogenesis and Developmental Angiogenesis 13*
   - *1.2. Blood vessel structure 14*
2. TUMOUR ANGIOGENESIS 15
3. THE ROLE OF GROWTH FACTORS AND GROWTH FACTOR RECEPTORS 19
   - *3.1. Fibroblast Growth Factor Family 19*
   - *3.2. Vascular Endothelial Growth Factors and Receptors 19*
   - *3.3. Anti-VEGF therapy 21*
4. CELL ADHESION AND INTEGRIN SIGNALING 22
   - *4.1. Endothelial cell Integrins 23*
   - *4.2. Tumour angiogenesis and Integrin signaling 24*
5. FOCAL ADHESION KINASE 25

FIGURE 1.4.2.1: FAK STRUCTURE AND SIGNALING. **26**

- *5.1. FAK protein domains 26*
  - 5.1.1. FAK FERM domain 26
  - 5.1.2. Kinase domain and involvement of Y397 27
  - 5.1.3. Proline rich motifs and involvement of Y861 28
  - 5.1.4. FAT domain 28
- *5.2. FAK phosphorylation mediated signaling 29*
- *5.3. FAK in cancer and pharmacological inhibition 30*
- *5.4. FAK Transgenic and Knock-Out mouse models 31*
- *5.5. Development point-mutant FAK knock-in mice 33*

RESEARCH AIMS **35**

CHAPTER II: MATERIALS AND METHODS **36**

1. MOUSE COLONY MANAGEMENT 36
   - *1.1 Reagents 36*
   - *1.2 DNA extraction 36*
   - *1.3 Genotyping PCR and DNA electrophoresis 36*
2. B16F0, CMT19T AND LLC CELL LINE CULTURE 38
3. POLYOMA-MIDDLE-T-ANTIGEN RETROVIRAL PRODUCTION 38
4. MOUSE LUNG ENDOTHELIAL CELL CULTURE 39
   - *4.1 Coating Mix composition for endothelial cell culture 39*
   - *4.2 Endothelial cell culture medium 39*
   - *4.3 Mouse Lung Endothelial Cell (MLEC) Isolation 39*
   - *4.4 Negative Sorting – removal of macrophages 40*
   - *4.5 Endothelial Cell Positive Sorting 40*
   - *4.6 Immortalisation of isolated endothelial cells 41*
   - *4.7 Transfection of immortalised endothelial cells 41*
5. REVERSE-TRANSCRIPTASE QUANTITATIVE POLYMERASE CHAIN REACTION 42
6. WESTERN BLOTTING AND CYTOKINE ARRAYS 43
   - *6.1. Endothelial cell lysis and Protein Concentration Assay 43*

6.2. SDS-PAGE and Protein Transfer……43
6.3.Immunoblotting……45
6.4. Cytokine array……45
7. ANIMAL EXPERIMENTS ……46
7.1. Tamoxifen formulation and treatment……46
7.2. Subcutaneous Tumour Growth……47
7.3. Ante-mortem procedures……47
7.3.1. PE-PECAM Injection ……47
7.3.2. PE-PECAM+Hoechst Injection ……48
7.3.3. Pimonidazole Injection ……48
7.4. Subcutaneous Sponge Assay……48
7.5. Aortic Ring Assay……49
8. HISTOLOGICAL ANALYSIS ……50
8.1. Tissue Section Preparation……50
8.2. Haematoxylin and Eosin (H&E) staining……50
8.3. Blood vessel immunofluorescence and quantitation……51
8.4. Blood vessel immunohistochemistry and microvessel quantitation in sponges……52
8.5. Functional Blood vessel quantitation……53
8.6. Hoechst Leakage quantitation……53
8.7. Blood vessel and pericyte double immunostaining and Pericyte coverage quantitation……54
8.8. Hypoxia staining and quantitation……55
9. ANALYSIS OF STATISTICAL SIGNIFICANCE ……56

CHAPTER III: RESULTS……57

1. ELUCIDATING THE EFFECTS OF ENDOTHELIAL FAK-Y397F AND FAK-Y861F MUTATIONS ON TUMOUR GROWTH AND ANGIOGENESIS……57
1.1. Generation and characterisation of mutant endothelial-specific FAK-Y397F and FAK-Y861F mice……58
1.3. Endothelial-specific FAK-Y397F mutation is sufficient to reduce B16F0 and CMT19T tumour growth, but not LLC tumour growth……73
1.4. Effect of endothelial-specific FAK-Y861F mutation on tumour growth and tumour angiogenesis……87
2. ELUCIDATING THE EFFECT OF ENDOTHELIAL FAK-Y397F AND FAK-Y861F MUTATIONS ON GROWTH FACTOR DRIVEN ANGIOGENESIS IN VIVO……102
2.1. Validation of the KO/KI system in sponge assays in vivo……103
2.2. Endothelial specific inactivation of FAK-Y397 phosphorylation impairs VEGF-, PlGF- and bFGF-driven angiogenesis……106
2.3. Endothelial specific inactivation of FAK-Y861 phosphorylation does not affect VEGF-, PlGF- and bFGF-driven angiogenesis and allows ANG2 to act as a pro-angiogenic growth factor……109
3. ELUCIDATING THE EFFECT OF ENDOTHELIAL FAK-Y397F AND FAK-Y861F MUTATIONS ON GROWTH FACTOR DRIVEN ANGIOGENESIS EX VIVO ……113
3.1. Validation of the KO/KI system in the ex vivo aortic ring assay……113
3.2. Endothelial-specific inactivation of FAK-Y397 phosphorylation impairs VEGF-driven sprouting……116
3.3. Endothelial-specific inactivation of FAK-Y861 phosphorylation impairs VEGF-driven sprouting……118
4. INVESTIGATING THE EFFECT OF ENDOTHELIAL FAK-Y397F AND FAK-Y861F MUTATIONS ON ENDOTHELIAL CYTOKINES……121
4.1. Validation of the KO/KI system for in vitro cytokine arrays……122
4.2. Endothelial-specific FAK-Y397F mutation leads to an increase of a limited number of cytokines……123

4.3. Endothelial-specific FAK-Y861F mutation leads to an increase of a substantial number of cytokines……123
4.4. Differentially modified cytokines……127

CHAPTER IV: DISCUSSION ……130
1. ROLE OF ENDOTHELIAL SPECIFIC FAK-Y397 AND FAK-Y861 PHOS-PHORYLATION IN TUMOUR GROWTH AND ANGIOGENESIS IN VIVO ……132
2. ROLE OF ENDOTHELIAL SPECIFIC FAK-Y397 AND FAK-Y861 PHOSPHORYLATION IN GROWTH-FACTOR INDUCED ANGIO-GENESIS IN VIVO……141
3. ROLE OF ENDOTHELIAL SPECIFIC FAK-Y397 AND FAK-Y861 PHOSPHORYLATION IN GROWTH-FACTOR INDUCED ANGIO-GENESIS EX VIVO ……146
4 ROLE OF FAK-Y397 AND FAK-Y861 PHOSPHORYLATION IN ENDOTHELIAL CELL CYTOKINE PRODUCTION IN VITRO……148

CONCLUDING REMARKS ……150

APPENDIX I ……152

AKNOWLEDGEMENTS ……158

BIBLIOGRAPHY ……159

LIST OF FIGURES

Figure 1.1: Balancing the Angiogenic Switch 16

Figure 1.2: Sprouting angiogenesis – a multi-step process. 17

Figure 1.3: Endothelial cell heterogeneity in sprouting angiogenesis. 18

Figure 1.4: FAK structure and signaling. 26

Figure 1.5: Development of point-mutant mice 34

Figure 3.1: Characterisation of the endothelial-specific FAK^{KI} mouse model 63

Figure 3.2: Reintroducing a WT version of FAK in endothelial cells does not affect B16F0 tumour growth *in vivo* 65

Figure 3.3: Reintroducing a WT version of FAK in endothelial cells does not affect B16F0 tumour angiogenesis *in vivo* 69

Figure 3.4: Reintroducing a WT version of FAK in endothelial cells does not affect B16F0 tumour endothelium or tumour hypoxia *in vivo* 70

Figure 3.5: Reintroducing a WT version of FAK in endothelial cells does not affect LLC tumour growth *in vivo* 72

Figure 3.6: Endothelial-specific inactivation of FAK-Y397 phosphorylation inhibits B16F0 tumour growth. 76

Figure 3.7: Endothelial-specific inactivation of FAK-Y397 phosphorylation is sufficient to reduce B16F0 tumour angiogenesis *in vivo* 77

Figure 3.8: Endothelial-specific inactivation of FAK-Y397 phosphorylation does not affect B16F0 tumour endothelium, but affects tumour hypoxia *in vivo* 78

Figure 3.9: Endothelial-specific inactivation of FAK-Y397 phosphorylation inhibits CMT19T carcinoma tumour growth.....81

Figure 3.10: Endothelial-specific inactivation of FAK-Y397 phosphorylation is sufficient to reduce CMT19T carcinoma tumour angiogenesis *in vivo*.....82

Figure 3.11: Endothelial-specific inactivation of FAK-Y397 phosphorylation does not affect LLC tumour growth in spite of impairing tumour angiogenesis *in vivo*.....84

Figure 3.12: Endothelial-specific inactivation of FAK-Y397 phosphorylation leads to a decrease LLC tumour angiogenesis *in vivo*.....85

Figure 3.13: Endothelial-specific inactivation of FAK-Y397 phosphorylation does not affect blood vessel perfusion in LLC tumours *in vivo*.86

Figure 3.14: Endothelial-specific inactivation of FAK-Y861 phosphorylation does not affect B16F0 tumour growth *in vivo*.....90

Figure 3.15: Endothelial-specific inactivation of FAK-Y861 phosphorylation decreases B16F0 tumour angiogenesis in the early stages of tumour formation.....91

Figure 3.16: Endothelial-specific inactivation of FAK-Y861 phosphorylation does not affect B16F0 tumour endothelium or tumour hypoxia *in vivo*.....92

Figure 3.17: Endothelial-specific inactivation of FAK-Y861 phosphorylation does not affect CMT19T carcinoma tumour growth. 95

Figure 3.18: Endothelial-specific inactivation of FAK-Y861 phosphorylation does not affect CMT19T carcinoma tumour angiogenesis.....96

Figure 3.19: Endothelial-specific inactivation of FAK-Y861 phosphorylation does not affect LLC tumour growth or tumour angiogenesis *in vivo*.....99

Figure 3.20: Endothelial-specific inactivation of FAK-Y861 phosphorylation does not affect LLC tumour growth or tumour angiogenesis *in vivo*..... 100

Figure 3.21: Endothelial-specific inactivation of FAK-Y861 phosphorylation does not affect blood vessel perfusion in LLC tumours *in vivo* 101

Figure 3.22: Validation of the KO/KI system in sponge assays *in vivo*. 105

Figure 3.23: Endothelial-specific inactivation of FAK-Y397 phosphorylation impairs VEGF-, PlGF and bFGF-driven angiogenesis. 108

Figure 3.24: Endothelial-specific inactivation of FAK-Y861 phosphorylation does not affect VEGF-, PlGF or bFGF-driven angiogenesis and allows Ang2 to act as a pro-angiogenic growth factor. 112

Figure 3.25: Reintroducting a WT version of FAK in endothelial cells does not affect VEGF-driven sprouting angiogenesis. 115

Figure 3.26: Endothelial specific FAK-Y397F mutation impairs VEGF-driven sprouting angiogenesis, but is partially rescued by Ang2 addition. 117

Figure 3.27: Endothelial specific FAK-Y861F mutation does not affect VEGF-driven sprouting angiogenesis, either in the presence, or in the absence of Ang2 120

Figure 3.28: Endothelial cells isolated from Cre-neg; FAK-WT^{KI} and Cre-pos; FAK-WT^{KI} mice present with a similar cytokine profile *in vitro* 124

Figure 3.29: Endothelial cells isolated from Cre-pos; FAK-Y397F^{KI} mice produce particularly high levels of CCL1 and CCL2 cytokines *in vitro* 125

Figure 3.30: Endothelial cells isolated from Cre-pos; FAK-Y861F^{KI} mice produce particularly high levels of several cytokines, including CCL2, IL-1F1 and CCL4 *in vitro* 126

Appendix Figure A3.1: Reintroducing a WT version of FAK in endothelial cells does not affect B16F0 tumour growth *in vivo* 153

Appendix Figure A3.2: Endothelial-specific inactivation of FAK-Y397 phospho-rylation inhibits B16F0 tumour growth. 154

Appendix Figure A3.3: Endothelial-specific inactivation of FAK-Y397 phosphorylation is sufficient to reduce B16F0 tumour angiogenesis *in vivo* 155

Appendix Figure A3.4: Endothelial-specific inactivation of FAK-Y397 phosphorylation leads to increased B16F0 tumour hypoxia *in vivo* 156

Appendix Figure A3.5: Endothelial-specific inactivation of FAK-Y861 phospho-rylation does not affect B16F0 tumour growth. 157

LIST OF TABLES

Table 3.1: Mouse genotypes and corresponding nomenclature. 60

Table 3.2: Differential fold increase in cytokine production between FAK-Y397F and FAK-861F mutated endothelial cells.....127

CHAPTER I: INTRODUCTION

1. Angiogenesis

Angiogenesis, the formation new blood vessels from pre-existing ones, is required for vertebrate embryonic development as well as wound healing and reproductive functions in adults (Carmeliet, 2000). Active angiogenesis is also involved in disease development and progression, such as cancer, retinopathies and rheumatoid arthritis (Ferrara, 2000; Carmeliet, 2003).

1.1. Vasculogenesis and Developmental Angiogenesis

In the mouse, the yolk sac vasculature starts to form at embryonic day (E) 6.5 when haemangioblasts derived from the mesoderm form blood islands. When exposed to basic Fibroblast Growth Factor (bFGF, also named FGF2), haemangioblasts give rise to angioblasts and hematopoietic stem cells (Choi, 1998). Angioblasts then form endothelial cords establishing the primitive vascular plexus of the embryo (Conway, 2001; Risau 1997). From embryonic day (E) 8.5, sprouting and intussusceptive angiogenesis allow the formation of the mature vascular tree.

The first step in sprouting angiogenesis is endothelial cell activation by nitric oxide and growth factors leading to the destabilization of the intercellular junctions in the existing endothelium (Gale and Yancopoulos, 1999). As the extracellular matrix is degraded, endothelial tip cells migrate towards to growth factor gradient, while the stalk cells proliferate allowing the elongation of the forming capillary (Gerhardt, 2008). Tube formation is followed by recruitment of supporting cells and basement membrane deposition. These supporting cells

and deposition and organization of vascular basement membrane help to maintain vascular integrity and diameter this controlling efficiency of blood flow.

Intussusception angiogenesis does not require endothelial cell proliferation but does involve the splitting and rejoining of existing blood vessels to generate new ones (Conway, 2001; Djonov, 2000). This process has been observed in physiological and pathological angiogenesis.

1.2. Blood vessel structure

Blood vascular network includes arteries, veins and capillaries. A sheet of endothelial cells lines the lumen of all blood vessels, but the proportion of supporting vascular cells and the basement membrane composition varies between the different vessel types.

The basement membrane is a specialized extracellular matrix that surrounds the basolateral side of the blood vessels. Vascular supporting cells and endothelial cells contribute to the basement membrane deposition and its composition varies from one organ to another, but is generally composed of collagen type IV, laminin, fibronectin, nidogen and heparin sulphate proteoglycan perlecan (Paulsson, 1992).

Pericytes and vascular smooth muscle cells support and stabilize the vascular endothelium. Capillaries and postcapillary venules are coated with pericytes that extend numerous protrusions through the basement membrane to establish cell contact with endothelial cells. Vascular smooth muscle cells surround larger vessels such as arteries and veins (Gerhardt and Betsholtz, 2003).

Pericytes are embedded in the endothelial basement membrane and have prominent nucleus and a multitude of cell protrusions that allow them to come in contact with more than one endothelial cell, through adhesion plaques and/or peg and socket contacts. Pericyte coverage is variable depending on the vascular bed and the pericyte to endothelial cell ration varies from 1:1 (in retina and brain) to as low as 1:100 (skeletal muscle).

The vascular network fulfills distinct function in different organs and this impacts pericyte coverage, morphology and molecular characteristics. Several markers are used to characterize pericytes such as smooth muscle α-actin (SMA), NG2 proteoglycan, desmin, platelet-derived growth factor receptor (PDGF)-β and others; but none of these markers is pericyte-specific or expressed in all pericytes (Armulik, 2005). Larger vessels are composed of an endothelial monolayer, covered by basement membrane and a separate layer of contractile vSMC.

2. Tumour Angiogenesis

Tumour angiogenesis occurs to supply the growing tumour mass with oxygen and nutrients, as well as to help evacuate the metabolic wastes resulting from the highly proliferating cancer cells. As the tumour mass grows, the tissue becomes hypoxic and tumour cells up-regulate the Hypoxia Induced Factor-1 (HIF-1) leading to the overexpression of pro-angiogenic growth factors, including Vascular Endothelial Growth Factor (VEGF), basic Fibroblast Growth Factor (bFGF), Platelet Derived Growth Factor (PDGF), Transforming Growth Factor β (TGFβ) and angiopoietins, and the decrease of anti-angiogenic signals, eg thrombospondin, interferon and cleaved products of plasminogen

(angiostatin) and collagen XVIII (endostatin) (Bergers and Benjamin, 2003; Wahl, 2005; Folkman 2005). The imbalance between naturally occurring pro-angiogenic and anti-angiogenic signals, also called the 'angiogenic switch' leads to pathological angiogenesis (**Figure 1.1**).

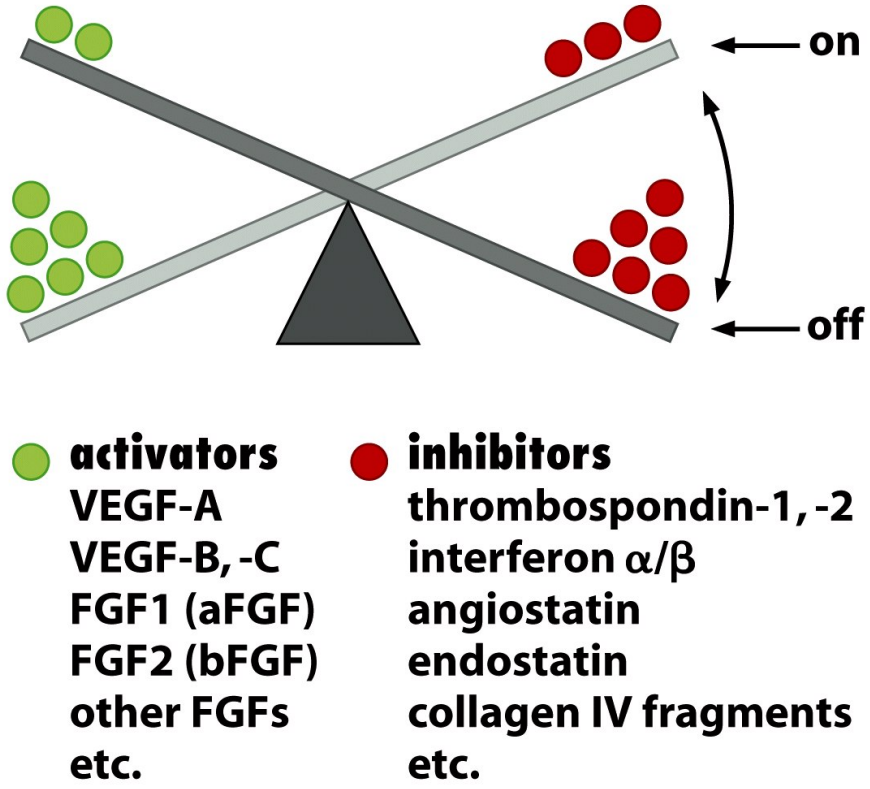

Figure 1.1: Balancing the Angiogenic Switch
Tumour angiogenesis results from an imbalance in the angiogenic signals in favour of pro-angiogenic factors. (Adapted from The biology of Cancer, R.A.Weinberg, 2007)

The endothelium, equipped with Growth Factor Receptors, responds to the angiogenic switch in several steps (**Figure 1.2**). Firstly the cell junctions between endothelial cells or endothelial and mural cells are loosened (Gale and Yancopoulos, 1999). This process, alongside the degradation of extracellular matrix by metalloproteases, allows endothelial cell proliferation and directional migration towards the hypoxic site and tube formation (Weis, 2011; Carmeliet, 2000; Hua, 2011). Proteolytic degradation of specific extracellular matrix

proteins can produce a variety of soluble fragments able to modulate the angiogenic response. For example, VEGF is normally tethered to the extracellular matrix, but is released during extracellular matrix degradation to stimulate angiogenesis. Growth Factor signaling pathways, including the VEGF/VEGFR2 signaling axis, crosstalk with integrin signaling pathways to allow the transition between an organized endothelial monolayer to a proliferating and migratory phenotype of the same cells. In quiescent vasculature, cell adhesion requires integrin binding to extracellular matrix and stable cell-cell junctions.

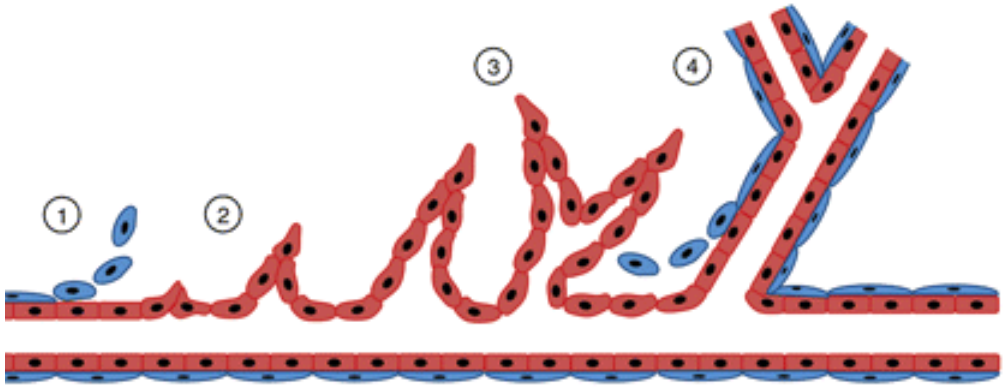

Figure 1.2.: Sprouting angiogenesis – a multi-step process.
Upon activation by pro-angiogenic growth factors, perivascular cells (in blue), such as pericytes and smooth muscle cells, detach from the vascular wall and endothelial cells (in red) release proteases, which degrade their basement membrane (1). This allows them to migrate into the surrounding interstitium, resulting in the formation of capillary buds and sprouts (2). The sprouts further elongate through endothelial cell proliferation, branch and interconnect with each other (3). This leads to the development of blood-perfused microvessels, whose wall is stabilised again by the recruitment of perivascular cells and the production of extracellular matrix compounds (4). (Adapted from M.W. Lashke, 2011)

The forming sprouts are composed of two types of endothelial cells: stalk cells and tip cells (**Figure 1.3**). The stalk cells are thought to be highly proliferative, whereas the tip cells integrate signals from the surrounding microenvironment and guide the growing vessels according to the growth

factor gradient. The stalk and tip cell phenotype is not definitive, and it has been shown that stalk cells are able to change phenotype and become tip cells at the edge of the forming vessel (Fruttiger, 2002).

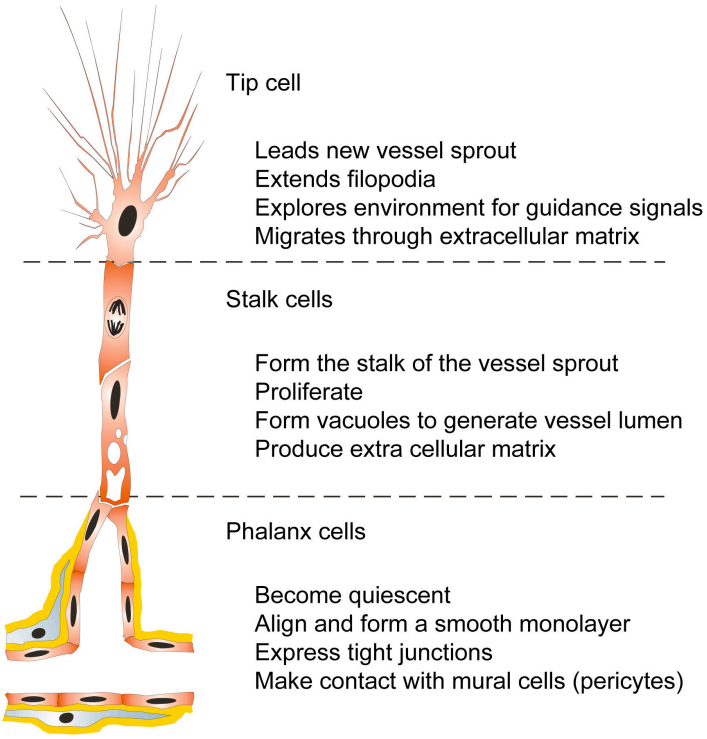

Figure 1. 1: Endothelial cell heterogeneity in sprouting angiogenesis.
The quiescent endothelium is formed on a monolayer of endothelial cells that express tight junctions and make contact with mural cells. During sprouting angiogenesis, the stalk cells proliferate in respond to growth factor stimulation, whereas the tip cells orientate the migration of the forming sprout according to growth factor gradient (Adapted from Gerhardt 2011).

Lastly, endothelial cells deposit basement membrane and secrete growth factors, such as platelet derived growth factor (PDGF), which attracts supporting cells, thus stabilizing the newly formed blood vessels. In spite of being continuously exposed to pro-angiogenic stimuli, a fraction of tumour blood vessels are covered with pericytes. Tumour vasculature, alongside the lymphatic system, is also involved in metastatic cancer dissemination (Hicklin and Ellis, 2005).

3. The Role of Growth Factors and Growth factor receptors

3.1. Fibroblast Growth Factor Family

The FGFs are a fimily of 22 growth factors and bFGF was the first pro-angiogenic factor identified (Shing, 1984). Heparin sulfate proteoglycans (HSPG) located on cell surface and in the extracellular matrix bind to bFGF with high affinity and their cell release is heparanase dependent (Turner, 2010). The biological effects of bFGF are mediated by four receptor tyrosine kinases: FGFR-1, -2, -3 and -4. After ligand binding, the activated FGFR receptors are able to phosphorylate tyrosine residues from intracellular proteins belonging to signaling pathways amongst which RAS-MAPK, PI3K-AKT that are highly relevant in cancer studies. Moreover bFGF is able to stimulate angiogenesis and was in fact the first pro-angiogenic molecule to be identified. Molecules from this family can be trapped in the extracellular matrix as a consequence of binding to Heparan Sulfate Proteoglycans, and can be later released in a coordinate manner due to heparanase activity. bFGF signaling can also to increased VEGF expression in endothelial cells through an autocrine and paracrine stimuli, thus potentiating the angiogenic response. Aside from being a pro-angiognic factor, bFGF also contributes to tumour development through cell proliferation and survival signaling.

3.2. Vascular Endothelial Growth Factors and Receptors

Placental Growth Factor (PlGF) and four other VEGF isoforms (A, B, C and D), encoded by different genes, have been identified and VEGF-A is

considered to be a major regulator of blood vessel formation, whereas VEGF-C and VEGF-D are specific to lymphatic vessels (Carmeliet, 2005). VEGF-B is the most abundant VEGF in the heart and was shown to stimulate coronary vessel growth and arterialization.

There are three spicing isoforms of VEGF-A in mouse: VEGF 121, VEGF 164 and VEGF 188. The loss of a single VEGF-A allele leads to embryonic lethality at (E) 11-12 due to lack of functional vasculature and absence of blood islands (Carmeliet 1996, Ferrara 1996). Interestingly certain VEGF-A splicing isoforms have anti-angiogenic effects (Qui, 2009). For example VEGF isoform resulting from differential splicing of terminal exon 8 is anti-angiogenic and is widely expressed in healthy tissues; however its expression is downregulated in cancers.

VEGF Receptors, VEGFR-1, VEGFR-2 and VEGFR-3, belong to a superfamily of receptors characterized by seven extracellular immunoglobulin loops and an intracellular tyrosine kinase domain (Stuttfeld, 2009). VEGFR-1 and VEGFR-2 are mainly expressed in endothelial cells, whereas VEGFR-3 expression is restricted to lymphatic cells and some tumour endothelial cells (Laakkonen, 2007). VEGFR-1 is thought to negatively regulate angiogenesis, because VEGFR-1 deficient embryos have excessive vascular growth and die in mid gestation (Fong, 1995). Lack of vascular development in VEGFR-2 deficient mice indicate that this receptor positively regulates angiogenesis (Shalaby, 1995). In addition, VEGF stimulated signaling involves coreceptors such as heparin sulfate proteoglycan and neuropilin -1 and -2 (Cebe-Suarez, 2006). Neuropilins were identified as Semaforin receptors for axonal guidance and later shown to play an essential role in development of vascular and lymphatic

vessels. Neuropilin-1 is involved in blood vessel formation by acting as a co-receptor of VEGFR-2 and was shown to be upregulated in tumour angiogenesis (Neufeld, 2002; Ellis, 2006). Neuropilin-2 acts as a coreceptor of VEGFR-3 and is thought to be restricted to the lymphatic system.

Upon VEGF-A signaling VEGFR-2 dimerisation triggers a signaling cascade involved in cell migration, survival and proliferation, important features in physiological and pathological angiogenesis.

Overexpression of VEGF is associated with tumour progression and poor prognosis in gastric, colorectal, pancreatic, prostate, lung and breast cancers (Takahashi, 1996; Lee, 2000; Ikeda 1999; George 2001; Fontanini, 1997; Manders, 2002).

3.3. Anti-VEGF therapy

The anti-VEGF therapy is used to decrease the vascularisation of the tumour mass, leading to tumour cell death. Two strategies are used to interfere with the VEGF/VEGFR2 signaling axis: neutralizing the VEGF molecule, thus interfering with extracellular activation or using tyrosine kinase inhibitors to block the intracellular VEGFR2 signaling. Bevacizumab, that has demonstrated survival benefits in patients with colorectal cancer, is a humanized antibody able to bind VEGF and sequester it away from its receptor (Hurwitz, 2004). In a similar way, Aflibercept has been designed to bind VEGF and PlGF and is used for advanced bowel cancer treatment (Gaya, 2012).

Preclinical trails showed that anti-VEGF treated tumours had increased FGF and FGFR expression, suggesting that this signaling axis is the resistance mechanism responsible for anti-VEGF therapy failure. Brivanib, a dual VEGFR

and FGFR inhibitor, has proven more effective in attenuating revascularization and tumour growth, when compared with single inhibitors (Allen, 2011).

Mechanisms of adaptation to anti-angiogenic therapies have in some cases been correlated with higher tumour malignancy and formation of distant metastasis (Paez-Ribes, 2009) and need to be addressed in clinics.

4. Cell adhesion and integrin signaling

Angiogenesis is dependent on the appropriate control of adhesive signals. Integrins are a family of heterodimeric transmembrane glycoproteins composed of non-covalently associated α and β subunits that mediate cell adhesion with the extracellular matrix (Hynes, 2002b). Mammalian cells have 8 β subunits and 18 α subunits that can assemble into 26 distinct integrins. There are four main groups of integrins: the RGD-integrin family (that binds to a arginine-glycine-aspartame consensus sequence), the collagen receptor family (that recognizes fibronectin and VCAM-1 amongst others), the leucocyte-specific receptor family and the laminin receptor family. The combination of α and β subunits confers ligand specificity to one or more substrates. Some heterodimers preferentially bind a single ligand, whereas others are able to bind to multiple ligands, as for example αIIbβ3 recognises fibrinogen, whereas αVβ3 can recognize vitronectin, fibronectin, thrombospondin, etc (Weis, 2011). The cytoplasmic tails of integrins are associated with adaptor proteins such as talin, vinculin, paxillin and α-actinin, that will assemble into clusters knows as focal contact sites and will facilitate intracellular signaling (Romer, 2006).

4.1. Endothelial cell Integrins

Endothelial cells express 8 integrins that mediate the interactions with endothelial cell matrix components: α5β1, αvβ3 and αvβ5 bind to the RGD tripeptide motive of fibronectin, fibrinogen, vitronectin, etc; α3β1, α6β1 and α6β4 primary bind to laminin; and α1β1 and α2β1 have affinity for collagen I and IV and denatured collagen (Albelda, 1989; Stromblad and Cheresh, 1996; Hodivala-Dilke, 2003). The upregulation of expression and activity of several integrins has been reported with nascent blood vessels (Hodivala-Dilke, 2003). αV integrins have received most attention in this field and have been associated with endothelial sprouts (Eliceiri and Cheresh, 1999). During angiogenic remodeling, endothelial αVβ5 and αvβ3 were shown to be upregulated (Stupack and Cheresh, 2002), but other integrins such as a5b1 and a2b1 are also upregulated. These observations together with the fact that integrins are transmembrane, made them ideal targets for anti-angiogenic therapy (Hodivala-Dilke, 2003; Zhang, 2015).

Some reports have suggested that integrins can also bind to growth factors, as for example α9β1, α3β1 and αVβ3 directly bind VEGF isoforms and others bind to angiopoietin (Hutchings, 2003; Rahman, 2005; Serini, 2008), but these data are still controversial. When interacting with specific integrins, select Growth Factor Receptors can be activated without ligand binding. VEGFR2 and αvβ3 form a physical complex to promote angiogenesis (Mahabeleshwar, 2007). Angiopoietin receptor Tie-2 physically interacts with α5β1 leading to amplification of angiogenic signals (Cascone, 2005). Integrin trafficking and internalization can modulate EGFR and VEGFR internalization and recycling (Caswell, 2008; Reynolds, 2009).

Together all these functions of integrins mean that they are central players in not only the adhesive biology of cells but also cell survival and signaling.

4.2. Tumour angiogenesis and Integrin signaling

Although integrins are not oncogenic *per se*, their elevated expression is often associated with tumour growth and invasion. Both genetic ablation and inhibition studies of α5β1, α1β1 and α2β1 inhibit angiogenesis, indicating that these integrins are pro-angiogenic (George, 1993; Kim 2000b, Pozzi 2000; Senger, 1997; Yang, 1993).

Function blocking antibodies and small peptides targeted to αvβ3 and αvβ5 integrins have been shown to inhibit angiogenesis in tumours and retinopathy models, suggesting that these integrins are pro-angiogenic (Brooks, 1994; Brooks, 1995; Friedlander, 1996; Hammes, 1996). However, mice lacking β3 or β3 and β5 undergo normal developmental angiogenesis and have enhanced pathological angiogenesis (Hodivala-Dilke, 1999; Reynolds, 2002; Robinson, 2004). These observations were determined to be a consequence of compensatory increased expression and activity of VEGFR2 (Reynolds, 2002). Mice expressing a non-phosphorylatable β3 did not show compensatory changes in VEGF signaling and presented with decreased angiogenesis, consistent with the antagonistic studies (Mahabeleshwar, 2008). Floxed mice with conditional deletion of β3 integrin in platelets have a bleeding phenotype, but no effect on tumour growth and angiogenesis (Morgan, 2009). Endothelial specific deletion of β3 resulted in a transient inhibition of tumour growth and

angiogenesis, suggesting that extended depletion of this molecule leads to an escape from angiogenesis inhibition (Robinson, 2013).

Integrins αvβ3 and αvβ5 promote two distinct cytokine-dependent pathways of angiogenesis. Angiogenesis induced by bFGF or TNF-α requires αvβ3 integrin, whereas angiogenesis induced by VEGF or TGF-α is αvβ5 dependent (Friedlander, 1995). This is due to the ability of β3 and β5 to differentially activate the Ras/Raf/MEK/Erk pathway in blood vessels (Hood, 2003).

5. Focal adhesion Kinase

Focal Adhesion Kinase (FAK) was identified as a 125 kD substrate of v-Src oncogene in chicken fibroblasts (Kanner, 1990) and was characterized as a ubiquitous cytoplasmic tyrosine kinase highly phosphorylated when localized at focal contacts (Schaller, 1992).

FAK contains a N-terminal FERM domain, a central kinase domain, three proline-rich domains and a C-terminal FAT domain (Girault, 1999). Upon growth factor or integrin signaling FAK is autophosphorylated on Y397, creating a binding site for Src and the p85 subunit of PI3K. This is followed by subsequent phosphorylations at Y576/Y577, allowing maximal catalytic activity and at Y861, that binds p130Cas and is thought to signal further downstream PI3K (**Figure 1.4**).

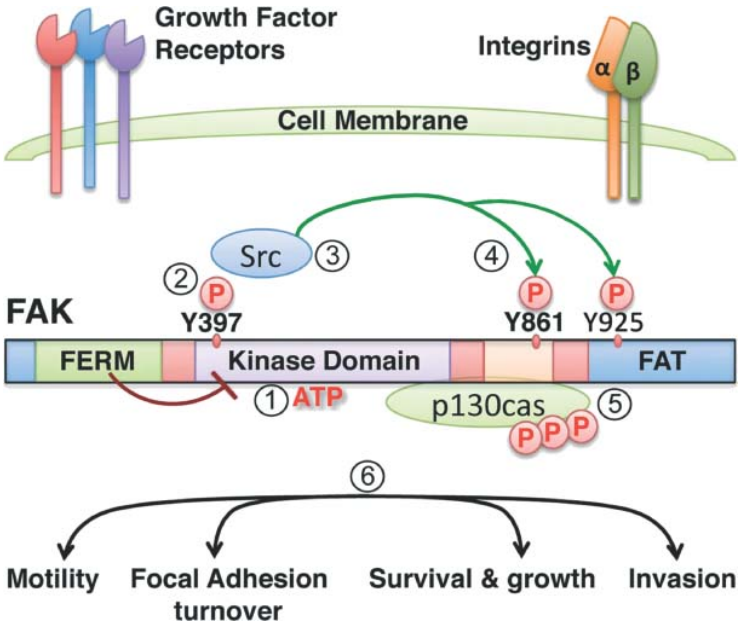

Figure 1.4: FAK structure and signaling.
FAK is composed of a FERM domain, a kinase domain containing the Y397, three proline-rich domains and a FAT domain where the Y925 is localized. Upon Growth factor and/or integrin stimulation, the FERM-Kinase autoinhibitory binding is disrupted (1) allowing FAK-Y397 autophosphorylation (2). This leads to the formation of an HS2 binding site recognized by Src (3). The dual FAK-Src enzyme can further phosphorylate FAK on Y861 and Y925 (4). FAK also contain a SH3 binding domains that is recognized by p130Cas (5). downstream signalling of activated FAK elicits changes in cellular morphology and behaviour, including changes in motility, focal adhesion turnover, survival, growth and invasion (6).

5.1. FAK protein domains

5.1.1. FAK FERM domain

The FAK FERM domain directly binds the FAK catalytic domain leading to an autoinhibitory effect of FAK kinase activity and phosphorylations (Dunty and Schaller, 2002; Cooper, 2003). In this conformation, FAK cannot be autophosphorylated on Y397, preventing Src binding and downstream signaling (Lietha, 2007). FAK FERM domain contains p53 binding domains and nuclear localization signals (Lim, 2008). Nuclear exporting sequences have been identified in the FERM and catalytic domains, suggesting that FAK could be involved in signal trafficking from the nucleus to the rest of the cell (Ossovskaya, 2008). FAK FERM domain is able to integrate signals from growth

factors and integrins. It directly binds the cytoplasmic tail of β1 integrin (Schaller, 1995) and is involved in signaling from PDGFR and EGFR (Sieg, 2000).

5.1.2. Kinase domain and involvement of Y397

FAK-Y397 autophosphorylation allows Src binding (Cobb, 1994; Schaller, 1994; Xing, 1994) and the FAK-Src dual enzymatic complex is involved in further FAK phosphorylation (for example on Y576/577, Y861 and Y925 residues) and in phosphorylation of substrates clustered at focal contacts, such as paxillin. FAK-Y576/Y577 phosphorylation leads to maximal catalytic activity, but the exact FAK or Src contribution to substrate phosphorylation remains unclear. When autophosphorylated on Y397, FAK can also bind to PI3K, growth-factor-receptor-bound protein-7 (Grb-7) and p120RasGAP (Mitra, 2005), but the sequential or preferential binding of various proteins to FAK is unknown.

It has been recently shown that in cancer cells FAK can be phosphorylated on the Y397 residue by oncogenic receptor tyrosine kinases even in the presence of FAK kinase inhibitors (Marlowe, 2016). This suggests that FAK kinase activity and FAK-Y397 phsophorylation are not necessarily always associated and that FAK-KD and FAK-Y397F mutations could impair different signaling pathways.

Inhibitors for FAK kinase domain and FAK-Y397 phosphorylation are being developed as cancer therapeutics. However the endothelial specific inactivation of this phosphorylation *in vivo* has not been studied.

5.1.3. *Proline rich motifs and involvement of Y861*

FAK contains three proline-rich motifs, one between the FERM and the kinase domains and two between the kinase and the FAT domains, in the C-terminal region. The proline-rich motifs are recognized by SH3-domain containing proteins, such as p130Cas, that is important for promoting cell migration through Rac activation (Hanks, 2003; Chodniewicz, 2004). FAK-Y861 phosphorylation is crucial for Ras transformation in fibroblasts (Lim, 2004) and was also shown to increase the binding of p130Cas (Mitra, 2005). ASAP1 and GRAF can also bind the FAK-SH3 domains and are involved in cytoskeletal dynamics (Parsons, 2003). Protection from cell detachment induced apoptosis (or anoikis) has also been linked with FAK-Y861 phosphorylation, suggesting that this tyrosine might play a role in survival during migration – an important feature for angiogenesis and metastatic spread (McLean, 2005). However the exact mechanisms leading to this preferential phosphorylation and the resulting downstream signals have not been studied *in vivo*.

5.1.4. *FAT domain*

The Focal Adhesion Targeting (FAT) domain is involved in targeting FAK to focal contacts (Hildebrans, 1993). There are two paxillin binding sites in the FAT domain and point mutations specifically disrupting paxillin binding highlighted the importance of FAK/paxillin interaction in FAK subcellular localization (Scheswohl, 2008). The first observations indicated that FAK deleted fibroblasts present with impaired migration, but have more numerous and larger focal contacts, suggesting a role of FAK in focal adhesion turnover, rather than formation (Ilic, 1995). Since then extensive studies have proven

that FAK-Y925 phosphorylation promotes FAK dissociation from the focal contacts, allowing focal adhesion turnover and efficient cell migration (Deramaudt, 2011).

5.2. FAK phosphorylation mediated signaling

After growth factor and/or integrin stimulation, FAK-Y397 autophosphorylation can occur in *cis* or *trans* (Toutant, 2002) and is considered a major signaling event that leads to the creation of an HS2-domain binding site. This allows FAK to complex with SH2 domain binding proteins, such as Src and the p85 subunit of PI3K amongst others (Mitra, 2005).

FAK/Src dual enzymatic complex can further phosphorylate FAK-Y576/Y577, FAK-Y861 and FAK-Y925 (Calalb, 1996; Schlaepfer, 2004). The FAK-Y861 phosphorylation has also been shown to be independent of FAK-Y397 phosphorylation in specific cellular settings (Abu-Ghazaleh, 2001). On the other hand, FAK-Y861 phosphorylation was observed when FAK/Src binding was impaired, suggesting that this phosphorylation is not exclusively dependent on the FAK/Src dual enzyme (Dunty, 2003). In endothelial cells, upon VEGF stimulation, FAK-Y861 is phosphorylated and forms a complex with αvβ5 integrin (Eliceiri, 2002).

VEGF-induced activation of PI3K, mediated by VEGFR2, is dependent on FAK (Abedi, 1997; Gerber, 1998, Qi, 2001). Activated PI3K generates PIP3 leading to the recruitment of AKT to the cell membrane through its PH domain, where it can be phosphorylated in its kinase domain on T-308 and in its C-terminal domain on S-473. The activated AKT is able to phosphorylate and therefore inhibit pro-apoptotic proteins, such as BAD and pro-caspase-9.

Phosphoinositide-dependent kinase 1 (PDK1) is able to phosphorylate AKT-T308 residue, however full AKT activation requires S-473 phosphorylation that can be performed by a wider range of kinases. FAK-KO in endothelial cells was shown to impair AKT-S473 phosphorylation, suggesting that FAK plays a role in transducing signals from the PI3K signaling pathway (Tavora, 2010).

FAK can also be phosphorylated on its Serine and Threonine residues by AKT (Wang, 2011). FAK has been shown to protect against apoptosis by upregulating the anti-apoptotic NF-kB signaling (Huang, 2007).

5.3. FAK in cancer and pharmacological inhibition

Generally, FAK is overexpressed in highly malignant tumour cells and has been associated, in most epithelial cancer types, with invasive cancer cell phenotype (Mitra, 2005; Zhao, 2009; Golubovskaya, 2009). However these observations do not always correlate with metastasis and show variable prognostic value (Madan, 2006).

The increased expression of FAK in a number of cancer types has led to the development of FAK inhibitors as an anti-cancer therapy. Pfizer has developed two ATP-binding inhibitors that inhibit tumour growth in the majority of tested mouse models and *in vitro* impair cell migration, but have no effect on cell survival, growth or apoptosis. Deletion of FAK from mouse skin blocked chemically-induced papilloma formation and malignant progression (McLean, 2004). In another study, FAK knock-out in cancer cells did not affect tumour growth, suggesting that the efficiency of FAK inhibitors is dependent on blocking FAK in tumour microenvironment rather than in the tumour cells

(Wendt, 2009). These data highlight the complex nature of the involvement of FAK in tumour growth and progression.

5.4. FAK Transgenic and Knock-Out mouse models

Genetic ablation of FAK results in embryonic lethality at (E) 8.5 due to gastrulation and vascular defects (Ilic, 1995) a phenotype that resembles to fibronectin-deficient mice. Global FAK Kinase dead mice are embryonically lethal at (E) 9.5, presenting similar vascular defects and haemorrhage (Lim, 2009). Global deletion of FAK exon 15 containing the Y397 resulted in mid-gestation mortality between (E) 14.5 and (E) 16.5, with developmental vasculature defects (Corsi, 2009). In a transgenic mouse model, the Tie2 promoter was used to overexpress chicken FAK in endothelial cells specifically (Peng, 2004). These mice presented with enhanced angiogenesis in skin wound healing and after ischemia.

The role of FAK in vascular development has been confirmed using a mouse model with endothelial-specific FAK deletion (Shen, 2005; Braren, 2006). Shen et al showed that endothelial specific FAK deletion caused lethality at (E) 11.5, two days later when compared to the total FAK KO. The vascular defects seen are linked with endothelial cell migration, proliferation and cell survival defects. Braren at al addressed the role of endothelial FAK in development using a Tie2Cre model and observed dilated capillaries starting from (E) 9.5 and lethality between (E) 10.5 and (E) 11.5. In this model endothelial cell migration and proliferation was not decreased and the phenotype was explained by aberrant lamellipodia, enhanced cell death and

vascular pruning. Together these data implicate FAK as essential to developmental angiogenesis.

Endothelial specific FAK Kinase Dead (KD) mutation in embryos revealed FAK Kinase dependent vascular barrier function (Zhao, 2010). The FAK-KD mutation was achieved by replacing the lysine at the 454 position with an arginine (FAK-K454R). The endothelial specific FAK-KD mice exhibited reduced blood vessel density in the embryo brain, increased vessel diameters and lethality at embryonic day (E) 13.5. In this study, the FAK-KD mutation seems to rescue the defective survival observed in FAK deleted endothelial cells, suggesting that other FAK elements are involved in endothelial cell pro-survival signaling. Endothelial specific FAK-KD knock-in mice also revealed a role for FAK in control of VEGF-stimulated vascular permeability (Chen, 2012) and further studies indicate that upon VEGF stimulation, FAK is able to directly phosphorylate VE-Cadherin, therefore tightening the vascular barrier (Jean, 2014).

To address endothelial FAK functions in adult pathological angiogenesis, inducible mouse models were engineered overcoming the embryonic lethality in endothelial specific FAK deleted or mutated mice. No changes in angiogenic response were observed in FAK floxed mice crossed with mice carrying a tamoxifen induced Cre under the control of the 5' endothelial enhancer of the stem cell leukaemia locus (End-SCL-Cre-ERT) and this is thought to be due to a compensatory effect of Pyk2 for the FAK loss (Weis, 2008). Immunocompromised mice were used in a tamoxifen-inducible Tie2-Cre^{ERT} FAK Knock-out model and highlighted FAK requirement in the Blood-Brain Barrier (BBB) integrity and tumoral angiogenesis in gliomas (Lee, 2010). Inducible

endothelial specific FAK deletion in the absence of Pyk2 compensation led to decreased tumour growth and angiogenesis (Tavora, 2010). In this study FAK floxed mice were crossed with mice carrying a tamoxifen inducible Cre, driven by the endothelial specific PDGFb promoter (Claxton, 2008). Together these studies suggest that endothelial FAK is a key player in tumourigenesis and malignant progression, but the contribution of FAK as a scaffolding protein, as a signaling molecule or as a kinase need to be better understood.

5.5. Development of point-mutant FAK knock-in mice

In our laboratory PDGFb-iCre^{ERT2};FAK$^{fl/fl}$;R26FAK^{KI} mice that display an inducible endothelial-specific FAK deletion and simultaneous mutant FAK expression were developed by crossing PDGFb-iCre^{ERT2};FAK$^{fl/fl}$ mice with mice carrying a WT or mutated version of chicken FAK preceded by a floxed STOP cassette, in the ROSA26 locus. The mutated chicken FAK protein knocked-in is non-phosphorylatable on either the 397 or 861 residue, due to the replacement of the respective tyrosine by a phenylalanine (Tavora, 2014a). **Figure 1.5** shows the genetic alterations present in PDGFb-iCre^{ERT2};FAK$^{fl/fl}$;R26FAK^{KI} mice before (**A**), during (**B**) and after (**C**) tamoxifen administration, as well as the impact of these genetic modifications on protein knockout and expression. This mouse model allows addressing the role of FAK-Y397 and FAK-Y861 phosphorylation in tumour growth and angiogenesis. These new models of point-mutant FAK have been used in my project.

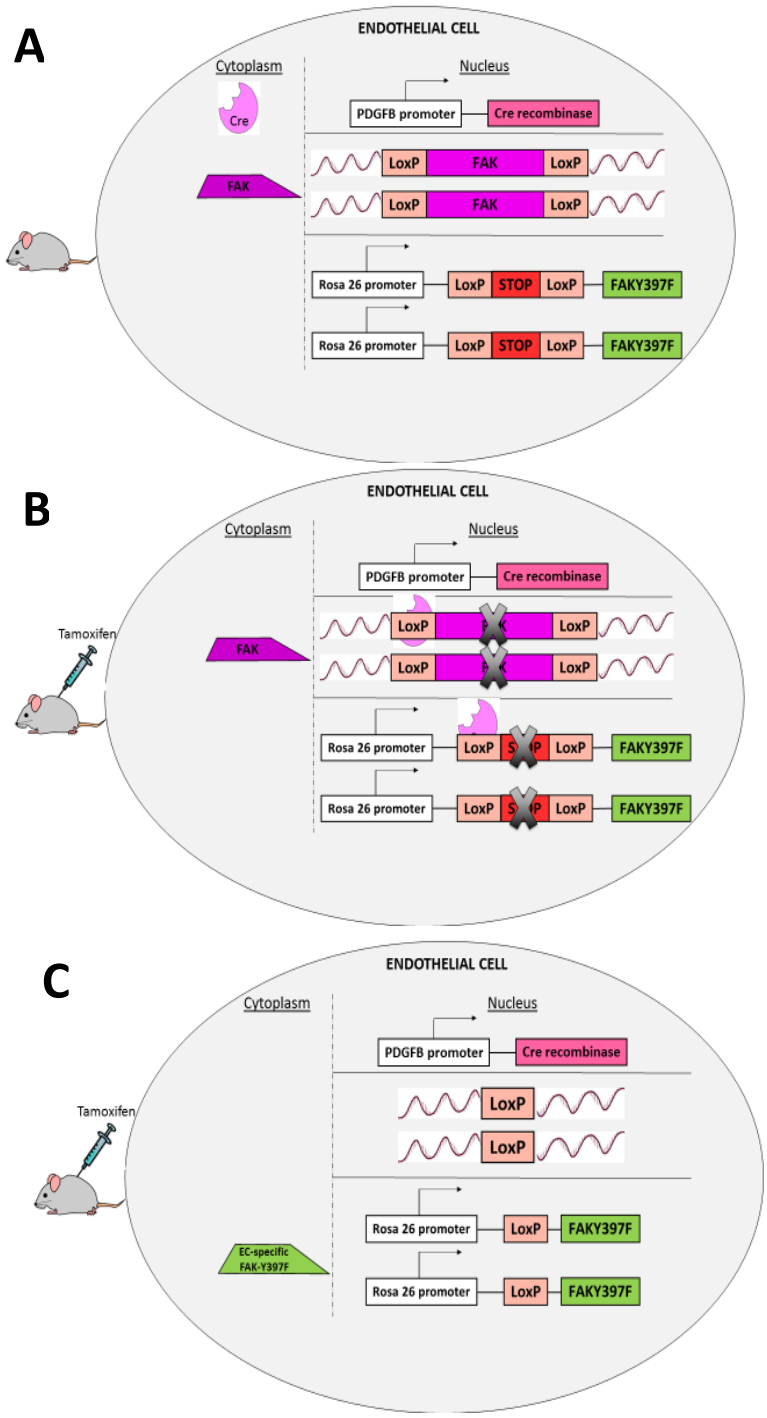

Figure 1.5: Development of point-mutant FAK mice

The Cre-positive inducible mouse contains the same genetic alterations as the Cre-negative mice, with the addition of a Cre transgene: (A) The Cre recombinase transgene is under the endothelial-specific Pdgfb promoter, allowing the expression of Cre only in endothelial cells, while the endogenous FAK gene and the STOP cassette are flanked by loxP sites. (B) Upon tamoxifen administration, Cre translocates to the nucleus, recognises the loxP sequences, and causes the removal of the endogenous gene FAK and the STOP cassette; (C) resulting in the expression of the desired FAK mutation in endothelial cells.

RESEARCH AIMS

The primary research aim of my thesis is to study the endothelial specific inactivation of FAK-Y397 and FAK-Y861 phosphorylation in tumour growth and angiogenesis *in vivo* for a panel of subcutaneous tumour models. The impact of the inactivation of these FAK phosphorylations on the tumour endothelial compartment as well as on the tumour mass itself will be analysed. The endothelial specific FAK-KO mouse model has shown a decrease in tumour growth and tumour angiogenesis and we have hypothesized that FAK-Y397F and FAK-Y861F mutations might have similar effects on tumour growth.

The endothelial compartment will be investigated for functional as well as morphological features, therefore blood vessel perimeter, perfusion, leakage and pericyte coverage will be investigated. The endothelial specific FAK-KO mouse model did not present with any differences in these parameters, and there is the possibility that the FAK point mutations yield in a similar result.

In vivo sponge assay and *ex vivo* aortic ring assay will be used to highlight potential signalling pathways impaired or activated by the endothelial specific FAK-Y397F and FAK-Y861F mutations.

To broaden the range of molecules and signalling pathways that can be affected by FAK-Y397F or FAK-Y861F mutation, mouse lung endothelial cells isolated from the transgenic mice will be used for preliminary studies to investigate cytokine production by endothelial cells *in vitro*.

CHAPTER II: MATERIALS AND METHODS

1. Mouse colony management

1.1 Reagents

Tail lysis buffer contains 50mM Trizma base/Trizma hypochloride at pH 8.5 (Sigma, Dorset, UK), 10mM EDTA at pH 8, 100mM NaCl (BDH Laboratory Supplies, Poole, UK) and 0.2% SDS. Proteinase K (Roche, Welwyn Garden City, UK) was diluted to 0.1mg/mL in Tail lysis buffer.

TE buffer contains 10mM Trizma base/Trizma hypochloride at pH 7.5 (Sigma, Dorset, UK) and 1mM EDTA (BDH Laboratory Supplies, Poole, UK).

1.2 DNA extraction

Ear or tail snips were digested overnight at 56°C in 100µL Tail lysis buffer, supplemented with 0.1mg/mL Proteinase K. To precipitate the DNA, equal volume of isopropanol was added prior to centrifuging the samples at 2600rpm for 30 minutes. After removing the supernatant, the DNA pellet was dried at 56°C for 2 hours, and then resuspended in 200µL TE buffer.

1.3 Genotyping PCR and DNA electrophoresis

The primers (Invitrogen, Paisley, UK) were resuspended to 100µm in TE buffer and stored at -20C. Prior to PCR, the primers were diluted to 10µmworking solution and 1µL of each primer was added to the PCR mix, except for the betaglobulin primers, in which case 0.75µL of each primer was used. For each PCR reaction 1µL DNA was used in a total volume of 25µL Megamix (Cambio, Cambridge, UK).

The PCR conditions for the LP2 genotyping were: 3 min at 94°C; 35 cycles of 45s at 94°C, 45s min at 56°C and 45s at 70°C; and 5 min at 72°C. The reaction was carried out using the following oligonucleotide primers:

LP2as: 5' – TTAATAAGACCAGAGGACTCAGC – 3'

LP2h: 5' – GGAAGAAGCTTGTATACTGTATG – 3'

LP2s: 5' – ATTGTGCTATACTCACATTTGGA – 3'

The PCR conditions for R26FAKKI/KI genotyping were: 5 min at 94°C; 35 cycles of 30 sec at 94°C, 1 min at 59.5°C and 30 sec at 72°C; and 10 min at 72°C. The following primers were used:

Rosa 1 (Forward WT): 5' – GTTATCAGTAAGGGAGCTGCAGTGG – 3'

Rosa 2 (Reverse WT): 5' – GGCGGATCACAAGCAATAATAACC – 3'

Rosa 3 (Reverse Targeted): 5' – AAGACCGCGAAGAGTTTGTCCTC – 3'

The PCR conditions for Pdgfb-iCreER genotyping 5 min at 94°C; 35 cycles of 30 sec at 94°C, 1 min at 65°C and 1 min 20 sec at 72°C; and 10 min at 72°C. The reaction was carried out using the following oligonucleotide primers:

PdgfbCre F: 5' – GCCGCCGGGATCACTCTC – 3'

PdgfbCre R: 5' – CCAGCCGCCGTCGCAACT – 3'

B2-1: 5' – CACCGGAGAATGGGAAGCCGAA– 3'

B2-2: 5' –TCCACACAGATGGAGCGTCCAG– 3'

The PCR products were separated on a 2% agarose (UltraPure Agarose, Life Technologies) gel at 100 volts and bands were visualized using UV light.

2. B16F0, CMT19T and LLC cell line culture

B16F0 melanoma cells, CMT19T carcinoma cells and LLC carcinoma cells were grown in Dulbecco's Modified Medium (DMEM, Invitrogen, Paisley, UK), supplemented with 10% foetal calf serum (FCS, PAA, UK). Cells were cultured in uncoated T175 flasks at 37°C/ 10% CO_2.

Tumour cells were 70-80% confluent when trypsinized, washed 3 times in 50mL PBS, passed through a 70µm cell strainer (BD Falcon, Bedford, MA, USA) and counted using the Automated Cell Counter (Scepter 2.0, Millipore). The cell suspension concentration was adjusted to 10^7 cells/mL (for B16F0 and CMT19T) or to $5x10^6$ cells/mL (for LLC) in PBS prior to 100µL tumour cell suspension subcutaneous injection.

3. Polyoma-middle-T-antigen retroviral production

The GgP+E packing cell line was grown Dulbecco's Modified Medium (DMEM, Invitrogen, Paisley, UK) supplemented with 15% FBS Hyclone. Cells were cultured in uncoated T75 flasks at 37°C/ 10% CO_2.

When cells were 70% confluent, the culture media was changed and 12 hours later media containing the retrovirus was collected, centrifuged at 2800 rpm for 15 minutes and passed through a 0.45µm filter. Polybrene (8µg/mL final concentration) was added after the filtration step.

Freshly prepared retrovirus was used to infect endothelial cells. In some cases, the prepared retrovirus was kept at -80°C for up to 2 years before infection.

4. Mouse Lung Endothelial Cell Culture

4.1 Coating Mix composition for endothelial cell culture

Distilled water was used to prepare 0.1% gelatine (Sigma, Dorset, UK). The solution was autoclaved 30min at 65°C and stored at 4°C. Tissue culture flasks were coated with 0.1% Gelatine, 1% Collagen (PureCol 5005-B, lot 6200, 1mg/mL, Advanced BioMatrix), 1% Fibronectin (Hu Plasma Fibronectin, 1mg/mL, lot 2272678, Millipore) mix and incubated at 37°C for 2 hours or at 4°C overnight. The coating mix was removed before the addition of culture medium and cells.

4.2 Endothelial cell culture medium

MLEC Medium contained 40% Low glucose DMEM (Gibco, 21885-025), 40% HAM-F12 (Sigma N6658), 20% Hyclone serum (Thermo Scientific SH 30071.03; lot SLBC9940V) and was supplemented with 10mg/mL Heparin (Sigma-Aldrich; H3149-1MU), Glutamine (Glutamax 35050, Invitrogen), Penicillin/Streptavidin (Sigma P4333) and Endothelial Cell Growth Supplements (Harbor Bio-Products; 1003).

MLEC Medium was supplemented with 500nM 4-hydroxytamoxifen (OHT) (Sigma, Dorset, UK) to activate the Cre recombinase *in vitro*. OHT was stored as a 10mM 95% ethanol solution.

4.3 Mouse Lung Endothelial Cell (MLEC) Isolation

Mice aged between 4 and 9 weeks were killed by cervical dislocation and lungs removed, stored in Optimem Medium on ice, any fat and blood clots removed, briefly rinced in 70% Ethanol and stored in ice-cold MLEC Medium. Lungs from each mouse were separately minced and incubated in 3 mL of 100

E.U. Type I Collagenase (Gibco Invitrogen, Paisley, UK) for 75 minutes. The digested tissue was then syringed up and down 3 times with the a 21G syringe (BD Microlance; 304432), then 2 times with 19G syringe (BD Microlance; 301500), followed by a passage through a 70µm cell strainer (BD Falcon; 352350). The single-cell suspension was spun down at 1200 rpm for 5 minutes; the supernatant was aspirated, leaving the pellet and 5mL solution. MLEC medium was used to resuspend the pellet and the 10mL cell suspension were plated on a pre-coated flask and incubated at 37°C, 5%CO_2.

4.4 Negative Sorting – removal of macrophages

Within 48h of the cell isolation, cells were incubated at 4°C for 20 minutes in ice-cold MLEC medium to prevent internalization of surface receptors, followed by 30 minutes incubation at 4°C with a rat anti-FCγRII/III antibody solution (BD Biosciences; 553142; 1/100 in PBS). Cells were then washed once with ice-cold PBS and incubated at 4°C for 30 minutes with a magnetic bead conjugated sheep anti-rat antibody (Invitrogen Dynabeads; 110.35). After 3 washes with ice-cold PBS cells were trypsinised, supplemented with medium and transferred in a tube placed in a magnetic holder. After 5 minutes the bead-attached macrophages were held in the wall of the tube. The medium was carefully removed from the tube and the macrophage-free cell suspension was plated in a pre-coated flask.

4.5 Endothelial Cell Positive Sorting

The procedure described in section 4.4 was repeated using a rat anti-ICAM2 antibody solution (BD Parmingen; 553326; 1/100 in PBS) and the bead attached endothelial cells were held in the wall of tube. The medium was

aspirated and discarded and the bead attached endothelial cells were resuspended in MLEC and plated in a pre-coated flask.

The positive sorting step was performed twice to ensure endothelial cell purity. The second endothelial cell positive sort was performed after the immortalisation procedure.

4.6 Immortalisation of isolated endothelial cells

MLEC were immortalised 24 hours after the first positive sort using polyoma-middle-T-antigen retroviral transfection. The retrovirus was prepared as described in section 3. Endothelial cells were infected for 4 hours and this procedure was repeated two consecutive days. After the second infection, endothelial cells were cultured in the presence of 4-OHT at 0.5mM. The second positive sort was performed at least 24 hours after the last viral transfection.

4.7 Transfection of immortalised endothelial cells

Endothelial cells were trypsined and counted; 10^6 endothelial cells were spanned for 10 minutes at 1200 rpm and resuspended in 100µL transfection solution (Nucleofactor Kit, VPB-1002, AmaxaTH HUVEC). The appropriate plasmid was added to the cell suspension and the transfection was performed using the Amaxa machine. The transfected cells were plated into a T25 pre-coated flask. Endothelial cells isolated from Cre positive mice were transfected with the pCAG-Cre-IRES2-GFP plasmid (Addgene, 26646) whereas cells isolated from Cre negative mice were transfected with pCAG-GFP (Addgene 11150).

5. Reverse-Transcriptase quantitative Polymerase Chain Reaction

The mouse FAK knock out and chicken FAK knock in was determined at the mRNA level using the RT-QPCR technique. For this endothelial cells were lysed using RNA lysis buffer (RPE + beta mercaptoethanol) and RNA was extracted with RNA Extraction Kit (Qiagen; 74104) and reverse transcribed with high-capacity cDNA Reverse Transcription kit (Applied Biosystems; 79254). Real time PCR was performed with custom made primers and probes specific for either chicken or mouse FAK (Applied Biosystems). Each Taqman reaction contained a FAM labelled chicken FAK or mouse FAK primer and a VIC labelled GAPDH primer, used as a loading control.

The sequence of the Chicken FAK primers and probe is the following:

Forward primer: CAACAGCAAGAGATGGAAGAAGATC:

Probe: ACGATTCCTGGTAATGAA;

Reverse primer: 5 CCGTCCTCCCGTTCAATG-3'.

FAM labeled/MGB probe

The sequence of the Mouse FAK primers and probe is the following:

Forward primer: GGCGTTGCCATCAATACCA

Probe: AAGGCATGCGGACACA

Reverse primer: GGTGTATGTGTCTTCCTCATCGAT

FAM labeled/MGB probe

6. Western blotting and Cytokine Arrays

6.1. Endothelial cell lysis and Protein Concentration Assay

Endothelial cells were plated in a 6-cm dish and left to grow overnight or until becoming 70-80% confluent. Cells were lysed with 100-150µL Sample Buffer (60mM Sucrose; 65 mM Tris-HCl pH 6.8; 3% SDS) and sonicated at 4C, 3 times for 5 seconds before protein concentration was determined.

BSA standard solutions were prepared at 0, 0.1, 0.2, 0.4, 0.8, 1, 1.2, 1.6, 2 mg/mL and the previously sonicated lysates were diluted 1/2 or 1/3 in Sample buffer. The Bio-Rad DC protein assay kit (Bio-Rad laboratories, Hercules, CA, USA) was used according to the manufacturer's guidelines to determine the protein concentration for each sample.

The protein concentration was adjusted between lysates using Sample Buffer and then the samples were prepared for western blotting by supplementing with 25% 4X NuPage, 10% 10X NuPage and boiling the samples for 5 minutes at 100°C.

6.2. SDS-PAGE and Protein Transfer

Resolving gels for 8% polyacrylamide gel was prepared according to the following recipe: 2.7ml 30% Acrylamide (National Diagnostics, UK), 2.5ml 4X Resolving Buffer (National Diagnostics, UK), 4.8ml Distilled Water, 100µL Ammonium persulphate (APS) 10% (w/v) (National Diagnostics, UK), 6µL TEMED (National Diagnostics, UK). This resolving gel was poured into pre-formed 1-1.5mm thick cassettes (Invitrogen, Paisley, UK) and overlaid with isopropanol, to prevent gel-air contact, which inhibits polymerisation. When the gels were polymerized, the isopropanol was discarded and the stacking gel was

poured on top and a lane comb was introduced. The stacking gel is composed of 330µL 30% Acrylamide (National Diagnostics, UK), 0.5mL Stacking Buffer (National Diagnostics, UK), 1.15mL Distilled Water, 20µL Ammonium persulphate (APS) 10% (w/v) (National Diagnostics, UK), 2µL TEMED (National Diagnostics, UK). The stacking gel was left to polymerise and the comb was then removed and the gel was placed in a gel tank (Invitrogen, Paisley, UK) and covered totally with 1X running buffer (0.025M Tris base, 0.192M glycine, 0.1% sodium dodecyl sulfate, Fisher Biotech, New Jersey, USA).

The protein samples and the protein marker ladder (GE, Paisley, UK) were loaded into the wells and the gel was run at 125 volts until the desired separation was achieved.

Resolved proteins were then transferred from the gel into a Hybond nitrocellulose transfer membranes (GE, Paisley, UK), by assembling a transfer 'sandwich' composed of, from bottom to top: two sponges, two Whatman paper sheets, the gel, the membrane, two Whatman paper sheets, two sponges. The transfer "sandwich" was placed in the transfer apparatus (Invitrogen, Paisley, UK), put in a transfer tank and immersed in 1X transfer buffer. The transfer buffer was composed of 0.025M Tris, 0.192M glycine (National Diagnostics, UK), 20% methanol (Fisher Scientific, Leicestershire, UK) and the transfer was performed at 35 volts for 1 hour and 30 minutes.

At the end of the transfer step, the membranes were immersed in Ponceau S (Sigma, Dorset, UK) and washed briefly in distilled water to access the efficiency of the transfer and were subsequently used for immunoblotting.

6.3. Immunoblotting

Membranes were blocked in 5% BSA/TBS-0.1%Tween-20 (Sigma, Dorset, UK) for 1 hour, then incubated with the primary antibody diluted 1/1000 in blocking solution overnight at 4C. After three 5-minute washes in TBS-0.1%Tween-20, the membrane was incubated with the appropriate horseradish-peroxydase (HRP) – conjugated secondary antibody diluted 1/1000 in 5% BSA/TBS-0.1%Tween-20 for 1 hour at room temperature. Three 5-minute washes in TBS-0.1%Tween-20 were performed, before incubating the membrane with ECL chemiluminescence reagents (Expedeon, UK) for 1 minute and exposing them in an autoradiographic film (Fujifilm, Pyser-SGI limited, UK). The films were developed with a Kodak X-OMAT 100A film processor (East Kodak Company, New York, USA). The following antibodies were used: Mouse anti-FAK (clone 77/FAK, BD Biosciences, Oxford, UK), Mouse anti-myc (Abcam, 9E10), Mouse anti-HSC70 (Santa Cruz Biotechnology, CA, USA), Polyclonal swine anti-rabbit-HRP (Dako P0217, Cambridgeshire, UK), Rabbit anti-pY397-FAK (Cell signalling; 3283S), Rabbit anti-pY861-FAK (Invitrogen; 44626G) and Polyclonal rabbit anti-mouse-HRP (Dako, Cambridgeshire, UK).

6.4. Cytokine array

Endothelial cells were plated in 6cm dishes, left to grow overnight and lysed using sample buffer. Protein concentration was determined as previously described and matched amongst lysates using sample buffer. The lysate was incubated with membranes containing antibodies against a panel of cytokines (Mouse Cytokine Array panel A, R&D Systems, Proteome Profiler Array, ARY006). All the steps and the quantifications were performed according to the manufacturer's protocol. Briefly, the array membranes were incubated for 1

hour in 2mL of Array Buffer 6 on a rocking platform shaker. Meanwhile the protein samples were prepared in Array Buffer 4 and 15µL of reconstituted Mouse Cytokine Array Panel A Detection Antibody Cocktail was added to each sample and left to incubate for one hour at room temperature. At the end of the incubation time, the membrane was incubated overnight in the cold room with the sample/antibody solution. The next day, the membranes were washed three times with 1X Wash Buffer and Streptavidin-HRP was added to the membranes and incubated for 30 minutes. After three washes in 1X Wash Buffer, 1mL of Chemi Reagent Mix was evenly pipetted into each membrane and incubated for 1 minute. The membrane was subsequently placed into a autoradiography film cassette and exposed to X-ray films for 30 seconds and up to 1 hour (several exposures were performed). The intensity of the signal was then quantified in the same way as for Western Blotting data.

7. Animal Experiments

Animal experiments were performed under the Personal Licence number ID FA07983 and the Project License PPL 70/7449 19b/2.

7.1. Tamoxifen formulation and treatment

To prepare Tamoxifen for intra-peritoneal injection 500 mg Tamoxifen (T5648-5G Sigma lot: SLBB0439V) was dissolved in 5mL 100% ethanol, for 30 minutes at 42°C with occasional vortexing, prior to the addition of 45mL autoclaved Corn Oil (Sigma C8267). The solution was vortexed for 2 minutes, aliquoted and stored at -20°C for up to 6 months. Each experimental mouse was

injected intra-peritonealy once a day, for two consecutive days, with 100µL of 10mg/mL Tamoxifen solution.

7.2. Subcutaneous Tumour Growth

Five to seven days after tamoxifen treatment, mice were anesthetised with Isofluorane (Abbot) and subcutaneously injected into the flank with 100µL of $1x10^7$ B16F0 mouse melanoma cells or $1x10^7$ CMT19T carcinoma cells or $0.5x10^7$ LLC carcinoma cells. When subcutaneous tumours became palpable (usually at day 5-7 for B16F) or at day 8-10 for CMT19T and LLC), the tumour size was measured with digital callipers every other day until the experimental endpoint.

When required, ante-mortem procedures were performed as described in the next section, and dissected tumours were snap-frozen in liquid nitrogen or fixed in 4% formalin.

7.3. Ante-mortem procedures

7.3.1. PE-PECAM Injection

Mice carrying subcutaneous size-matched tumours were intra-venously injected with 100µL of anti-PE-PECAM antibody (BioLegends, clone 390, 102498) 10 minutes prior to tumour dissection. The tumours were snap-frozen, kept at -80°C and stained for endomucin as described in section 8.3; this allowed to quantify perfused blood vessels and the total number of blood vessels and determine the percentage of perfused blood vessels.

7.3.2. PE-PECAM+Hoechst Injection

Mice carrying subcutaneous size-matched tumours were intra-venously injected with 100µL of anti-PE-PECAM antibody as described in the previous section. Hoechst 33342 was injected intra-venously 1 minute prior to tumour dissection. The tumours were snap-frozen and kept at -80C. This methodology allows quantifying the level of Hoechst leakage out of the perfused blood vessels and into the tumour tissue.

7.3.3. Pimonidazole Injection

Mice carrying subcutaneous size-matched tumours were intra-peritoneally injected with 60mg/kg of pimonidazole (Hypoxiprobe Plus Kit; HP2-100K) 1 hour prior to tumour dissection. The tumours were snap-frozen, kept at -80°C and stained for hypoxia as described in section 8.8.

7.4. Subcutaneous Sponge Assay

Two sterile polyether sponges (approximately 1 x 0.8 x 0.8 cm) (Caligen Foam) were inserted subcutaneously in the flanks of adult mice, previously injected with tamoxifen as described in Section 7.1.

The sponges were injected every other day with 100µL of 10ng/mL of VEGF (Peprotech, 450-32) or 100µL of 10ng/mL of PlGF (R&D Systems, 465-PL-010) or 100µL of 5ng/mL of bFGF (Peprotech, 450-33) or 100µL of 10ng/mL of ANG2 (R&D Systems, 7186-AN-025) or 100µL of PBS as a negative control.

After 15 days, the experimental mice were culled and sponges removed and fixed in 4% formalin overnight. The next day, sponges were transferred in 70% ethanol, paraffin embedded and 5µm sections were cut.

To evaluate the blood vessel infiltration sections were immunostained for endomucin as described in section 8.4.

7.5. Aortic Ring Assay

A week prior to dissection, mice was injected with tamoxifen as described in Section 8.1. The mice were killed by cervical dislocation and the heart and lungs removed and the aortic ring assay was performed as described previously (Masson et al, 2002; Reynolds et al, 2004). The aortas were gently separated from the spine and placed in OptiMEM (Life Technologies, 51985-026) supplemented with 100U/mL of penicllin/streptomycin (Invitrogen, Paisley, UK). The aortas were cleaned of fat, blood/blood cloths, and conjunctive tissue under sterile conditions using a dissecting microscope and were subsequently cut into 20-25 rings per aorta. The rings were starved overnight in OptiMEM at 37°C / 10% CO_2 and at the end of the starvation time were embedded in 50µL of Collagen matrix. The collagen matrix was prepared by mixing 1.2 mg/mL Collagen Type I (Millipore, 08-115) and 1.1mL of 10X DMEM (Gibco, 12800-017) supplemented with distilled water to 10mL. The aortic ring containing collagen matrix was left to polymerize for 30 minutes at 37°C / 10% CO_2 and 150µL of OptiMEM containing 2.5% FCS and either VEGF (30ng/mL) or Ang2 (10ng/mL) or VEGF+Ang2 (30ng/mL + 10ng/mL, respectively) or PBS (as a control) were added per well. Media was changed on Monday/Wednesday/Friday by removing 75µL of the media and adding 75µL of fresh media supplemented with the appropriate growth factor or growth factor combination and the aortic ring sprouts were counted starting with Day 5 and until the end of the experiment (Day 14).

8. Histological Analysis

8.1. Tissue Section Preparation

Mouse tissue and tumours were immersed in formalin for 24 hours, then in 70% ethanol for up to one week. The Barts Cancer Institute Pathology Department performed sample paraffin-embedding procedures and 5µm thick sections were mounted onto glass slides and kept at room temperature. Prior to staining, paraffin sections were de-waxed in two separate xylene baths (BDH Laboratory Supplies, Poole, UK) for 5 minutes each and re-hydrated in five separate baths of graded ethanol (100%, 100%, 80%, 70% and 50%) for 2 minutes each. The slides were immediately used for immunofluorescence staining.

If immunohistochemistry had to be performed on paraffin embedded tissue, endogenous peroxidase was inactivated using Methanol (Fisher scientific, Leicestershire, UK) with 3% H_2O_2 (Sigma Dorset, UK) and this step was performed between the two 100% Ethanol baths.

Mouse tissue, previously snap frozen in liquid nitrogen, was sectioned on a cryostat and 5µm thick sections were mounted onto glass slides and kept at -80°C. The frozen sections were fixed in ice-cold acetone at -20°C for 10 minutes and immediately used for immunofluorescence staining.

8.2. Haematoxylin and Eosin (H&E) staining

The H&E staining was routinely performed by the Barts Cancer Institute Pathology Department. H&E counterstaining was also performed as part of immunohistochemistry protocols for sponge assay.

8.3. Blood vessel immunofluorescence and quantitation

Immunofluorescence technique was used to stain for blood vessels on snap-frozen tumour sections. After having been thawed and fixed as described in section 9.1, sections were blocked in 5% BSA (PAA, Somerset, UK) in PBS for 1 hour at room temperature. The sections were incubated with anti-endomucin antibody (clone V7C7, Santa Cruz Biotechnology, CA, USA) diluted 1/200 in 5%BSA/PBS overnight at 4C. After three 10-minute washes with PBS 0.02% Triton X-100, the slides were incubated with Alexa fluoro 488 goat anti-rat antibody (Invitrogen, Paisley, UK) diluted 1/100 in 5%BSA/PBS for 45 minutes at room temperature. Sections were washed three times with PBS 0.02% Triton X-100, one time with distilled water and mounted in Prolong Gold anti-fade reagent with DAPI (Invitrogen, Paisley, UK). Alternatively, after the last wash, sections were incubated for 5 minutes with DAPI (Invitrogen, Paisley, UK) diluted 1/10 000 in water, followed by a 10 minute was in water and mounted in Prolong Gold anti-fade reagent (without DAPI) (Invitrogen, Paisley, UK).

The endomucin-positive blood vessels were visualised and counted at the Zeis Axioplan microscope and tumour blood vessel density was calculated by dividing the number of endomucin-positive blood vessels counted across the entire midline tumour sections by the section area. Representative pictures were taken at the confocal microscope at 40X magnification.

Pictures were also taken at 10X magnification with at the Axioplan microscope and blood vessel perimeter was determined using ImageJ software.

8.4. Blood vessel immunohistochemistry and microvessel quantitation in sponges

Immunohistochemistry technique was used to stain for blood vessels in sponge sections. Sections cut from paraffin-embedded sponges were dewaxed, rehydrated and fixed with Methanol+H_2O_2, as previously described. Antigen retrieval was done using 10mM Tri-Sodium Citrate pH6. The solution was microwaved alone until boiling, them slides were added further microwaved for 10 minutes and then left to cool until reaching RT. Distilled water was used to wash the slides twice, before incubating with the blocking buffer containing 2% Goat serum / 1% BSA / 0.1% TritonX100 / PBS. The anti-endomucin (Endomucin clone C7 Santa Cruz; 1/200 in blocking buffer) primary antibody was incubated overnight at 4C. The next day slides were washed three times for 5min with PBS 1X and anti-rat biotinylated (BA4001 Dako; 1/100 in blocking buffer) secondary antibody was incubated for 30min at RT. Slides were then washed twice for 5 min in PBS1X and Elite ABC reagent (Vector kit PK6100 or 6102) was made up according to the manufacturer's instructions and incubated for 30min at RT. After another two PBS 1X washes, slides were incubated with DAB substrate (Vector kit SK4100) until blood vessels could be visualised in brown colour (usually after 8-10 min), after what the reaction was stopped by adding tap water for 3min. Slides were then incubated with H&E for 3-4min and washed in running tap water for 3min. Lastly, slides were dehydrated, cleared (by being incubated for 5min in each of these baths: 50%, 70%, 95%, 99%, 99% alcohol, xylene) and mounted with DPX (Sigma, Dorset, UK).

DPX-mounted slides were left to dry overnight and the next day slides ere scanned using the Pannoramic 250 Scanner. Infiltrated microvessels were

quantified across the width of the sponge at 30X magnification. The H&E stainig was used to determine if the analysed field was infiltrated by cells. The number of microvessels was quantified for the fields that presented with infiltrated cells and the average number of microvessels per field was determined for each sponge. To determine if the studied mutations affected microvessels formation into the sponge, the Cre pos group was compared to the Cre pos group.

8.5. Functional Blood vessel quantitation

Tumour sections from tumour-burdened mice that had undergone ante-mortem anti-PE-PECAM antibody injections, as described in section 7.3.1 were stained for endomucin following the immunofluorescence protocol previously described.

PE-PECAM-positive blood vessels (perfused blood vessels) and endomucin-positive blood vessels (all blood vessels) were counted at 40X magnification at the Axioplan microscope and at least 100 PE-PECAM-positive blood vessels were counted per tumour. The percentage of functional blood vessels was calculated by dividing the number of PE-PECAM-positive blood vessels by the number of endomucin-positive blood vessels and multiplied by 100%. The percentage of functional blood vessels was compared between Cre negative and Cre positive groups.

8.6. Hoechst Leakage quantitation

At the experimental endpoint tumour-bearing mice were injected with anti- PE-PECAM antibody into the tail vein 10 minutes prior to sacrifice, and with Hoechst 33342 into the tail vein 1 minutes prior to sacrifice. At the end of

these ante-mortem procedures, mice were culled, tumours were dissected and snap frozen as previously described.

The frozen tumours were processed in the dark and sections were cut, mounted using anti fade reagent (without DAPI) and 5 fields per tumour were photographed at 40X magnification using the Axioplan microscope. The same threshold was used across all the fields and tumours for the blue channel (DAPI) and also for the red channel (PE-PECAM).

Image J software was used to determine the Hoechst-positive area and the PE-PECAM positive area for each field and the Hoechst/PE-PECAM ratio was calculated for each field. Hoechst/PE-PECAM ratios from each of the 5 photographed fields were averaged to obtain Hoechst/PE-PECAM ratio for each tumour.

To determine if the studied endothelial mutations have an effect on Hoechst leakage, Hoechst/PE-PECAM ratios were compared between Cre negative and Cre positive groups.

8.7. Blood vessel and pericyte double immunostaining and Pericyte coverage quantitation

Tumour sections were fixed with Acetone as previously described, blocked with 5%BSA/PBS and incubated with a solution containing anti-Endomucin antibody (Endomucin clone C7 Santa Cruz; 1/200 in in 5%BSA/PBS) and anti-NG2 antibody (Millipore AB5320; 1/200 in 5%BSA/PBS) at 4°C overnight. The next day, slides were washed three times in PBS 1X for 5min and incubated with a secondary antibody mixture containing anti-rat Alexa 546 antibody (Invitrogen, Paisley, UK; 1/100 in 5%BSA/PBS) and anti-

rabbit Alexa 488 antibody (Invitrogen, Paisley, UK; 1/100 in 5%BSA/PBS) for 1hour at RT. Slides were washed three times in PBS 1X for 5min and mounted using the Antifade reagent with DAPI (Invitrogen, Paisley, UK). The slides were left to set overnight at RT and were then stored at 4°C.

A CDD camera Hamamatsu C4742-95 and a Zeiss Axioplan microscope were used to acquire fluorescence images at 40X magnification of approximately 10 fields per tumour. For each tumour, blood vessels were classified as naked (when no pericyte was present), partially covered or fully covered by pericytes. The percentage of blood vessels falling into each of these categories was calculated and these data were compared between Cre negative and Cre positive groups.

8.8. Hypoxia staining and quantitation

Tumour sections from tumour-burdened mice that had undergone ante-mortem Pimonidazole injections were blocked in 5% BSA (PAA, Somerset, UK) in PBS for 1 hour at room temperature. The sections were next incubated overnight at 4°C with FITC-conjugated antibody (HPI Burlington; MA01803) diluted 1/10 in PBS. After three PBS washes, the sections were mounted in Prolong Gold anti-fade reagent with DAPI (Invitrogen, Paisley, UK).

Fluorescence images were captured using a CDD camera Hamamatsu C4742-95 and a Zeiss Axioplan microscope. The area positive for staining was determined using the ImageJ software and the hypoxic index was calculated as the area of pimonidazole staining/area of tumour section and was used for statistical analysis.

9. Analysis of statistical significance

Prism software was used to analyse the generated data set with the Student t-test.

CHAPTER III: RESULTS

Here I will present my data on the effects of endothelial FAK-Y397F and FAK-Y861F mutations on tumour growth and *in vivo* tumour angiogenesis, as well as on growth factor induced angiogenesis *in vivo* and *ex vivo*. Mouse lung endothelial cells isolated from the mutated mice were used for preliminary mechanistic studies *in vitro* and the effects of endothelial FAK-Y397F and FAK-Y861F mutations on cytokine production will be presented at the end of this chapter.

1. Elucidating the effects of endothelial FAK-Y397F and FAK-Y861F mutations on tumour growth and angiogenesis

This section will present the *in vivo* effect of endothelial specific FAK-Y397F and EC-FAK-Y861F mutations on tumour growth and angiogenesis. Tumour experiments were carried out using three commercially available murine syngeneic cell lines: B16F0 mouse melanomas; CMT19T carcinomas and Lewis Cell Lung carcinomas (LLC). The B16F0 cells were derived from mouse melanoma and represent a model for skin cancer. Since B16F0 cells have been injected under the skin, the tumours are able to develop in an environment that is very similar to the one they were derived from. CMT19T and LLC cell lines were isolated from lung cancers. LLC tumour cells have been shown to secrete high amounts of VEGF and lower amounts of PlGF, whereas B16F10 cancer cells (which are derived from B16F0 melanoma cells) secrete high levels of PlGF (Zhang, 2008). The aim of this section is to investigate if and how the

endothelial specific FAK-Y397F and FAK-Y861F mutations impact tumour growth, in three distinct tumour models that differ in terms of tissue of origin and growth factor secretion profile.

The generation and characterisation of the transgenic mice will briefly be presented in the next part, before presenting the tumour growth and angiogenesis data.

1.1. Generation and characterisation of mutant endothelial-specific FAK-Y397F and FAK-Y861F mice

PDGFb-iCre^{ERT2}; FAK fl/fl; R26FAK-KI mice that display inducible endothelial-specific simultaneous FAK-deletion and mutant FAK expression were developed in our laboratory (Tavora et al., Genesis 2014b). All mice were generated on a mixed C57Bl/6J/129Sv background.

The series of transgenic mice presented in this thesis were obtained by crossing PDGFb-iCre^{ERT2}; FAK fl/fl mice (aslo referred to as EC-FAK^{KO} mice) with mice bearing one of the following constructs (WT or FAK-Y397F or FAK-Y861F) in the Rosa26 locus. After a series of crossings, PDGFb-iCre^{ERT2}; FAK fl/fl; R26FAK-KI/KI mice were obtained and experiments addressing the involvement in tumour angiogenesis and tumour growth of two residues FAK-Y397 and FAK-Y861 when mutated specifically in endothelial cells were performed. Similar experiments (B16F0 and CMT19T tumour growth, sponge assay and aortic assay) have been conducted with the endothelial specific FAK-KO mice, have been published (Tavora, 2010) and are regularly referred to throughout this thesis as the EC-FAK^{KO} phenotype.

Since the endothelial specific knock out and knock in mutation is tamoxifen-inducible, the mice did not present with antenatal or post-natal mortality. Tamoxifen administration lead to the knock out of the endogenous mouse FAK and the knock in of the mutated version of FAK in the Rosa26 locus. Mice were given a diet containing tamoxifen throughout the experimental procedure, as well as two consecutive tamoxifen injections intra-peritoneally five to seven days before the injection of tumour cells, to avoid major variations in tamoxifen administration due to variation in diet up-take. In the case of tumour studies the characterisation of the tumour tissues was performed at least 24 days after the first tamoxifen injection.[1]

I was additionally responsible for managing the backcross of these and other FAK-mutant mice onto a pure C57Bl/6 background using the Speed Congenics technology. These animals are now fully backcrossed onto a C57Bl/6 background and will be used in future experiments in the laboratory.

Table 3.1 shows the detailed nomenclature for various genotypes and the abbreviations that will be used throughout the thesis.

[1] For the sponge assay, microvessel infiltration was determined 21 days after

Genotype	Abbreviation used	Proteins expressed
$FAK^{fl/fl}$	Cre-neg; $FAK^{control}$	mFAK expressed
Pdgfb-$iCre^{ERT2}$;$FAK^{fl/fl}$;	Cre-pos; FAK^{KO}	mFAK not expressed
$FAK^{fl/fl}$;$R26FAK^{WT/WT}$	Cre-neg; FAK-WT^{KI}	mFAK expressed chFAK-WT not expressed
Pdgfb-$iCre^{ERT2}$;$FAK^{fl/fl}$; $R26FAK^{WT/WT}$	Cre-pos; FAK-WT^{KI}	mFAK not expressed chFAK-WT expressed
$FAK^{fl/fl}$;$R26FAK^{Y397F/Y397F}$	Cre-neg; FAK-$Y397F^{KI}$	mFAK expressed chFAK-Y397F not expressed
Pdgfb-$iCre^{ERT2}$;$FAK^{fl/fl}$; $R26FAK^{Y397F/Y397F}$	Cre-pos; FAK-$Y397F^{KI}$	mFAK not expressed chFAK-Y397F expressed
$FAK^{fl/fl}$;$R26FAK^{Y861F/Y861F}$	Cre-neg; FAK-$Y861F^{KI}$	mFAK expressed chFAK-Y861F not expressed
Pdgfb-$iCre^{ERT2}$;$FAK^{fl/fl}$; $R26FAK^{Y861F/Y861F}$	Cre-pos; FAK-$Y861F^{KI}$	mFAK not expressed chFAK-Y861F expressed

Table 3.1: Mouse genotypes and corresponding nomenclature.
(mFAK=mouse FAK; chFAK=chicken FAK)

During my PhD I was responsible for maintaining the FAK-WT^{KI}, FAK-$Y397F^{KI}$ and FAK-$Y861F^{KI}$ colonies (approximately 200 cages) and was responsible for all the breeding, weaning, genotyping, experimental mouse allocation and protocols. DNA sequencing identified the mutations in each of the mutant lines (**Figure 3.1 A**). PCR genotyping was carried out on all mice and identified the presence of the floxed sequences in the endogenous FAK gene (on both alleles), the presence of the FAK-knockin construct (on both alleles) and the presence or absence of the Cre recombinase (**Figure 3.1 B**). Mice were born at normal Mendelian and male:female ratios with no gross defects (**Figure 3.1**

C). The knockin for each genotype was confirmed by RT-qPCR, where chicken[1] FAK knockin and mouse FAK deletion was confirmed for each Cre positive endothelial cell line isolated from these mice (**Figure 3.1D**). Additionally, Western blot analysis confirmed FAK expression in Cre-neg and Cre-pos endothelial cell lines, with myc-tagged FAK expression only in Cre-pos endothelial cells line as expected. The biochemical outcome of the mutants was confirmed by reduced phospho-Y379 in the Cre-pos; FAK-Y397F^{KI} endothelial cells and reduced phospho-Y861 in the Cre-pos; FAK-Y861F^{KI} endothelial cells (**Figure 3.1 E**). Cre pos; FAK-Y397F^{KI} cell line also presents with a reduced FAK-Y861 phosphorylation indicating that when FAK-Y397 autophosphorylation site is mutated, subsequent phosphorylation at FAK-Y861 residue is impaired, at least in basal conditions (i.e. non-stimulated with exogenous Growth Factors). The total amount of FAK protein, as visualized after probing for total FAK and for myc indicates that FAK-Y397F protein is expressed in slightly higher mounts when compared to FAK-WT, whereas FAK-Y861F protein is less expressed when compared to FAK-WT. Cre pos; FAK-Y861F^{KI} cell line presents with some residual signal as detected by the anti-FAK-Y861 phospho antibody. This might be due to the quality of the antibody and its ability to detect exclusively phosphoY861-FAK, as the intensity of the signal is still much lower when compared to Cre pos; FAK-WT^{KI} and all the Cre neg cell lines.

[1] Chicken FAK gene and mouse FAK gene share 92% homology and chicken FAK has been used as a substitute for mouse FAK in a variety of studies. The results generated during my PhD also show that the wild-type chicken FAK protein is equivalent to the wild-type mouse FAK protein, at least for the investigated parameters.

1.2. Endothelial-specific FAK-WT^{KI} rescues the tumour growth and tumour angiogenesis EC-FAK^{KO} defect

It has been published that FAK-deletion in endothelial cells delays B16F0 tumour growth (Tavora, 2010). Thus to test if the KO/KI system functions efficiently, a WT version of FAK was knocked-in to determine if this leads to phenotype rescue thus validating the system. Cre-neg; FAK-WT^{KI} and Cre-pos; FAK-WT^{KI} mice were injected subcutaneously with B16F0 melanoma cells a week after tamoxifen administration, and tumour growth was monitored. B16F0 tumour cells injected in Cre-pos; FAK-WT^{KI} mice grow in a similar way to B16F0 tumour cells injected in Cre-neg; FAK-WT^{KI} mice (**Figure 3.2**). This result is representative of 2 experimental repeats; the second repeat is shown in **Appendix I Figure A3.1**. This result indicates that knocking-in a WT version of FAK using the KO/KI model developed in our group is sufficient to rescue the previously observed EC-FAK^{KO} phenotype.

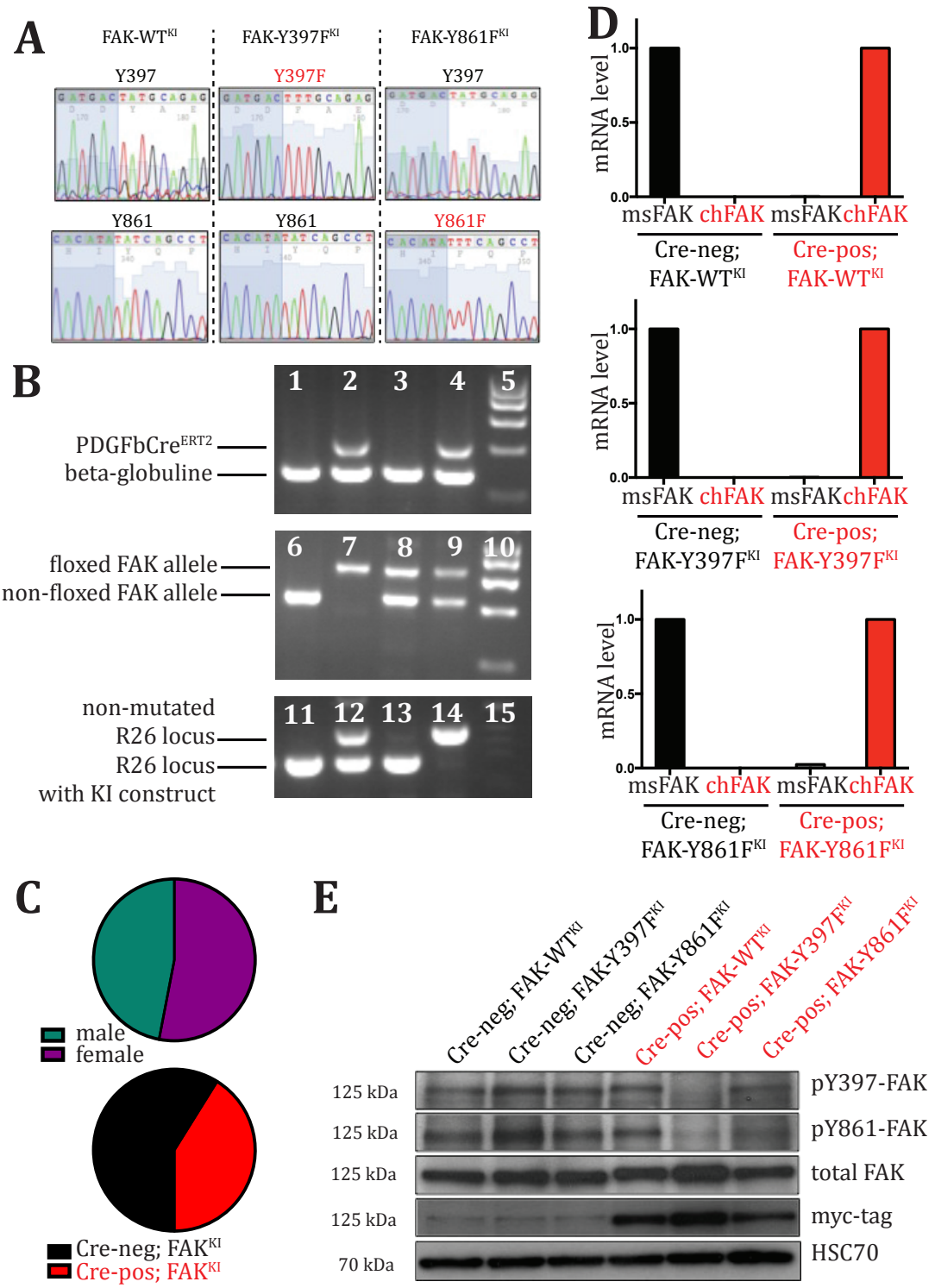

Figure 3.1: Characterisation of the endothelial-specific FAK^{KI} mouse model
Legend on next page

Figure 3.1: Characterisation of the endothelial-specific FAK^{KI} mouse model
(**A**) Mice from all genotypes were earsnipped and DNA was extracted, after protein K digestion. The fragment around amino acid 397 or around amino acid 861 was amplified and sequenced and the sequencing traces for both fragments are presented for the FAK-WT^{KI}, FAK-Y397F^{KI} and FAK-Y861F^{KI} mice. The FAK-WT^{KI} mice have the TAT DNA codon encoding for a tyrosine at position 397 and 861. The FAK-Y397F^{KI} mice have the TTT DNA codon encoding for a phenylalanine at the 397 position and an intact TAT DNA codon encoding for a tyrosine at position 861. The FAK-Y861F^{KI} mice have the TAT DNA codon encoding for a tyrosine at position 397 and a TTT DNA codon encoding for a phenylalanine at position 861. The sequencing traces also confirm that the mice are homozygous for all the cited sites.
(**B**) Mice were earsnipped and genotyping PCR was performed to determine which mice were homozygous for the floxed FAK gene (example lane 7) and for the presence of the KI construct (example lane 11 and 13). Mice were also genotyped for the presence (example lane 2 and 4) or absence (example lane 1 and 3) of the PdgfbCre^{ERT2} and β-globuline was amplified to control for the presence of DNA in the PCR mix (example lanes 1-4). The PCR products were run an agarose gel, photographed under UV light and an example of PCR product bands is shown. Mice homozygous for the floxed FAK gene and homozygous for KI construct, and either Cre-negative or Cre-positive were used for experiments.
(**C**) The ratio between Cre-negative and Cre-positive mice, as well as the ratio between male and female were calculated and found to be close to mendelial expectations, suggesting that the inducible cre activity does not affect development of Cre-positive mice or the male:female ratio.
(**D**) Mouse lung endothelial cells were isolated from mice from all the genotypes and mRNA was extracted from the cell lysates, reverse transcribed and qPCR was performed to determine the amount of mouseFAK (msFAK) mRNA and of chickenFAK (chFAK) in all the cell lines. Results show that msFAK was present in Cre-negative cell lines and absent in Cre-positive cell lines, whereas chFAK was absent in Cre-negative cell lines and present in Cre-positive cell lines.
(**E**) Mouse lung endothelial cells were isolated from mice from all the genotypes and protein lysates were used to determine the total FAK protein, as well as pY397-FAK and pY861-FAK phosphorylations and the myc-tagged chFAK protein. Results show that FAK is phosphorylated at Y397 in all lysates except for the lysate generated using the Cre-pos; FAK-Y397F^{KI} endothelial cells, indicating that FAK is not phosphorylated at this residue when this mutation is present. Similarly FAK is phosphorylated on Y861 in all lysates except for the lysate generated using the Cre-pos; FAK-Y397F^{KI} and Cre-pos; FAK-Y861F^{KI} endothelial cells, suggesting that FAK is not phosphorylated on the mutated Y861F residue; additionally this data indicate that, in baseline conditions, FAK-Y861 phosphorylation is decreased in Cre-pos; FAK-Y397F^{KI} when comparing to Cre-negative controls. In all cell lysates similar levels of total FAK protein are observed, whereas only the Cre-positive cell lines show the presence of the myc-tagged chFAK protein. HSC70 serves as loading control.

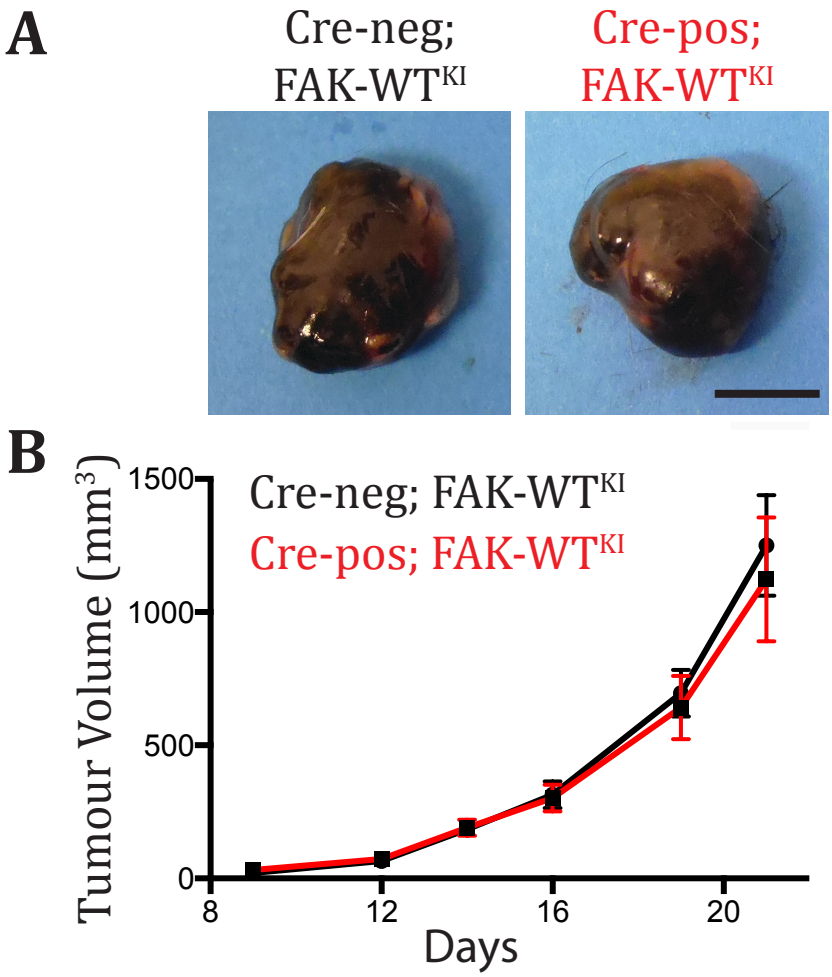

Figure 3.2: Reintroducing a WT version of FAK in endothelial cells does not affect B16F0 tumour growth *in vivo*

Cre-neg; FAK-WT^{KI} and Cre-pos; FAK-WT^{KI} mice were given subcutaneous injections of syngeneic B16F0 melanoma cells, 5-7 days after tamoxifen injection. Tumour dimensions were measured from day 9 to day 21 and tumour volumes calculated (Volume = 0.52 x Length x Width^2). At day 21 tumours were dissected and photographed (**A**). No significant difference in tumour growth was determined between Cre-neg; FAK-WT^{KI} and Cre-pos; FAK-WT^{KI} mice (**B**) indicating that knocking-in a WT version of FAK does not affect B16F0 melanoma tumour growth. Scale bar = 1 cm. n=10-11 mice/genotype.

To determine tumour blood vessel density, endomucin-positive blood vessels were counted across the midline sections of size-matched, age-matched tumours and the number of blood vessels was divided by the area of the tumour section. Results indicate that there is no difference in blood vessel density between the tumours grown in Cre-neg; FAK-WT^{KI} and Cre-pos; FAK-WT^{KI} (**Figure 3.3**). The results suggest that the KO/KI system functions efficiently and that re-introducing the WT version of FAK in endothelial cells rescues the delayed tumour angiogenesis phenotype observed in the EC-FAK^{KO}.

Tumour blood vessels can vary in their functionality and morphology. To examine this I measured changes in blood vessel perimeter (indicative of possible changes in blood flow and vessel maturation); blood vessel leakage (indicative of changes in vessel maturation); perciyte coverage (also indicative of vessel maturation) and tumour hypoxia (a indicator of oxygen delivery into the tumour). Studying these parameters is important as it can indicate which features of the tumour vasculature can be affected by FAK mutations and can also offer a direction regarding the signalling pathways that could be affected by these mutations. Tumour blood vessel perimeter was analysed using Image J software. The perimeter of at least fifty blood vessels per sample was determined. The percentage of vessels that were less than 50μm; 50-100 μm; 100-200 μm or 200 μm or more were calculated and results show that there is no different in tumour blood vessel perimeter between Cre-neg; FAK-WT^{KI} and Cre-pos; FAK-WT^{KI} (**Figure 3.4 A**). In ante-mortem processing tumour burdened mice were injected via the tail vein with anti-PE-PECAM antibody and Hoechst dye (33342). Freshly cut tumour sections were mounted with anti-fade

reagent (without any immunostaining) and the levels of Hoechst leakage assessed by measuring the areas of Hoechst-stained nuclei around PE-PECAM-positive vessels (as detected by the PE-conjugated anti-PECAM-antibody injected in the tail vein 10 minutes before culling the mice and dissecting the tumours). Results showed that the levels of Hoechst leakage were similar in Cre-neg; FAK-WT^{KI} and Cre-pos; FAK-WT^{KI} mice (**Figure 3.4 B**). Blood vessel maturation was measured by counting the numbers of pericyte-positive blood vessels. Tumour sections were double stained for endomucin and NG2 marker of pericytes and the percentage of vessels with associated pericytes was calculated after histological examination. Results showed no significant difference in blood vessel pericyte coverage between the Cre-neg; FAK-WT^{KI} and Cre-pos; FAK-WT^{KI} mice (**Figure 3.4 C**). In order to determine if knocking-in a WT version of FAK in endothelial cells affects tumour hypoxia, pimonidazole was injected in tumour bearing mice one hour prior to sacrifice and tumour sections were analysed for areas of tumour hypoxia. No difference in the percentage of hypoxic tumour area between Cre-neg; FAK-WT^{KI} and Cre-pos; FAK-WT^{KI} was apparent (**Figure 3.4 D**).

Lastly, to confirm the tumour growth results in a second tumour type, Lewis Lung Carcinoma (LLC) cells were injected subcutaneously in Cre-neg; FAK-WT^{KI} and Cre-pos; FAK-WT^{KI} mice, one week after tamoxifen administration. As for the B16F0 tumour growth, LLC tumour growth was the same between Cre-neg; FAK -WT^{KI} and Cre-pos; FAK-WT^{KI} (**Figure 3.5**) thus providing further validation that the KO/KI system is working.

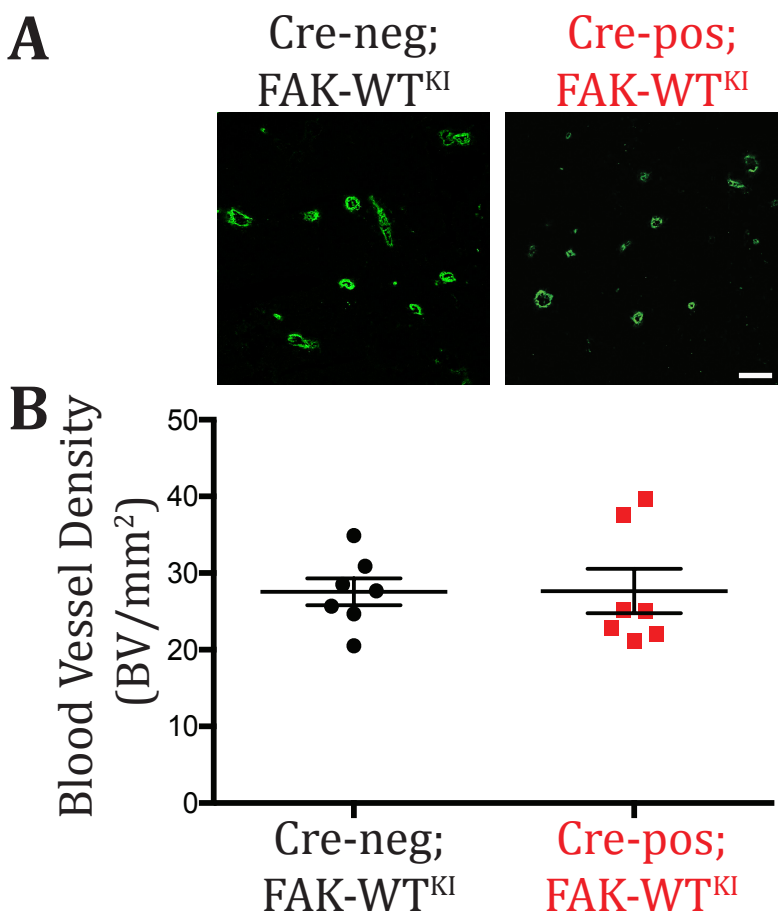

Figure 3.3: Reintroducing a WT version of FAK in endothelial cells does not affect B16F0 tumour angiogenesis *in vivo*

Cre-neg; FAK-WT^{KI} and Cre-pos; FAK-WT^{KI} mice were given subcutaneous injections of syngeneic B16F0 melanoma cells after tamoxifen treatment. Tumour blood vessel density was calculated by counting all the endomucin-positive blood vessels across the entire midline tumour section from size-matched tumours. Representative pictures of endomucin stained blood vessels and blood vessel density quantification are shown in (**A**) and (**B**) respectively. No difference in B16F0 tumour blood vessel density was observed between Cre-neg; FAK-WT^{KI} and Cre-pos; FAK-WT^{KI} mice, suggesting that knocking-in a WT version of FAK does not affect B16F0 tumour angiogenesis. Scale bar = 100 µm. n=7 mice/genotype.

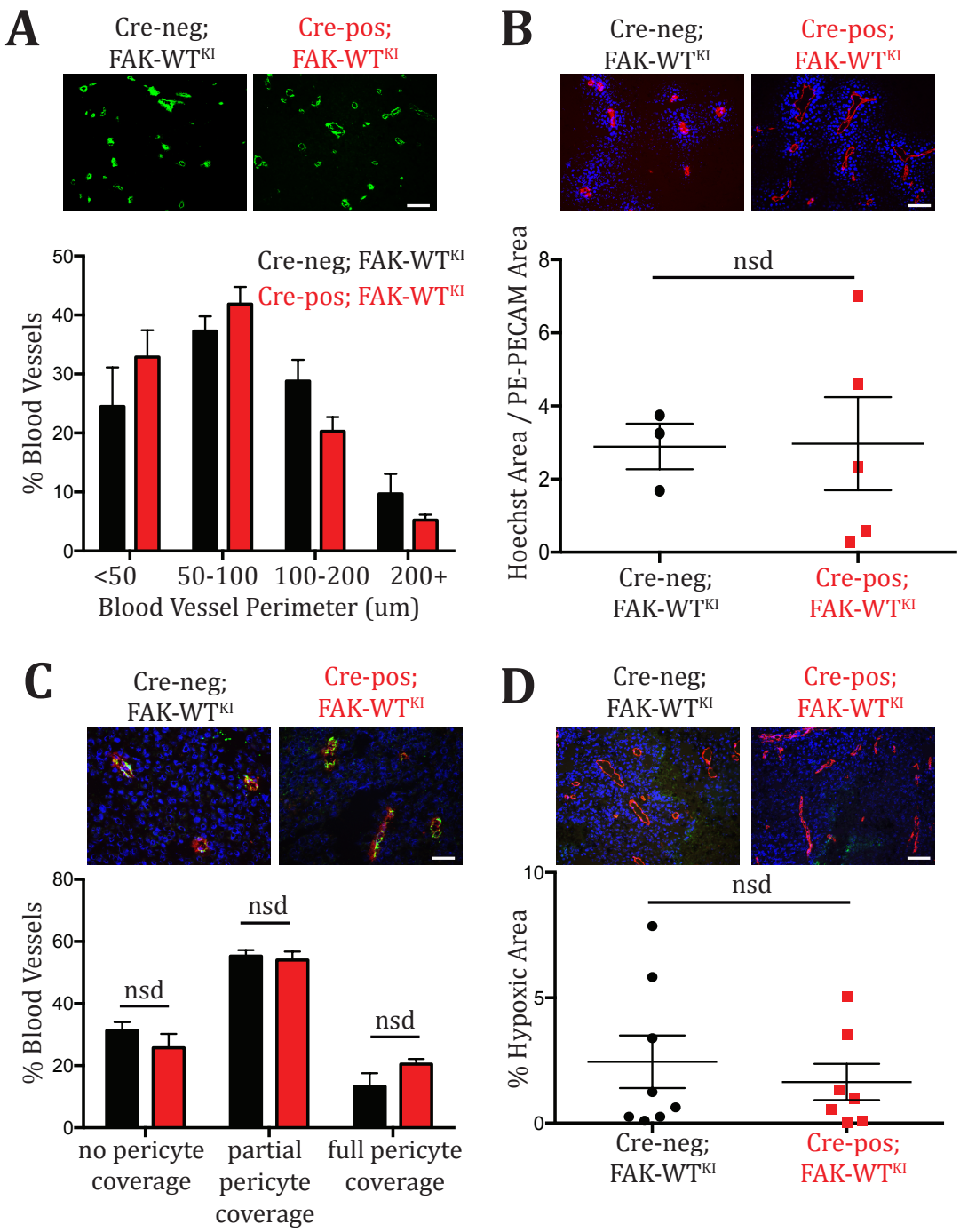

Figure 3.4: Reintroducing a WT version of FAK in endothelial cells does not affect B16F0 tumour endothelium or tumour hypoxia *in vivo*

Legend on next page.

Figure 3.4: Reintroducing a WT version of FAK in endothelial cells does not affect B16F0 tumour endothelium or tumour hypoxia *in vivo*

(**A**) Endomucin-stained tumour sections were photographed at the Axioplan microscope and representative pictures show blood vessels stained in green. The perimeter of at least fifty blood vessels per sample was measured using the Image J software. The percentage of blood vessels that were less than 50mm; 50-100 mm; 100-200 mm or 200 mm or more was determined for Cre-neg; FAK-WT^{KI} and Cre-pos; FAK-WT^{KI} samples and no significant difference was observed between the two genotypes. Scale bar = 300 μm.

(**B**) Cre-neg; FAK-WT^{KI} and Cre-pos; FAK-WT^{KI} mice bearing 21-day-old B16F0 subcutaneous tumours, were given tail vein injections of anti-PE-PECAM antibody and Hoechst. Midline tumour sections were mounted from size-matched tumours (without any immunofluorescence staining). Representative pictures show Hoechst signal in blue and PE-PECAM signal in red. The area of Hoechst/area of PE-PECAM ratio indicates that re-introducing a WT version of FAK does not affect Hoechst Leakage.

(**C**) Endomucin- and NG2-double stained tumour sections were photographed at the Axioplan microscope and representative pictures show endomucin-stained endothelial cells in red and NG2-stained perycites in green. The percentage of naked blood vessels (no pericyte coverage) and the percentage of blood vessels partially or completely covered by pericytes was calculated and shows that there is no difference in pericyte coverage between the two genotypes.

(**D**) B16F0 tumour-burdened Cre-neg; FAK-WT^{KI} and Cre-pos; FAK-WT^{KI} mice were given tail vein injections of Pimonidazole probe. FITC-anti-Pimonidazole antibody was used to detect hypoxic regions (in green) and blood vessels are detected by endomucin staining (in red). Pictures taken at the Axioplan were quantified and the percentage of hypoxic area was determined by dividing the Pimonidazole stained area by the total field area. These data indicate that reintroducing a WT version of FAK does not affect B16F0 tumour hypoxia levels.

Scale bar = 100 μm. Values are given as means + s.e.m. n=3-9 mice/genotype.

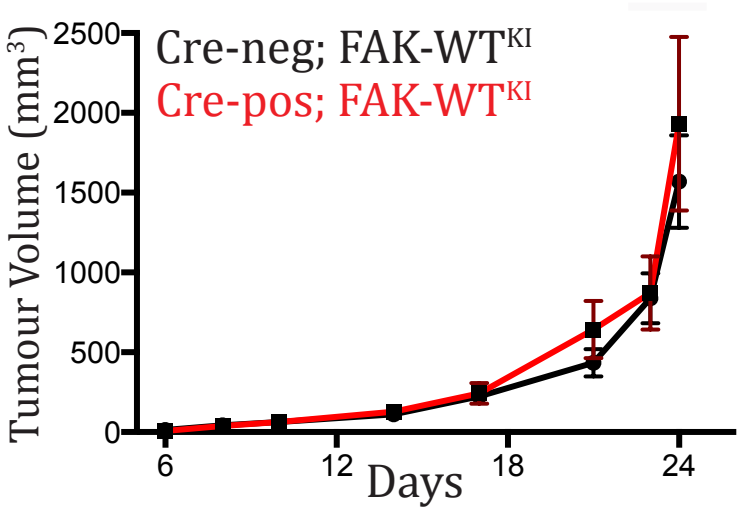

Figure 3.5: Reintroducing a WT version of FAK in endothelial cells does not affect LLC tumour growth *in vivo*

Cre-neg; FAK-WT^{KI} and Cre-pos; FAK-WT^{KI} mice were given subcutaneous injections of syngeneic LLC carcinoma cells, 5-7 days after tamoxifen injection. Tumour dimensions were measured from day 6 to day 24 and tumour volumes calculated (Volume = 0.52 x Length x Width^2). No significant difference in LLC tumour growth was determined between Cre-neg; FAK-WT^{KI} and Cre-pos; FAK-WT^{KI} mice indicating that knocking-in a WT version of FAK does not affect LLC carcinoma tumour growth. n=6-12 mice/genotype.

1.3. Endothelial-specific FAK-Y397F mutation is sufficient to reduce B16F0 and CMT19T tumour growth, but not LLC tumour growth

A week after tamoxifen administration, Cre-neg; FAK-Y397F^{KI} and Cre-pos; FAK-Y397F^{KI} mice were injected subcutaneously with B16F0 melanoma cells and tumour volumes were determined over time. Results showed that B16F0 tumour growth was significantly inhibited in Cre-pos; FAK-Y397F^{KI} mice when compared with Cre-neg; FAK-Y397F^{KI} mice (**Figure 3.6**). Results shown in **Figure 3.6** are representative of four independent repeats[1] shown in **Appendix I Figure A3.2**.

To determine if the observed tumour growth delay was accompanied by a reduction in tumour angiogenesis, blood vessel density was calculated for two of the experimental repeats. **Figure 3.7 A** shows representative pictures of endomucin stained blood vessels from size-matched tumours grown in Cre-neg; FAK-Y397F^{KI} and Cre-pos; FAK-Y397F^{KI} mice. Blood vessel quantification indicates that there is a significant decrease in tumour angiogenesis in tumours grown in Cre-pos; FAK-Y397F^{KI} mice when compared to tumours grown in Cre-neg; FAK-Y397F^{KI} mice (**Figure 3.7 B**). This result indicated that the endothelial

[1] It can be challenging to perform three different ante-mortem procedures at the end of a tumour growth experiment containing up to 15 mice per group, therefore at least two experimental repeats were necessary. Later on, concerns were raised about the length of the tumour growth experiment and the impact that this could have on the statistical outcome, therefore the tumour growth experiment was stopped at Day 15, Day 17 and Day 21. Noteworthy is that tumour growth is impaired in Cre-pos; FAK-Y397F^{KI} mice when compared with Cre-neg; FAK-Y397F^{KI} mice independently of the length of the experiment. Further concerns were raised regarding performing the tumour growth experiments independently for each KI colony, therefore a tumour growth experiment with mice from the three KI colonies (WT-KI, FAK-Y397F KI and FAK-Y861F KI) was performed. Noteworthy is that the same results as previously were obtained for each KI.

specific inactivation of FAK-Y397F phosphorylation is sufficient to decrease tumour angiogenesis. **Appendix I Figure S3.3** shows data from the second experimental repeat and confirms the delayed tumour angiogenesis.

In order to determine if delayed tumour growth is a consequence of delayed tumour angiogenesis, B16F0 tumour cells were injected subcutaneously in Cre-neg; FAK-Y397F^{KI} and Cre-pos; FAK-Y397F^{KI} mice, a week after tamoxifen administration and allowed to grow until Day 8. Tumours were dissected at this early time point and blood vessel density was determined. Representative pictures are shown in **Figure 3.7** C and results indicate that tumour angiogenesis is decreased in tumours grown in Cre-pos; FAK-Y397F^{KI} mice when compared to Cre-neg; FAK-Y397F^{KI} mice and suggest that a defect in tumour angiogenesis is present before a delay in tumour growth is observed (**Figure 3.7 D**). Overall this data indicates that impaired tumour growth might be a consequence of delayed angiogenesis.

Although blood vessel density was reduced in B16F0 tumours grown in Cre-pos; FAK-Y397F^{KI} mice when compared with Cre-neg; FAK-Y397F^{KI} mice, no differences in tumour blood vessel perfusion in 8-day old (**Figure 3.8 A**) and in 15-day old B16F0 tumours (**Figure 3.8 B**) was observed, indicating that endothelial FAK-Y397F mutation does not affect tumour blood vessel perfusion. Tumour blood vessel perimeter (**Figure 3.8 C**)**,** Hoechst leakage (**Figure 3.8 D**) or pericyte coverage (**Figure 3.8 E**) was also analysed and no difference was observed between genotypes. Lastly, the reduced number of blood vessels in Cre-pos; FAK-Y397F^{KI} mice was associated with a significant increase in tumour hypoxia (**Figure 3.8 F**). Tumour hypoxia result is representative of two

independent experiments and the second repeat is shown in **Appendix I Figure A3.4**.

In short, the results indicate that the mutation in EC-FAK-Y397F is sufficient to delay B16F0 subcutaneous tumour growth and tumour angiogenesis but does not affect other parameters of blood vessels. Nevertheless, FAK-Y397F mutation in endothelial cells specifically increases tumour hypoxia, presumably as a consequence of decreased blood vessel density.

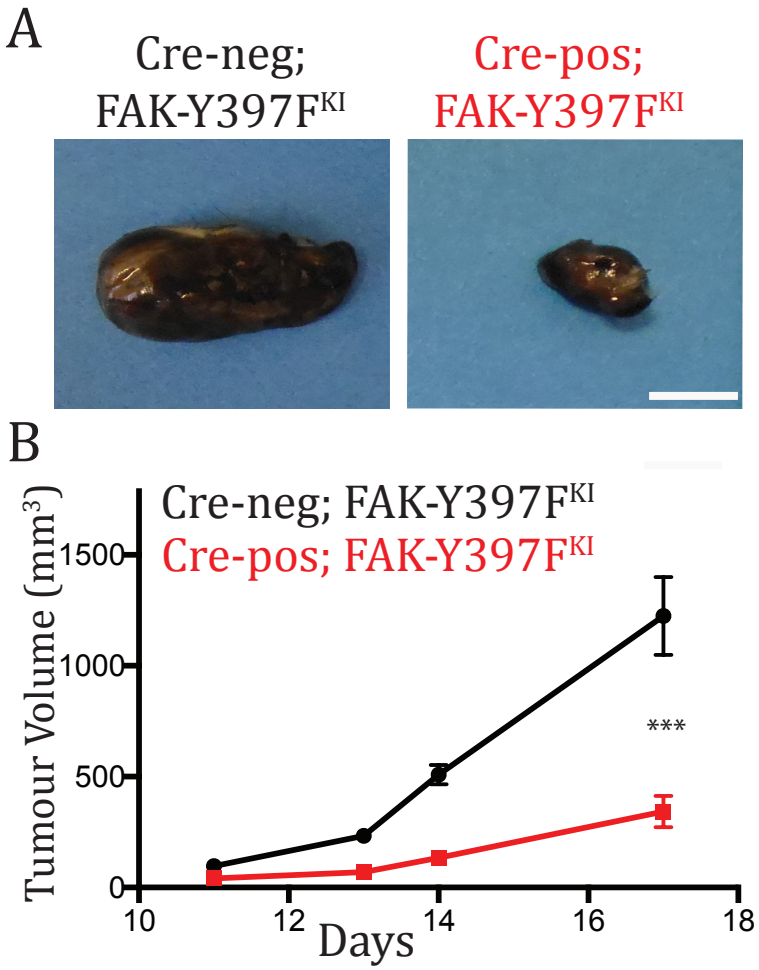

Figure 3.6: Endothelial-specific inactivation of FAK-Y397 phosphorylation inhibits B16F0 tumour growth.

Cre-neg; FAK-Y397F^{KI} and Cre-pos; FAK-Y397F^{KI} mice were given subcutaneous injections of syngeneic B16F0 melanoma cells, 5-7 days after tamoxifen injection. Tumour dimensions were measured from day 11 to day 17 and tumour volumes calculated (Volume = 0.52 x Length x Width^2). At day 17 tumours were dissected and photographed (**A**). Tumour growth was significantly retarded in Cre-pos; FAK-Y397F^{KI} mice when compared to Cre-neg; FAK-Y397F^{KI} (**B**) indicating that the endothelial-specific FAK-Y397 phosphorylation is required for B16F0 tumour growth. Scale bar = 1 cm. *** P<0.005. n=6-9 mice/genotype.

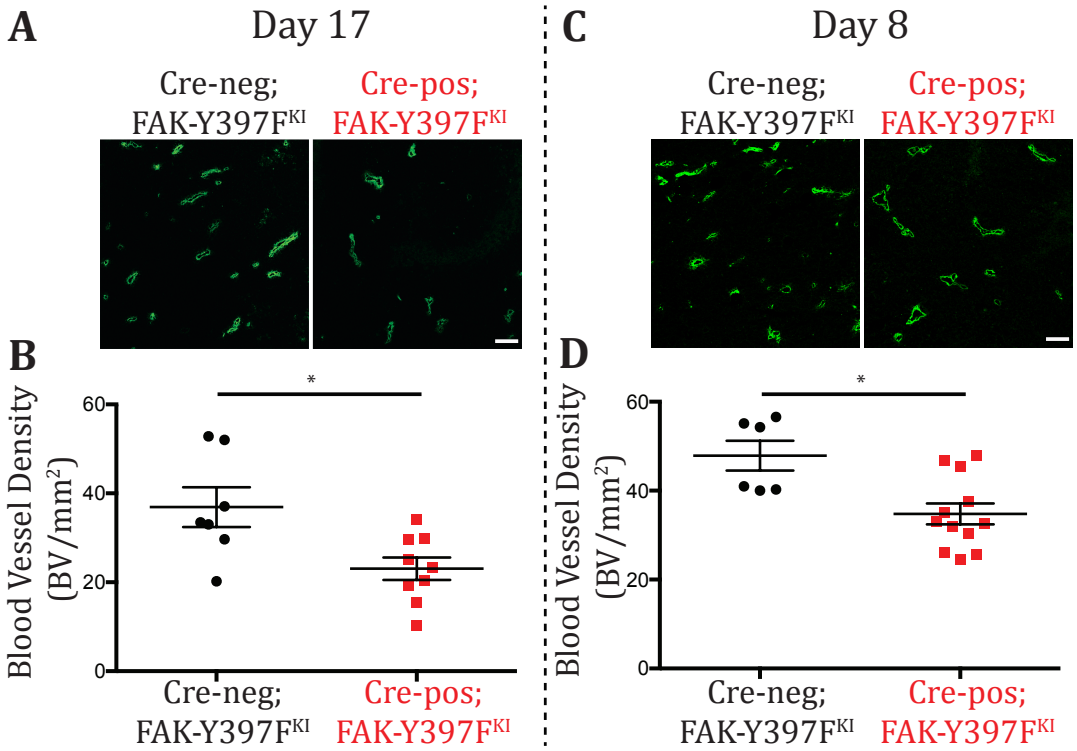

Figure 3.7: Endothelial-specific inactivation of FAK-Y397 phosphorylation is sufficient to reduce B16F0 tumour angiogenesis *in vivo*

B16F0 tumour blood vessel density was calculated by counting all the endomucin-positive blood vessels across the entire midline tumour section from size-matched 17-day-old or 8-day-old tumours. Representative images of endomucin-stained blood vessels from 17-day-old tumours from both genotypes are shown (**A**) and the quantified data indicated that FAK-Y397F mutation in endothelial cells delays B16F0 tumour angiogenesis (**B**). To determine if the delay in angiogenesis occurs before the difference in tumour volumes is observed, blood vessel density was quantified in 8-day-old B16F0 tumours. Representative images and quantification are shown in (**C**) and (**D**) respectively and indicate that endothelial-specific FAK-Y397F mutation impairs angiogenesis before its effect can be observed on tumour volumes. Scale bar = 100 µm. Values are given as means + s.e.m. * $P<0.05$. n=7-12 mice/genotype.

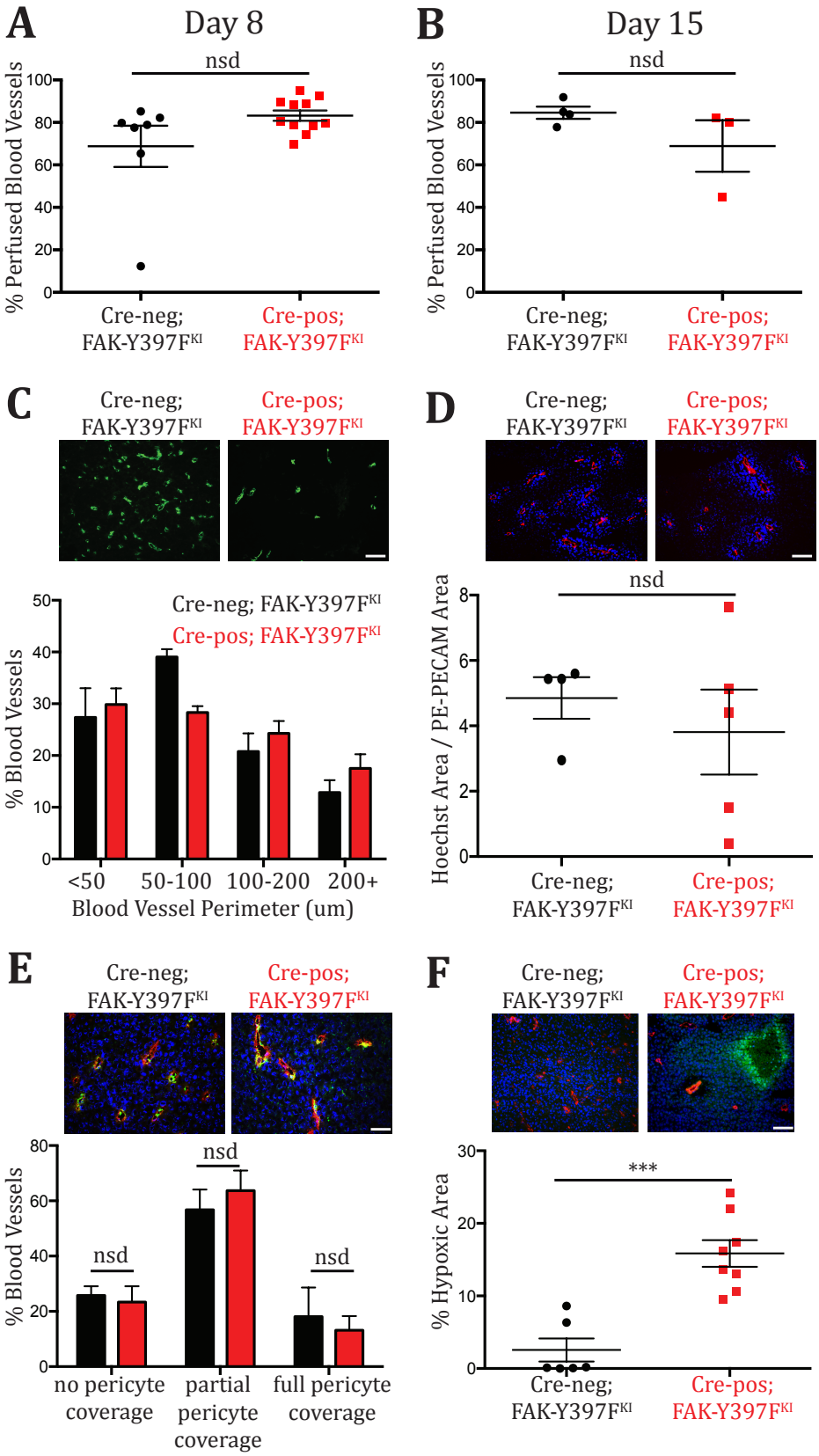

Figure 3.8: Endothelial-specific inactivation of FAK-Y397 phosphorylation does not affect B16F0 tumour endothelium, but affects tumour hypoxia *in vivo*

Legend on next page.

Figure 3.8: Endothelial-specific inactivation of FAK-Y397 phosphorylation does not affect B16F0 tumour endothelium, but affects tumour hypoxia *in vivo*

Cre-neg; FAK-Y397F^{KI} and Cre-pos; FAK-Y397F^{KI} mice bearing 7-day old B16F0 tumours (**A**) or 15-day-old B16F0 tumours (**B**) were given anti-PE-PECAM antibody injection into the tail vein ten minutes prior to sacrifice. Midline B16F0 tumour sections from size-matched tumours were stained for endomucin. The total number of PE-PECAM-antibody perfused tumour blood vessels was counted across the midline section from size-matched tumours. The percentage of perfused vessels was calculated by dividing the number of PE-PECAM-antibody perfused tumour blood vessels/ total number of tumour blood vessels. Statistical analysis indicates that the endothelial specific FAK-Y397F mutation does not affect tumour blood vessel perfusion.

(**C**) Endomucin-stained tumour sections were photographed at the Axioplan microscope and the perimeter of at least fifty blood vessels (stained in green) per sample was measured using the Image J software. The percentage of blood vessels that were less than 50mm; 50-100 mm; 100-200 mm or 200 mm or more was determined for Cre-neg; FAK-Y397F^{KI} and Cre-pos; FAK-Y397F^{KI} samples and no significant difference was observed between the two genotypes. Scale bar= 300μm.

(**D**) Cre-neg; FAK-Y397F^{KI} and Cre-pos; FAK-Y397F^{KI} mice bearing 21-day-old B16F0 subcutaneous tumours, were given tail vein injections of anti-PE-PECAM antibody (red signal) and Hoechst (blue signal). Midline tumour sections were mounted from size-matched tumours (without any immunofluorescence staining). Representative pictures and area of Hoechst/area of PE-PECAM ratio is shown and statistical analysis indicates that introducing FAK-Y397F mutation in the endothelium does not affect Hoechst Leakage. Scale bar = 100μm.

(**E**) Endomucin- and NG2-double stained tumour sections were photographed at the Axioplan microscope and the percentage of naked blood vessels (no pericyte coverage) and the percentage of blood vessels partially or completely covered by pericytes was calculated and results show that there is no difference in pericyte coverage between the two genotypes. Endomucin-stained endothelial cells are shown in red, whereas NG2-stained perycites are shown in green. Scale bar = 100μm.

(**F**) B16F0 tumour-burdened Cre-neg; FAK-Y397F^{KI} and Cre-pos; FAK-Y397F^{KI} were given intraperitoneal injections of Pimonidazole probe. FITC-anti-Pimonidazole antibody was used to detect hypoxic regions (shown in green). Endomucin-positive endothelial cells are shown in red. Pictures taken at the Axioplan were quantified and the percentage of hypoxic area was determined by dividing the Pimonidazole stained area by the total field area. This data indicate that endothelial specific inactivation of FAK-Y397 phosphorylation leads to an increase in tumour hypoxia. Scale bar = 100μm.

Values are given as means + s.e.m. n=3-11mice/genotype.

CMT19T carcinoma cells were used as a second subcutaneous tumour model and were injected in Cre-neg; FAK-Y397F^{KI} and Cre-pos; FAK-Y397F^{KI} mice a week after tamoxifen administration. The results were similar to those of the B16F0 tumours grown in Cre-neg; FAK-Y397F^{KI} and Cre-pos; FAK-Y397F^{KI} mice. CMT19T tumour volumes were measured over time and a significant difference was seen starting from Day 15 (**Figure 3.9**). At Day 24 the tumours grown in Cre-pos; FAK-Y397F^{KI} mice were significantly smaller than the tumours grown in the Cre-neg; FAK-Y397F^{KI} mice, indicating that endothelial specific inactivation of FAK-Y397 phosphorylation is sufficient to reduce CMT19T tumour growth. At Day 24 a large proportion of Cre negative mice developed tumours at the legal limit and had to be culled. The remaining tumours were dissected at the experimental endpoint (Day 28) and statistical analysis returned a p value of p=0.050 for the remaining set of data.

Size-matched tumours from Day 28 were used to quantify tumour angiogenesis. **Figure 3.10** A shows representative pictures of blood vessels stained for endomucin in green. Blood vessel density was significantly reduced in CMT19T tumours grown in Cre-pos; FAK-Y397F^{KI} mice (**Figure 3.10 B**) when compared to Cre-neg; FAK-Y397F^{KI} controls.[1]

Overall the CMT19T carcinoma model recapitulates the B16F0 melanoma model findings, as for both tumour types, endothelial specific inactivation of FAK-Y397 phosphorylation leads to delayed tumour growth and delayed angiogenesis.

[1] Paraskevi Natalia Georgiou, B.Sc student, whom I supervised, quantified blood vessel density for CMT19T tumour model.

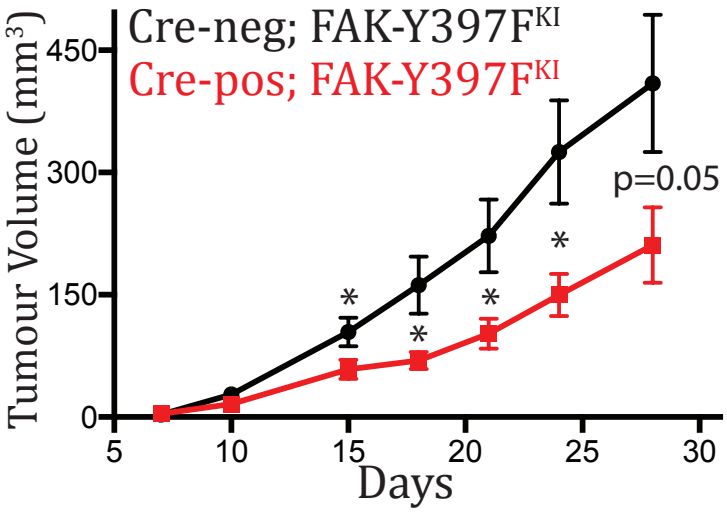

Figure 3.9: Endothelial-specific inactivation of FAK-Y397 phosphorylation inhibits CMT19T carcinoma tumour growth.

Cre-neg; FAK-Y397F^{KI} and Cre-pos; FAK-Y397F^{KI} mice were given subcutaneous injections of syngeneic CMT19T carcinoma cells, 5-7 days after tamoxifen injection. Tumour dimensions were measured from day 7 to day 28 and tumour volumes calculated (Volume = 0.52 x Length x Width^2). Tumour growth was significantly retarded in Cre-pos; FAK-Y397F^{KI} mice when compared to Cre-neg; FAK-Y397F^{KI} indicating that the endothelial-specific FAK-Y397 phosphorylation is required for CMT19T carcinoma tumour growth. * P<0.05. n=8-9 mice/genotype.

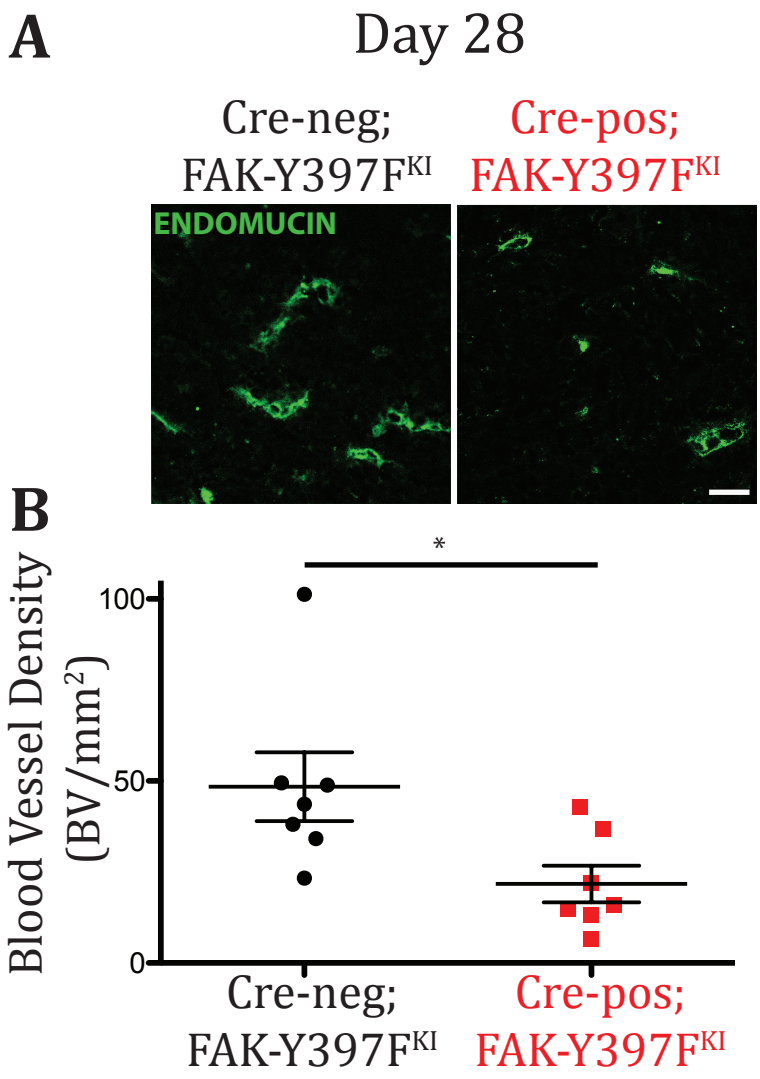

Figure 3.10: Endothelial-specific inactivation of FAK-Y397 phosphorylation is sufficient to reduce CMT19T carcinoma tumour angiogenesis *in vivo*

Cre-neg; FAK-Y397F^{KI} and Cre-pos; FAK-Y397F^{KI} mice were given subcutaneous injections of syngeneic CMT19T carcinoma cells after tamoxifen treatment. Tumour blood vessel density was calculated by counting all the endomucin-positive blood vessels across the entire midline tumour section from size-matched tumours. Representative pictures of endomucin stained blood vessels and blood vessel density quantification are shown in (**A**) and (**B**) respectively. The quantified data indicate that FAK-Y397F mutation in endothelial cells delays CMT19T tumour angiogenesis. Scale bar = 100 μm. * P<0.05. n=7 mice/genotype.

As a third subcutaneous model, LLC carcinoma cells were injected in Cre-neg; FAK-Y397F^{KI} and Cre-pos; FAK-Y397F^{KI} mice a week after tamoxifen administration. Tumour volumes were measured across time and are presented in **Figure 3.11**. In contrast to the B16F0 or CMT19T, these results indicate that there is no difference in LLC tumour growth between Cre-neg; FAK-Y397F^{KI} and Cre-pos; FAK-Y397F^{KI}, suggesting that the endothelial specific FAK-Y397F mutation does not affect LLC tumour growth. However, in line with my previous results with B16F0 and CMT19T, blood vessel density in LLC tumours was decreased significantly in Cre-pos; FAK-Y397F^{KI} mice (**Figure 3.12**).[1] Thus, these results indicate that endothelial specific inactivation of FAK-Y397 phosphorylation is sufficient to decrease LLC tumour angiogenesis, without affecting LLC tumour growth. Noteworthy, blood vessel perfusion was not affected by the endothelial specific FAK-Y397F mutation, indicating that this mutation leads to delayed angiogenesis without affecting the ability of the blood vessels that form to be perfused (**Figure 3.13**).[1]

[1] Paraskevi Natalia Georgiou, B.Sc student, whom I supervised, quantified blood vessel density and perfusion parameters for LLC tumour model.

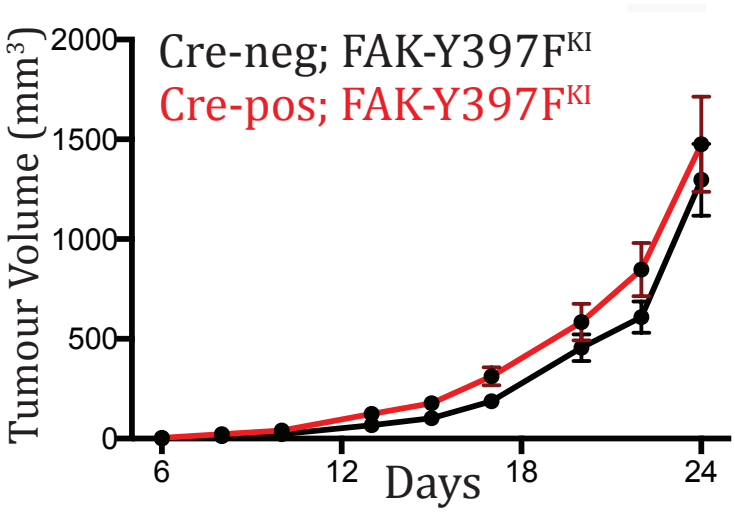

Figure 3.11: Endothelial-specific inactivation of FAK-Y397 phosphorylation does not affect LLC tumour growth in spite of impairing tumour angiogenesis *in vivo*

Cre-neg; FAK-Y397F^{KI} and Cre-pos; FAK-Y397F^{KI} mice were given subcutaneous injections of syngeneic LLC carcinoma cells, 5-7 days after tamoxifen injection. Tumour dimensions were measured from day 6 to day 24 and tumour volumes calculated (Volume = 0.52 x Length x Width^2). No significant difference in LLC tumour growth was determined between Cre-neg; FAK-Y397F^{KI} and Cre-pos; FAK-Y397F^{KI} mice. n=8-14 mice/genotype.

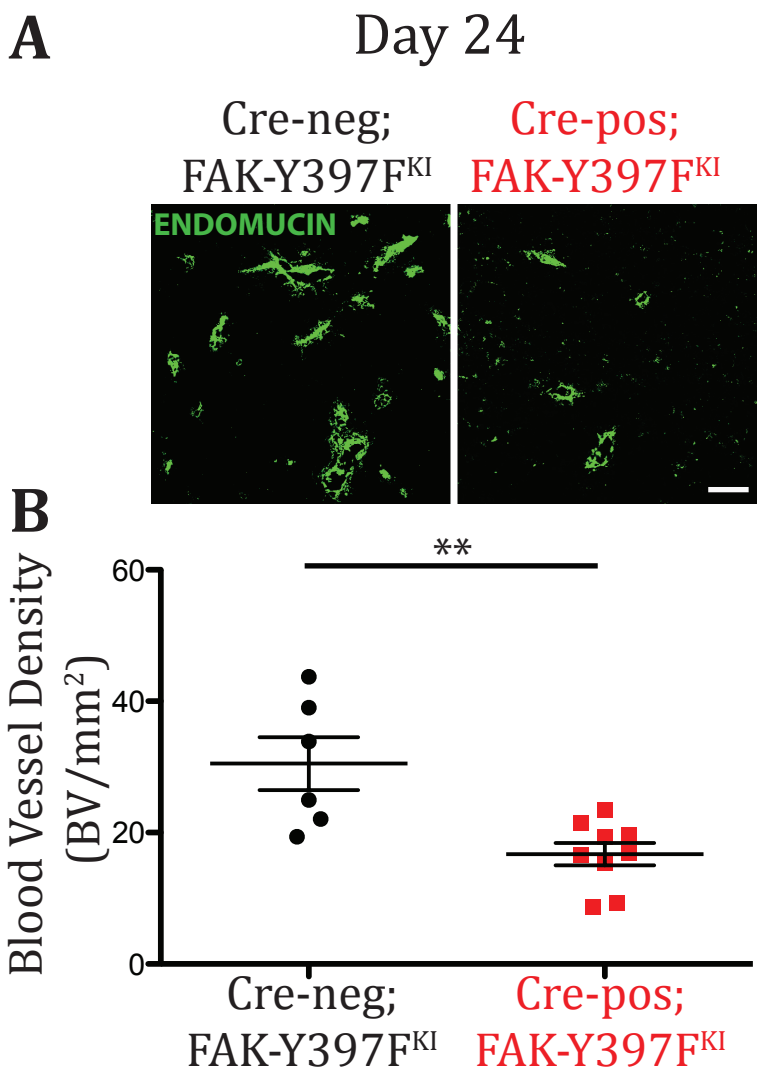

Figure 3.12: Endothelial-specific inactivation of FAK-Y397 phosphorylation leads to a decrease LLC tumour angiogenesis *in vivo*

Cre-neg; FAK-Y397F^{KI} and Cre-pos; FAK-Y397F^{KI} mice were given subcutaneous injections of syngeneic LLC carcinoma cells, 5-7 days after tamoxifen injection. Tumours were grown for 24 days and then dissected. Tumour sections were cut, stained for endomucin (**A**) and endomucin-positive blood vessels were counted across the midline section of LLC size matched tumours to the blood vessel density (**B**). Statistical analysis shows that endothelial-specific FAK-Y397F mutation impairs tumour angiogenesis. Scale bar = 100 µm. ** P<0.001. n=6-9 mice/genotype.

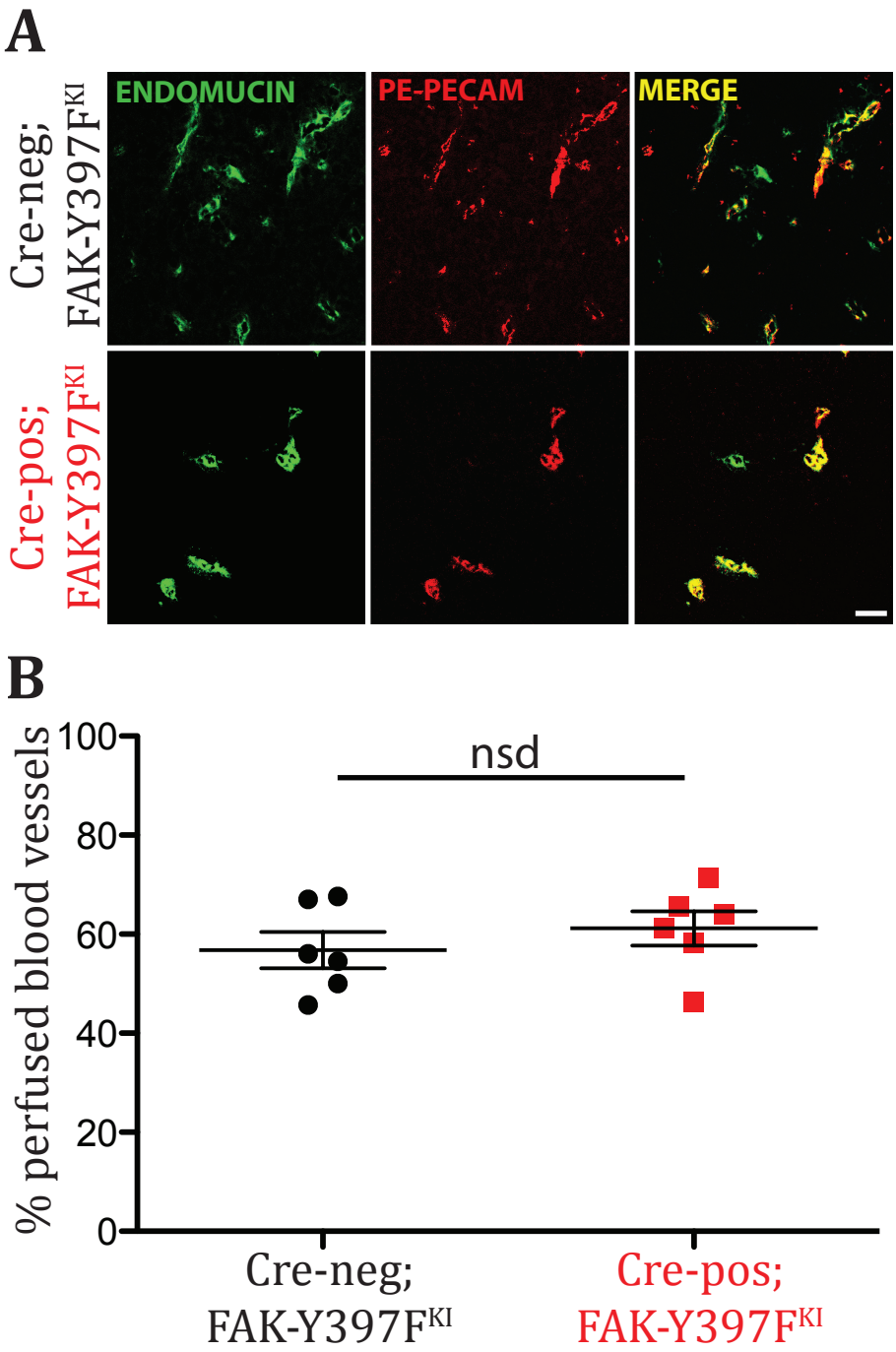

Figure 3.13: Endothelial-specific inactivation of FAK-Y397 phosphorylation does not affect blood vessel perfusion in LLC tumours *in vivo*

LLC tumour bearing Cre-neg; FAK-Y397F^{KI} and Cre-pos; FAK-Y397F^{KI} mice, were injected with anti-PE-PECAM antibody into the tail vein ten minutes prior to sacrifice. Midline LLC tumour sections from size-matched tumours were stained for endomucin and representative pictures were taken at the Confocal microscope. Blood vessels (in green), PE-PECAM-antibody perfused blood vessels (in red) and their merge from Cre-neg; FAK-Y397F^{KI} and Cre-pos; FAK-Y397F^{KI} samples are shown (**A**). The percentage of perfused vessels was calculated by dividing the number of PE-PECAM-antibody perfused tumour blood vessels/ total number of tumour blood vessels (**B**). Quantification indicates that the endothelial specific FAK-Y397F mutation does not affect tumour blood vessel perfusion. Scale bar = 100 µm. n=6 mice/genotype.

1.4. Effect of endothelial-specific FAK-Y861F mutation on tumour growth and tumour angiogenesis

To determine if endothelial specific FAK-Y861F mutation affects tumour growth and angiogenesis, Cre-neg; FAK-Y861F^{KI} and Cre-pos; FAK-Y861F^{KI} mice were used and B16F0, CMT19T or LLC tumours were grown subcutaneously after the mutation was induced.

B16F0 tumours were grown in Cre-neg; FAK-Y861F^{KI} and Cre-pos; FAK-Y861F^{KI} until Day 17 and results are presented in **Figure 3.14** A. These data indicate that endothelial-specific FAK-Y861F mutation does not affect B16F0 tumour growth. These results are representative of two independent experimental repeats and the second repeat is shown in **Appendix I Figure A 3.5**. Dissected B16F0 tumours from Cre-neg; FAK-Y861F^{KI} and Cre-pos; FAK-Y861F^{KI} were photographed and are shown in **Figure 3.14** B. As there seemed to be a tendency for the Cre-pos; FAK-Y861F^{KI} tumours in being smaller that the controls, the tumour growth experiment was repeated again and tumours were allowed to grow for a longer period – until Day 21 (**Figure 3.14 C**). In spite of the persistent tendency in Cre-pos; FAK-Y861F^{KI} tumours in being smaller, the difference in tumour volume was never significant, confirming that endothelial specific FAK-Y861 phosphorylation is dispensable for B16F0 tumour growth.

Blood vessel density was analysed in the B16F0 tumours after 17 days of subcutaneous growth (**Figure 3.15 A**). Tumour sections were stained for endomucin and representative pictures are shown in **Figure 3.15** B. Blood

vessel density quantification indicates that the endothelial specific FAK-Y861F mutation is able to impair angiogenesis in 17-day old B16F0 tumours.

Blood vessel density was also analysed at an early time point in tumour growth (Day 7) and Cre-pos; FAK-Y861F^{KI} tumours presented with significantly reduced blood vessel density when compared to Cre-neg; FAK-Y861F^{KI} (**Figure 3.15 C**). This result indicates that tumour angiogenesis is affected by the endothelial specific FAK-Y861F mutation as early as Day 7 post B16F0 tumour cell inoculation. Surprisingly when this parameter was analysed in 21-day old B16F0 tumours, no delay in tumour angiogenesis was observed between the two genotypes (**Figure 3.15 D**). This data highlights the possibility that FAK-Y861F mutated endothelium is able to compensate the initially observed angiogenesis impairment.

Overall these results suggest that the endothelial specific inactivation of FAK-Y861 phosphorylation reduces tumour angiogenesis at least until Day 17 post tumour cell inoculation, but does not affect tumour growth.

Tumour blood vessel perfusion was determined in 7-day old (**Figure 3.16 A**) and in 17-day old B16F0 tumours (**Figure 3.16 B**) and results show that endothelial FAK-Y861F mutation does not affect tumour blood vessel perfusion. Blood vessels in B16F0 tumours were assessed for blood vessel perimeter measurements (**Figure 3.16 C**), Hoechst leakage (**Figure 3.16 D**) and pericyte coverage (**Figure 3.16 E**). No significant differences between genotypes were observed. Lastly, analysis of tumour hypoxia also showed no significant differences in B16F0 tumours grown in Cre-pos; FAK-Y861F^{KI} mice when compared with Cre-neg; FAK-Y861F^{KI} controls (**Figure 3.16 F**). This result is particularly intriguing since blood vessel density is decreased in these

tumours, but this does not seem to impact the levels of hypoxia, as measured by the pimonidazole probe.

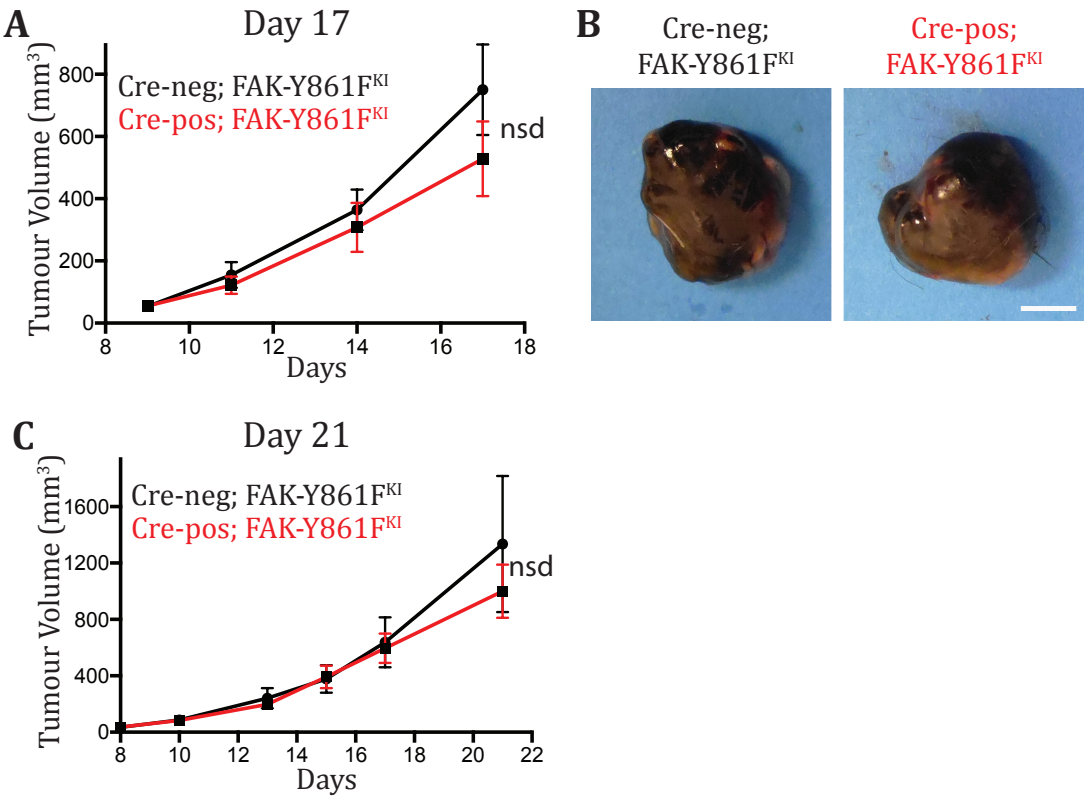

Figure 3.14: Endothelial-specific inactivation of FAK-Y861 phosphorylation does not affect B16F0 tumour growth *in vivo*

Cre-neg; FAK-Y861F^{KI} and Cre-pos; FAK-Y861F^{KI} mice were subcutaneously injected with syngeneic B16F0 melanoma cells, 5-7 days after tamoxifen administration. Tumour size was measured from day 8 to day 17 and tumour volumes calculated (Volume = 0.52 x Length x Width^2). At day 17, tumours were dissected and photographed (**A**). The endothelial-specific FAK-Y861F mutation does not impair tumour growth, as no significant difference was observed between Cre-neg; FAK-Y861F^{KI} and Cre-pos; FAK-Y861F^{KI} mice at day 17 (**B**). When tumours were let to grow until at day 21 there was still no significant difference between the genotypes (**C**). Scale bar = 1 cm. n=8-15 mice/genotype.

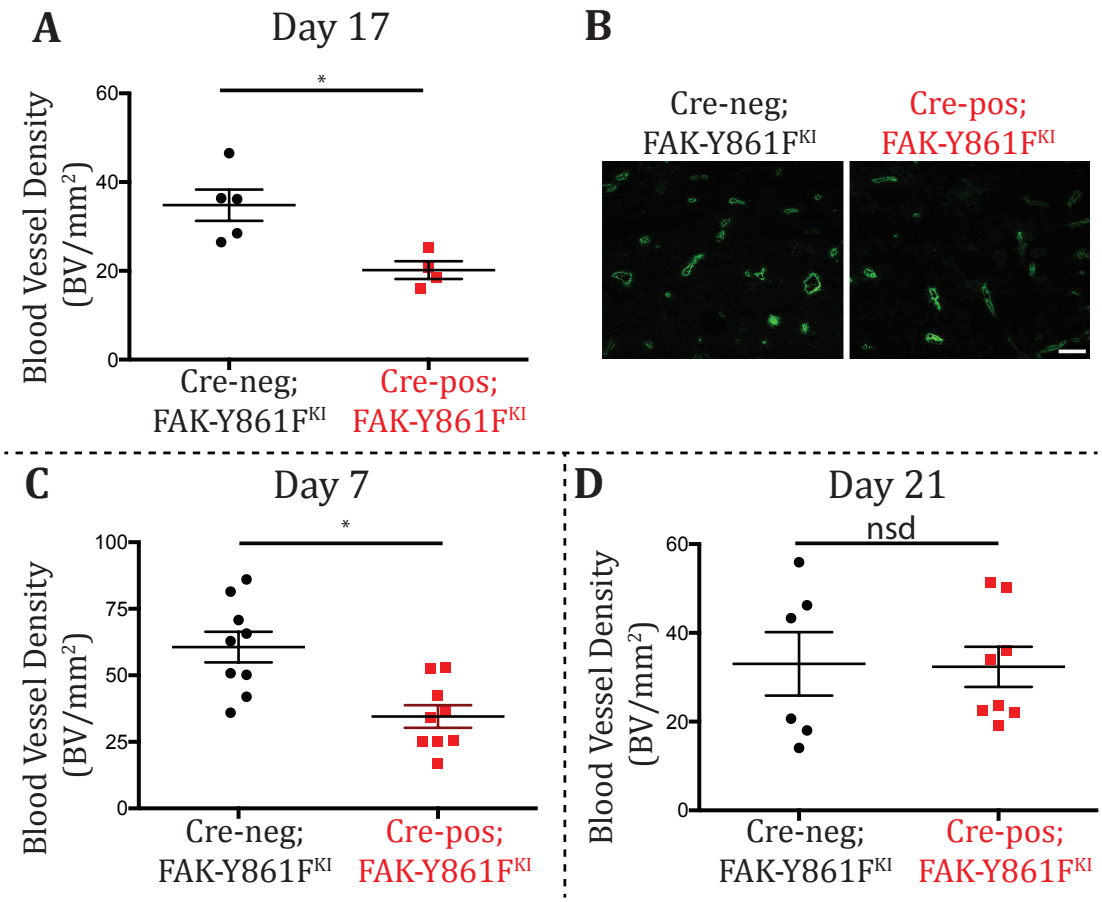

Figure 3.15: Endothelial-specific inactivation of FAK-Y861 phosphorylation decreases B16F0 tumour angiogenesis in the early stages of tumour formation

Cre-neg; FAK-Y861F^{KI} and Cre-pos; FAK-Y861F^{KI} mice were subcutaneously injected with syngeneic B16F0 melanoma cells, 5-7 days after tamoxifen administration. Tumour cells were allowed to grow until Day 17 and blood vessel density was quantified in age-matched, size-matched tumours (**A**). A decrease in tumour angiogenesis was observed and representative pictures are shown (**B**). Blood vessel density was quantified in 7-day old (**C**) and 21-day old (**D**) B16F0 tumours, and statistical analysis shows that the decrease in blood vessel density observed in early stages of tumour formation is overcome at day 21. Scale bar = 1 cm. * $p<0.05$. n=4-9 mice/genotype.

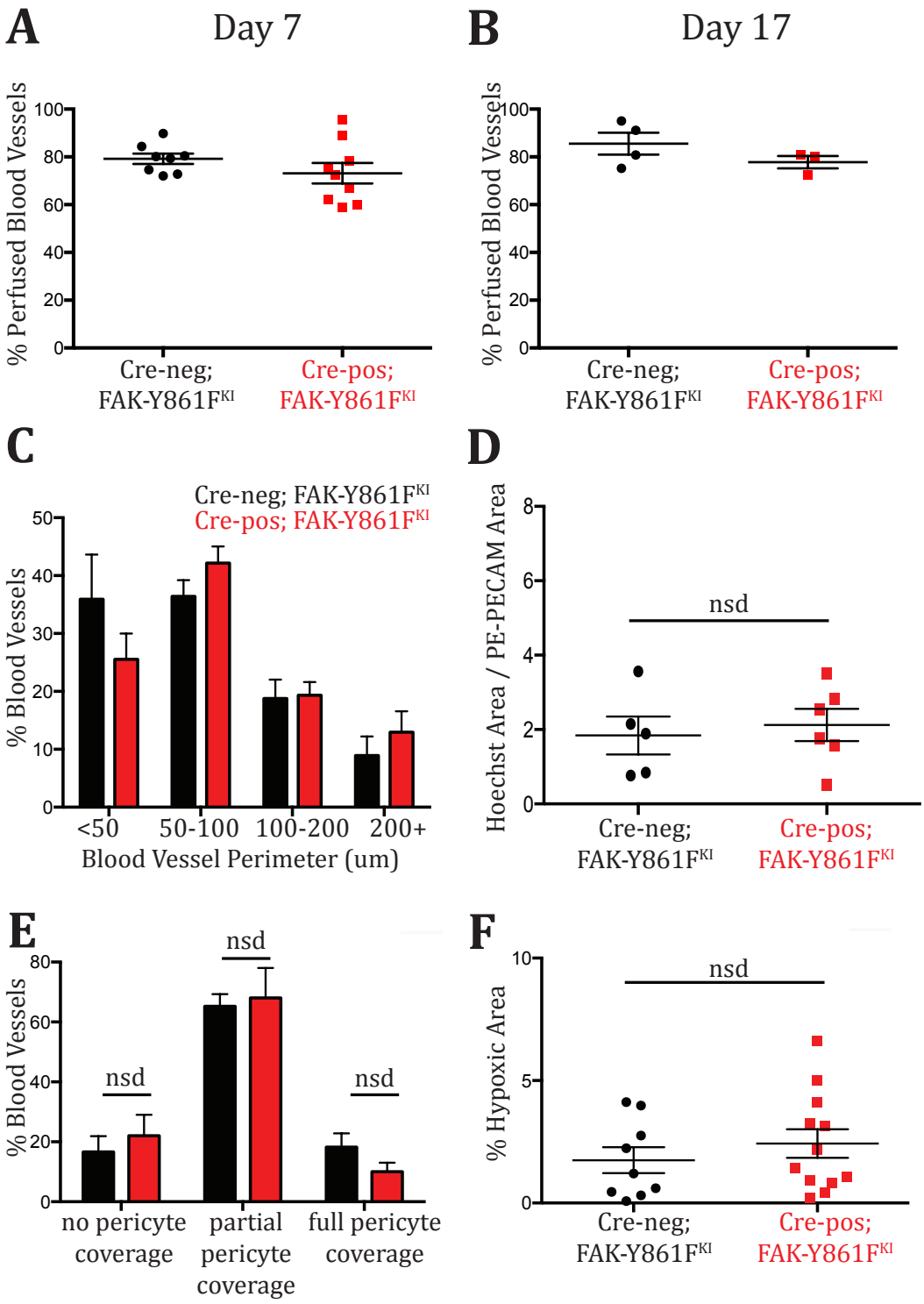

Figure 3.16: Endothelial-specific inactivation of FAK-Y861 phosphorylation does not affect B16F0 tumour endothelium or tumour hypoxia *in vivo*

Legend on next page.

Figure 3.16: Endothelial-specific inactivation of FAK-Y861 phosphorylation does not affect B16F0 tumour endothelium or tumour hypoxia *in vivo*

Cre-neg; FAK-Y861F^{KI} and Cre-pos; FAK-Y861F^{KI} mice bearing 8-day old B16F0 tumours (**A**) and 17-day old B16F0 tumours (**B**) were given anti-PE-PECAM antibody injection into the tail vein ten minutes prior to sacrifice. Midline B16F0 tumour sections from size-matched tumours were stained for endomucin. The number of PE-PECAM-antibody perfused tumour blood vessels was counted across the entire midline section from size-matched tumours. The percentage of perfused vessels was calculated by dividing the number of PE-PECAM-antibody perfused tumour blood vessels/ total number of tumour blood vessels. Quantification indicates that the endothelial specific FAK-Y861F mutation does not affect tumour blood vessel perfusion.
(**C**) Endomucin-stained tumour sections were photographed at the Axioplan microscope and the perimeter of at least fifty blood vessels per sample was measured using the Image J software. The percentage of blood vessels that were less than 50mm; 50-100 mm; 100-200 mm or 200 mm or more was determined for Cre-neg; FAK-Y861F^{KI} and Cre-pos; FAK-Y861F^{KI} samples and no significant difference was observed between the two genotypes.
(**D**) Cre-neg; FAK-Y861F^{KI} and Cre-pos; FAK-Y861F^{KI} mice bearing 21-day-old B16F0 subcutaneous tumours, were given tail vein injections of anti-PE-PECAM antibody and Hoechst. Midline tumour sections were mounted from size-matched tumours (without any immunofluorescence staining). Statistical analysis indicates that introducing FAK-Y861F mutation in the endothelium does not affect Hoechst Leakage.
(**E**) Endomucin- and NG2-double stained tumour sections were photographed at the Axioplan microscope and the percentage of naked blood vessels (no pericyte coverage) and the percentage of blood vessels partially or completely covered by pericytes was calculated and shows that there is no difference in pericyte coverage between the two genotypes.
(**F**) B16F0 tumour-burdened Cre-neg; FAK-Y861F^{KI} and Cre-pos; FAK-Y861F^{KI} mice were given intraperitoneal injections of Pimonidazole probe. FITC-anti-Pimonidazole antibody was used to detect hypoxic regions. Pictures taken at the Axioplan were quantified and the percentage of hypoxic area was determined by dividing the Pimonidazole stained area by the total field area. This data indicate that endothelial specific inactivation of FAK-Y861 phosphorylation does not affect tumour hypoxia. Values are given as means + s.e.m. n=3-12 mice/genotype.

As a second subcutaneous tumour model, the CMT19T carcinoma cell line was used to investigate the effect of endothelial-specific FAK-Y861F mutation on tumour growth and angiogenesis. Cre-neg; FAK-Y861F^{KI} and Cre-pos; FAK-Y861F^{KI} mice were injected with CMT19T cells a week after tamoxifen injection and tumour volumes were monitored across time until Day 28 post tumour cell injection. **Figure 3.17** shows that there is no difference in CMT19T tumour growth between Cre-neg; FAK-Y861F^{KI} and Cre-pos; FAK-Y861F^{KI} mice. Blood vessel density was quantified in these 28-day old CMT19T tumours and results indicate there is no significant difference in CMT19T tumour blood vessel densities (**Figure 3.18**).[1] This result indicates that endothelial FAK-Y861F mutation does not affect tumour angiogenesis as analysed at Day 28. Whether this mutation impairs tumour angiogenesis in early stages of tumour formation with this effect being overcome at a later stage (as it is the case for the B16F0 tumour model) needs to be further investigated.

[1] Paraskevi Natalia Georgiou, B.Sc student, whom I supervised, quantified blood vessel density for CMT19T tumour model.

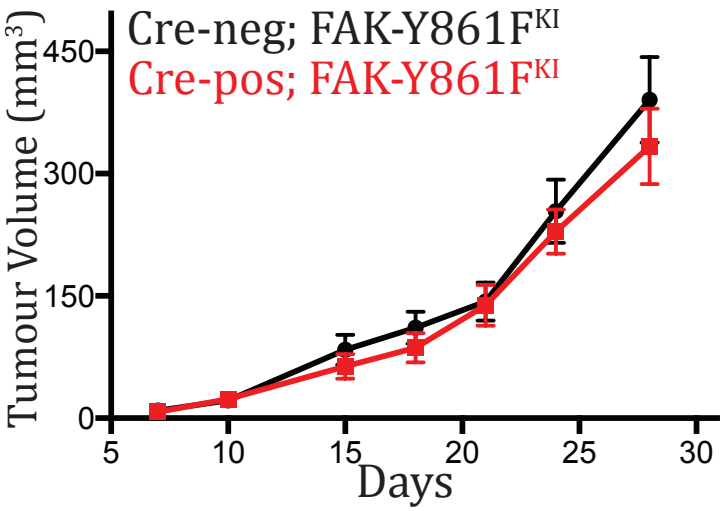

Figure 3.17: Endothelial-specific inactivation of FAK-Y861 phosphorylation does not affect CMT19T carcinoma tumour growth.

Cre-neg; FAK-Y861F^{KI} and Cre-pos; FAK-Y861F^{KI} mice were given subcutaneous injections of syngeneic CMT19T carcinoma cells, 5-7 days after tamoxifen injection. Tumour dimensions were measured from day 6 to day 28 and tumour volumes calculated (Volume = 0.52 x Length x Width^2). CMT19T tumour growth was not affected by the endothelial-specific FAK-Y861F mutation. n=8-9 mice/genotype.

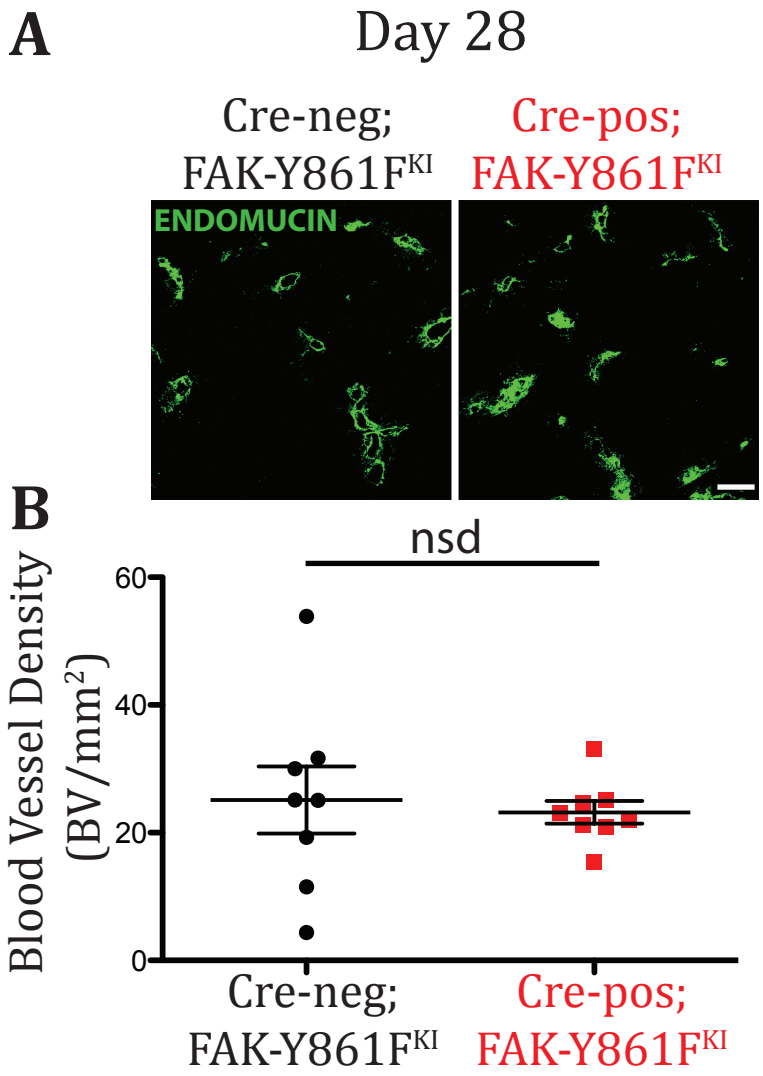

Figure 3.18: Endothelial-specific inactivation of FAK-Y861 phosphorylation does not affect CMT19T carcinoma tumour angiogenesis.

Cre-neg; FAK-Y861F^{KI} and Cre-pos; FAK-Y861F^{KI} mice were given subcutaneous injections of syngeneic CMT19T carcinoma cells, 5-7 days after tamoxifen injection. CMT19T tumour blood vessel density was calculated by counting all the endomucin-positive blood vessels across the entire midline tumour section from size-matched tumours. Representative pictures of endomucin stained blood vessels and blood vessel density quantification are shown in (**A**) and (**B**). Statistical analysis indicates that FAK-Y861F mutation in endothelial cells does not affect CMT19T tumour angiogenesis. Scale bar = 100 µm. n=8 mice/genotype.

In a third tumour model Lewis Lung Carcinoma (LLC) cells were injected subcutaneously into Cre-neg; FAK-Y861F^{KI} and Cre-pos; FAK-Y861F^{KI} mice previously administered with tamoxifen. Results indicate that there is no difference in LLC tumour growth between Cre-neg; FAK-Y861F^{KI} and Cre-pos; FAK-Y861F^{KI} (**Figure 3.19**). In addition, no difference in LLC tumour angiogenesis was observed between the two genotypes (**Figure 3.20**). The analysis was performed in 24-day old LLC tumours and whether a delay in tumour angiogenesis is present at earlier staged in tumour formation still needs to be investigated.

As previously observed in the B16F0 tumour model, blood vessel perfusion was not affected by the endothelial specific FAK-Y861F mutation in LLC tumours (**Figure 3.21**).[1]

Summary: tumour growth and tumour angiogenesis in vivo

The findings presented in this section show that inactivating the endothelial specific FAK-Y397 phosphorylation leads to a delay in tumour angiogenesis, for the three studied subcutaneous tumour models and is accompanied by an increase in tumour hypoxia. None of the studied blood vessel parameters (such as blood vessel perimeter, perfusion, leakage or pericyte coverage) were affected by the FAK-Y397F mutation.

For two of the studied models (B16F0 and CMT19T) delayed angiogenesis is accompanied by delayed tumour growth; but in the case of LLC model delayed angiogenesis does not impair tumour growth.

[1] Paraskevi Natalia Georgiou, B.Sc student, whom I supervised, quantified blood vessel density and perfusion parameters for LLC tumour model.

Inactivation of endothelial specific FAK-Y861 phosphorylation leads to delayed tumour angiogenesis in the early stages of B16F0 tumour formation and at least until Day 17 post tumour cell inoculation. This defect is overcome by Day 21 suggesting that alternative mechanisms that are independent of FAK-Y861 phosphorylation become activated. Noteworthy is that the observed delayed angiogenesis did not impair B16F0 tumour growth.

Tumour angiogenesis was analysed in 28-day old CMT19T and 24-day old LLC tumour models and the endothelial FAK-Y861F mutation did not affect tumour angiogenesis in neither of these models. Investigating tumour angiogenesis at an earlier stage of tumour formation would indicate if the data obtained for 7- and 17-day old B16F0 tumours can be generalized to all the studied models or if it is specific to B16F0 melanoma tumours.

In addition none of the three studied tumour types have their growth impaired by the endothelial specific FAK-Y861F mutation.

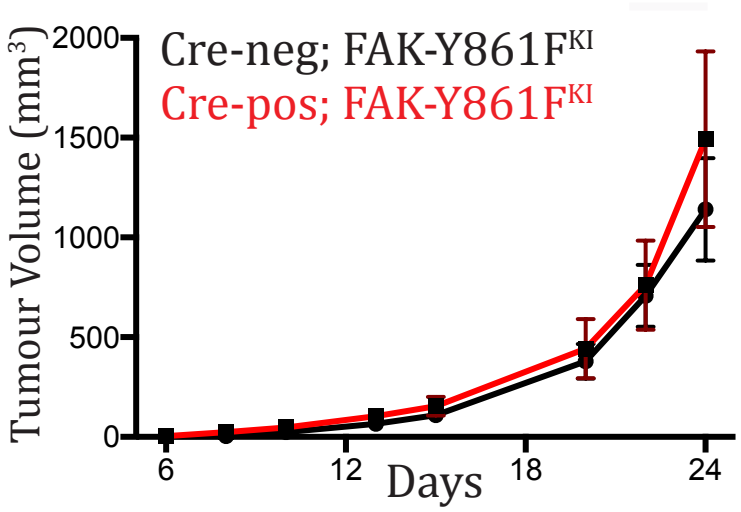

Figure 3.19: Endothelial-specific inactivation of FAK-Y861 phosphorylation does not affect LLC tumour growth or tumour angiogenesis *in vivo*
Cre-neg; FAK-Y861F^{KI} and Cre-pos; FAK-Y861F^{KI} mice were given subcutaneous injections of syngeneic LLC carcinoma cells, 5-7 days after tamoxifen injection. Tumour dimensions were measured from day 6 to day 24 and tumour volumes calculated (Volume = 0.52 x Length x Width^2). No significant difference in LLC tumour growth was determined between Cre-neg; FAK-Y861F^{KI} and Cre-pos; FAK-Y861F^{KI} mice. n=7-8 mice/genotype.

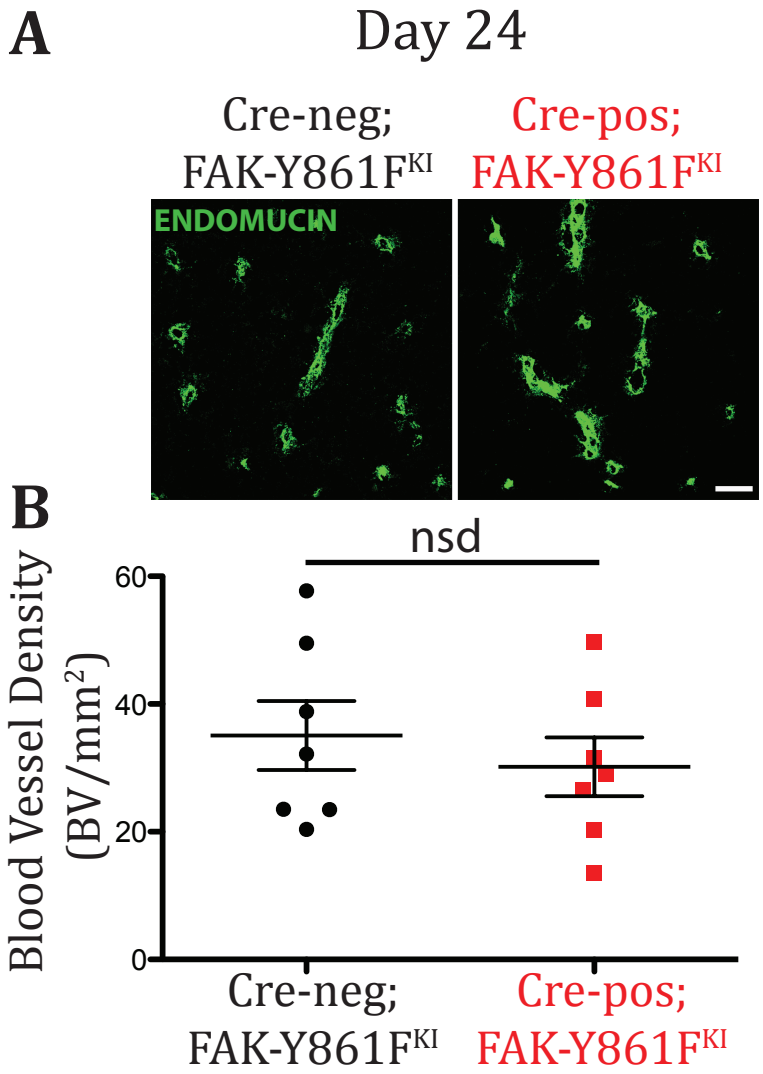

Figure 3.20: Endothelial-specific inactivation of FAK-Y861 phosphorylation does not affect LLC tumour growth or tumour angiogenesis *in vivo*

Cre-neg; FAK-Y861F^{KI} and Cre-pos; FAK-Y861F^{KI} mice were given subcutaneous injections of syngeneic LLC carcinoma cells, 5-7 days after tamoxifen injection. Endomucin-positive blood vessels were counted across the midline section of LLC size matched tumours and the blood vessel density was determined. Statistical analysis shows that endothelial-specific FAK-Y861F mutation does not affect tumour angiogenesis. Scale bar = 100 μm. nsd – no significant difference. n=7 mice/genotype.

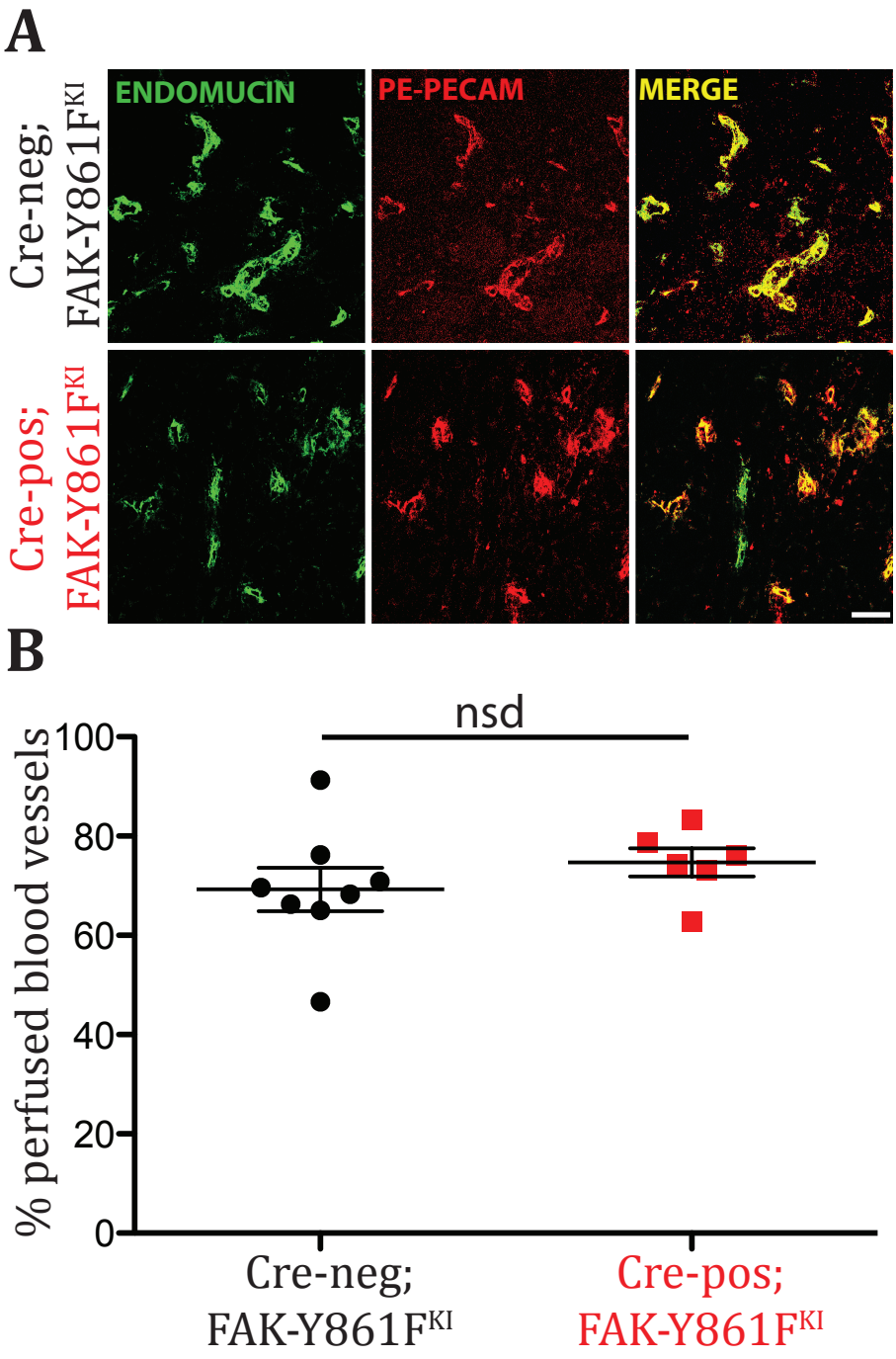

Figure 3.21: Endothelial-specific inactivation of FAK-Y861 phosphorylation does not affect blood vessel perfusion in LLC tumours *in vivo*

LLC tumour bearing Cre-neg; FAK-Y861F^{KI} and Cre-pos; FAK-Y861F^{KI} mice, were injected with anti-PE-PECAM antibody into the tail vein ten minutes prior to sacrifice. Midline LLC tumour sections from size-matched tumours were stained for endomucin and representative pictures were taken at the Confocal microscope. Blood vessels (in green), PE-PECAM-antibody perfused blood vessels (in red) and their merge from Cre-neg; FAK-Y397F^{KI} and Cre-pos; FAK-Y397F^{KI} samples are shown (**A**). The percentage of perfused vessels was calculated by dividing the number of PE-PECAM-antibody perfused tumour blood vessels/ total number of tumour blood vessels (**B**). Quantification indicates that the endothelial specific FAK-Y861F mutation does not affect tumour blood vessel perfusion. Scale bar = 100 µm. n=6 mice/genotype.

2. *Elucidating the effect of endothelial FAK-Y397F and FAK-Y861F mutations on growth factor driven angiogenesis in vivo*

Several hypotheses could explain the difference between B16F0, CMT19T and LLC tumour growth and the associated tumour angiogenesis for the two studied FAK mutants. For sustained tumour growth different tumour types seem to depend more or less on tumour angiogenesis and the way they trigger tumour angiogenesis might be different. More precisely, the main growth factor, or the cocktail of growth factors, secreted by these tumours might be different and, the effect of the endothelial FAK mutations can be different, depending on the growth factor(s) that drive angiogenesis. To determine if FAK-Y397F and FAK-Y861F mutated endothelial cells react differently when angiogenesis is driven by various growth factors (such as VEGF, PlGF, bFGF and Ang2), sponge assay was performed.

The sponge assay was used to determine if individual growth factors trigger angiogenesis differently and if the endothelial specific FAK-Y397F and the FAK-Y861F mutations affect angiogenesis differently depending on which growth factor is driving angiogenesis *in vivo*. Briefly, the procedure involved treating mice with tamoxifen to induce the WT-knockin or mutant FAK-knockin followed by subcutaneous implantation of a synthetic sponge that was injected with growth factors to induce microvessel invasion. Approximately two weeks post implantation, sponges were excised and blood vessel invasion assessed by quantitative immunohistochemistry.

2.1. Validation of the KO/KI system in sponge assays in vivo

The sponge assay was designed in such a way as to resemble as much as possible the conditions and timings of the subcutaneous tumour growth experiments. Firstly Cre-neg; FAK-WT^{KI} and Cre-pos; FAK-WT^{KI} mice were given tamoxifen five days prior to sponge implantation, which is similar to what was done in tumour growth experiments, where tumour cells where injected 5-7 days after the first tamoxifen administration. Secondly, the sponges were implanted under the skin, on the flank of the mice, similarly to where the tumour cells are injected. To mimic the early time point as previously described in the tumour growth experiments, sponges were dissected at Day 7, but very few microvessels had infiltrated the sponges and it was unclear if the growth factors had a pronounced angiogenic effect at this early time point (data not shown). This was in contrast to what had been observed in 7-day old tumours that presented with a substantial blood vessel density; and this is presumably due to tumours containing a multitude of growth factors acting together, as opposed to the one growth factor regularly injected into the sponge. Therefore to study the effect of one specific growth factor on microvessel infiltration, sponge assay studies at a later time point, namely at Day 14. To this purpose, growth factors or PBS were injected into the sponge on Mondays, Wednesdays, Fridays and a total of five injections per sponge were performed over 2 weeks. At the end of the experiment the sponges were dissected and formalin-fixed; thin sections were cut and stained for the endothelial marker endomucin. **Figure 3.22 A** shows sponge fields containing blood vessels (stained for

endomucin in brown) as well as other cell types (stained with H&E) for the following groups: Cre-neg; FAK-WT^{KI} mice treated with PBS, Cre-pos; FAK-WT^{KI} mice treated with PBS, Cre-neg; FAK-WT^{KI} mice treated with VEGF and Cre-pos; FAK-WT^{KI} treated with VEGF. The number of blood vessels was determined in areas infiltrated by cells across the width of the sponge and normalized by the number of quantified fields. PBS-injected sponges showed baseline microvessel invasion that was the same in Cre-neg; FAK-WT^{KI} and Cre-pos; FAK-WT^{KI} mice **(Figure 3.22 B)**. VEGF injected sponges showed an increase in micovessel invasion when compared with PBS baseline. No difference in VEGF-stimulated microvessel invasion was observed between Cre-neg; FAK-WT^{KI} and Cre-pos; FAK-WT^{KI} mice **(Figure 3.22 B)** indicating that the two genotypes respond to VEGF in a similar way. The results also indicate that knocking-in WT-FAK is sufficient to rescue the FAK-KO phenotype (Tavora, 2010).

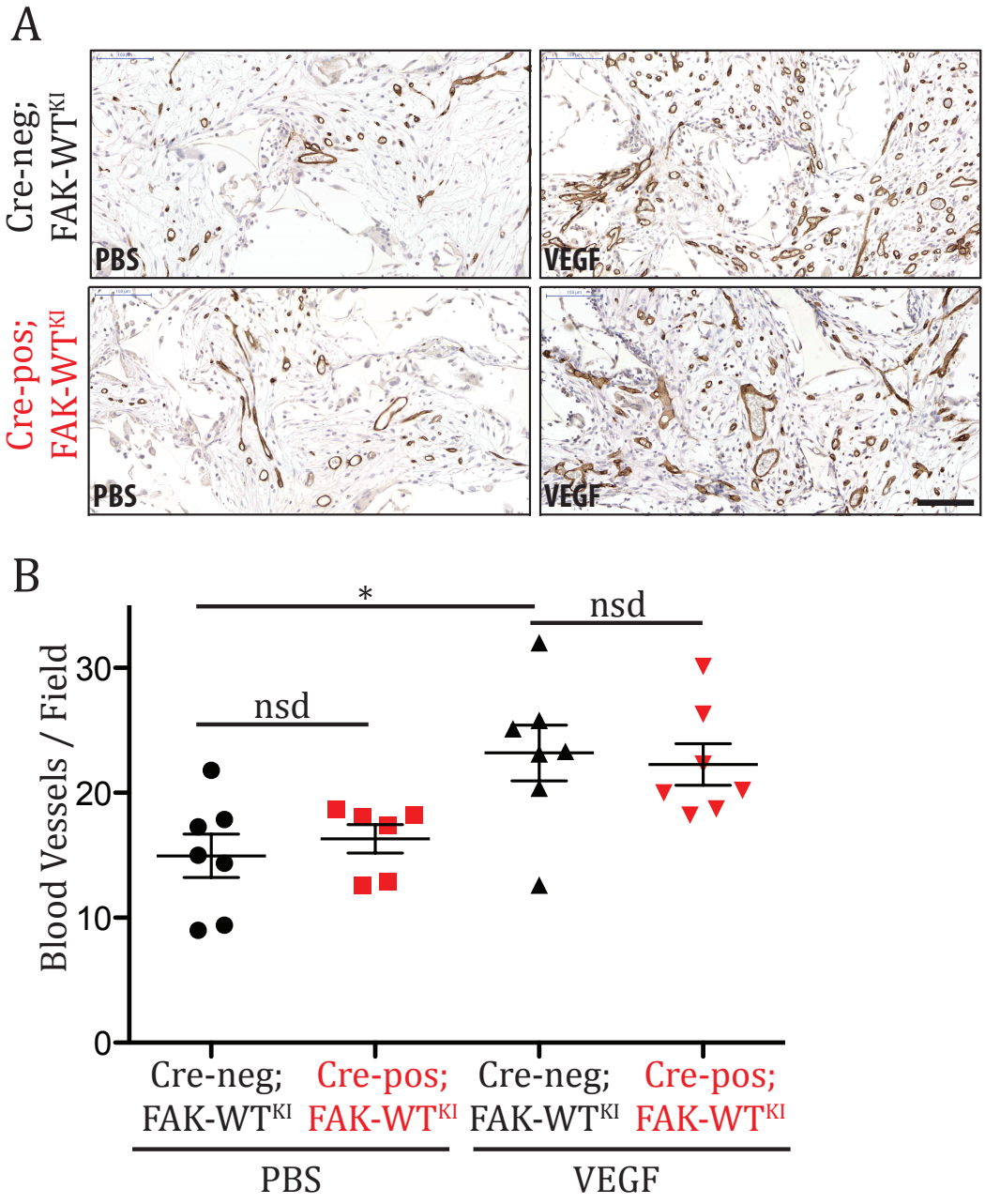

Figure 3.22: Validation of the KO/KI system in sponge assays *in vivo*.
Cre-neg; FAK-WT^{KI} and Cre-pos; FAK-WT^{KI} mice were given subcutaneous sponge implants, two days after tamoxifen administration. The sponges were injected with either 100 µL PBS or VEGF every other day starting with Day 2 postimplantation. At Day 14 postimplantation, sponges were harvested, fixed in formalin and the cut sections were stained for endomucin (**A**). Angiogenesis was quantified by counting the endomucin-positive blood vessels across the sponge width at 30X magnification and normalized to the number of counted fields (**B**). VEGF administration increases angiogenesis similarly in Cre-neg; FAK-WT^{KI} and Cre-pos; FAK-WT^{KI} sponges when compared to PBS injected controls, indicating that reintroducing a WT version of FAK in endothelial cells is sufficient to rescue the previously observed KO phenotype. Scale bar=100µm. Scatter plots show mean ± s.e.m; * P<0.05; nsd no significant difference. n=6-7 mice per condition per genotype.

2.2. Endothelial specific inactivation of FAK-Y397 phosphorylation impairs VEGF-, PlGF- and bFGF-driven angiogenesis

The sponge assay was performed using Cre-neg; FAK-Y397F^{KI} and Cre-pos; FAK-Y397F^{KI} mice and sponges were treated with one of the following: VEGF, PlGF, bFGF, Ang2 or PBS, as a control.

A statistically significant increase in the number of blood vessels per field was observed in VEGF- (**Figure 3.23 A**), PlGF- (**Figure 3.23 B**) or bFGF- (**Figure 3.23 C**) treated sponges implanted in the Cre-neg; FAK-Y397F^{KI} mice when compared to PBS-treated sponges implanted in mice with the same genotype, indicating that each of these growth factors is able to trigger angiogenesis in our experiments.

To determine the effect of the endothelial specific FAK-Y397F mutation on in VEGF-, PlGF- or bFGF-driven angiogenesis, the number of blood vessels per field was compared between growth factor-treated sponges implanted in Cre neg; FAK-Y397F^{KI} and Cre pos; FAK-Y397F^{KI} mice. VEGF-, PlGF- and bFGF-stimulated microvessel invasion was reduced in Cre-pos; FAK-Y397F^{KI} mice when compared with Cre-neg; FAK-Y397F^{KI} controls (**Figure 3.23 A, B and C**). These results indicate that the endothelial specific inactivation of FAK-Y397 phosphorylation is sufficient to impair VEGF-, PlGF and bFGF-driven angiogenesis.

Noteworthy is the statistically significant decrease in the number of blood vessels per field for PBS-treated sponges implanted in Cre-pos; FAK-Y397F^{KI} mice when compared to PBS-treated sponges implanted in Cre-neg;

FAK-Y397F^{KI} mice (**Figure 3.23 B, C and D**)[1]. This data indicates that the endothelial specific inactivation of FAK-Y397 phosphorylation may impair baseline angiogenesis even in PBS controls.

Statistical analysis of the data presented in **Figure 3.23 D** returns a p value of p=0.0566 when comparing microvessel infiltration in sponges treated with Ang2 vs PBS in Cre-neg; FAK-Y397F^{KI} mice, which is very close to statistical significance. In itself this data suggests that Ang2 is not able to promote angiogenesis in the Cre-neg control mice and therefore cannot be considered as a pro-angiogenic growth factor in this experimental setting. Nevertheless, increasing n-numbers, or fine tuning the experimental design by administering Ang2 more often or in higher concentrations would allow to obtain a more clear cut result in terms of the ability of Ang2 to induce or sustain angiogenesis. However Ang2 stimulated microvessel invasion was reduced in Cre-Pos; FAK-Y397F^{KI} mice when compared with Cre-neg; FAK-Y397F^{KI} mice (**Figure 3.23 D**). Since decreased microvessel infiltration was also observed in PBS treated sponges between the two genotypes, the reduction in angiogenesis cannot be incurred solely to Ang2 treatment.

Overall this data indicates that the endothelial specific FAK-Y397 phosphorylation is required for VEGF-, PlGF- and bFGF-driven angiogenesis *in vivo*.

[1] The PBS data presented in **Figure 3.23 A** did not yield significant difference.

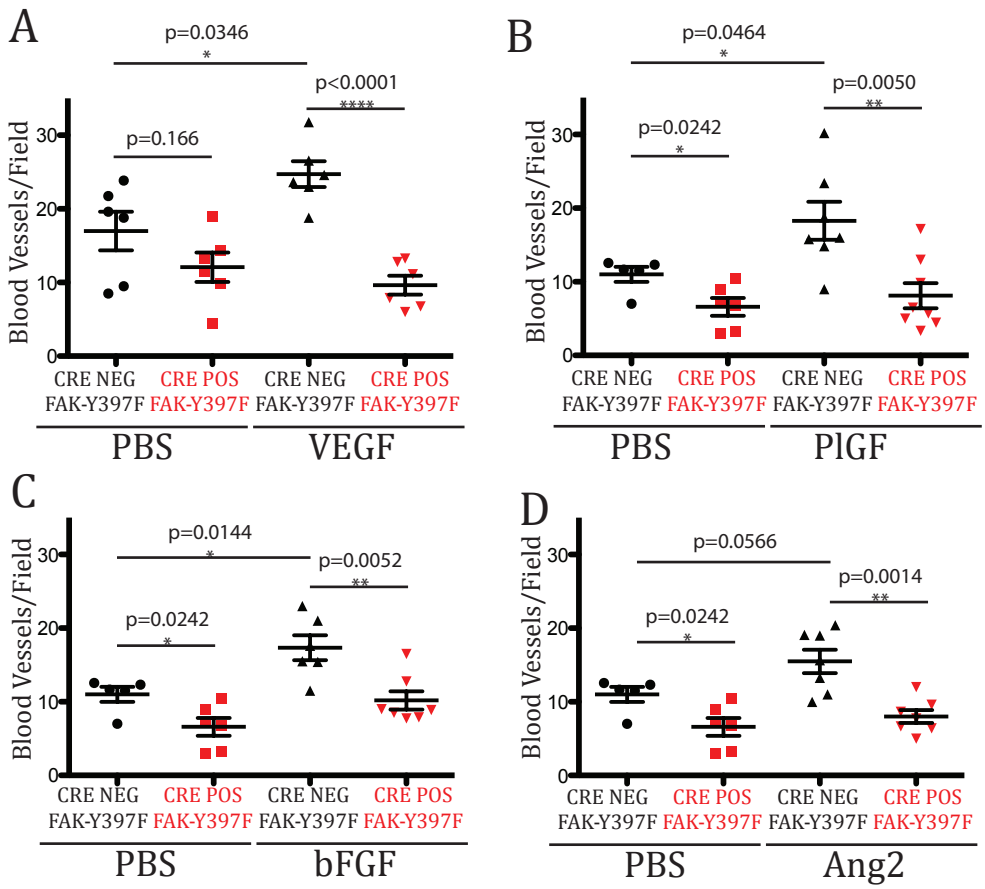

Figure 3.23: Endothelial-specific inactivation of FAK-Y397 phosphorylation impairs VEGF-, PlGF and bFGF-driven angiogenesis.

Cre-neg; FAK-Y397F^{KI} and Cre-pos; FAK-Y397F^{KI} mice were given subcutaneous sponge implants, two days after tamoxifen administration. The sponges were injected with PBS, VEGF, PlGF, bFGF or Ang2 every other day starting with Day 2 postimplantation. At Day 14 postimplantation, sponges were harvested, fixed in formalin and the cut sections were stained for endomucin. Angiogenesis was quantified by counting the endomucin-positive blood vessels across the sponge width at 30X magnification and normalized to the number of counted fields. VEGF (**A**), PlGF (**B**) or bFGF (**C**) administration increased microvessel formation in Cre-neg; FAK-Y397F^{KI} when compared to PBS treated Cre-neg; FAK-Y397F^{KI} sponges. Conversely VEGF, PlGF and bFGF were not able to trigger angiogenesis in Cre-pos; FAK-Y397F^{KI} sponges to the same extend as in Cre-neg; FAK-Y397F^{KI} sponges. (**D**) Ang2 failed to trigger angiogenesis in Cre neg control mice; nevertheless FAK-Y397F mutation impaired microvessel invasion in Cre-pos; FAK-Y397F^{KI} sponges when compared to Cre-neg; FAK-Y397F^{KI} Ang2 treated sponges. Noteworthy FAK-Y397F mutation leads to a delay in microvessel infiltration even in the PBS control group. Scatter plots show mean ± s.e.m; * p<0.05, **p<0.01, ****p<0.0001; nsd no significant difference. n=5-8 mice per condition per genotype.

2.3. Endothelial specific inactivation of FAK-Y861 phosphorylation does not affect VEGF-, PlGF- and bFGF-driven angiogenesis and allows ANG2 to act as a pro-angiogenic growth factor

To study the effect of the endothelial specific FAK-Y861F mutation, sponges were implanted in Cre-neg; FAK-Y861F^{KI} and Cre-pos; FAK-Y861F^{KI} mice five days after tamoxifen administration and VEGF (**Figure 3.24 A**), PlGF (**Figure 3.24 B**), bFGF (**Figure 3.24 C**) or Ang2 (**Figure 3.24 D**) was injected into the sponges as previously described. PBS treatment was used as a negative control. Results indicated that in Cre-neg; FAK-Y861F^{KI} control mice VEGF, PlGF and bFGF administration leads to increased microvessel invasion when compared with PBS. This data confirms that VEGF, PlGF and bFGF act as pro-angiogenic growth factors in Cre-neg control mice.

To determine if the endothelial specific FAK-Y861F mutation impairs VEGF-, PlGF- or bFGF-driven microvessel invasion into the sponges, the number of blood vessels per field in either VEGF-, PlGF- or bFGF-treated sponges was compared between Cre-neg; FAK-Y861F^{KI} and Cre-pos; FAK-Y861F^{KI}. The outcome of this comparison indicates that there is no significant difference between Cre-neg; FAK-Y861F^{KI} and Cre-pos; FAK-Y861F^{KI} in terms of microvessel infiltration in either VEGF-, PlGF- or bGFG-treated sponges, suggesting that the endothelial specific FAK-Y861 phosphorylation is dispensable for VEGF-, PlGF- or bFGF-driven angiogenesis in this *in vivo* experimental setting.

Of note is that the endothelial specific FAK-Y861F mutation does not affect baseline microvessel infiltration, as proven by comparing Cre-neg; FAK-Y861F^{KI} and Cre-pos; FAK-Y861F^{KI} blood vessel counts after PBS treatment (**Figure 3.24**).

In this *in vivo* experimental setting, ANG2 does not act as a pro-angiogenic growth factor. Indeed the number of blood vessels per field in ANG2-treated sponges implanted in Cre-neg; FAK-Y861F^{KI} mice was unchanged when compared to PBS-treated sponges implanted in mice with the same genotype (**Figure 3.24 D**)[1]. Surprisingly microvessel infiltration was increased in Ang2-treated sponges implanted in Cre-pos; FAK-Y861F^{KI} mice, suggesting that Ang2 is sensed as a pro-angiogenic growth factor by the FAK-Y861F mutated endothelium (**Figure 3.24 D**).

Together these results suggested that the endothelial specific FAK-Y861F mutation does not affect VEGF-, PlGF- or bFGF-driven angiogenesis and that in the presence of this mutation Ang2 acts as a pro-angiogenic growth factor.

Summary: growth factor induced angiogenesis in vivo

The sponge assay has allowed dissection of the effect of four different growth factors – VEGF, PlGF, bFGF and ANG2 on FAK-Y397F or FAK-Y861F mutated endothelium in a tumour-free environment *in vivo*. The endothelial specific inactivation of FAK-Y397 phosphorylation impairs VEGF-, PlGF- and bFGF-driven angiogenesis (as well as baseline angiogenesis) and this is in line

[1] Noteworthy is that this result is different from the one obtained for Cre neg; FAK-Y397F^{KI} mice.

with the finding that this mutation delays tumour angiogenesis for the three studied subcutaneous tumour models (B16F0, CMT19T and LLC). In contrast, VEGF-, PlGF- and bFGF-stimulated angiogenesis was not affected in FAK-Y861F mutated endothelium and this finding is in line with unaffected tumour angiogenesis in late time point B16F0 CMT19T and LLC tumour models. The reason for delayed tumour angiogenesis, when FAK is mutated on the Y861 residue, in the early time point of B16F0 tumour model needs further investigation.

The studied growth factors can be secreted by a variety of cell types, including immune cells and endothelial cells and this raises the possibility that the results obtained with the sponge assay could be due to other growth factors that are secreted into the sponges *in vivo*. In order to dissect the contribution of these *in vivo* secreted factors, the *ex-vivo* aortic ring assay was used to investigate the affect of the endothelial specific FAK-Y397F and FAK-Y861F mutation on sprouting angiogenesis in presence of VEGF, Ang2 or both combined.

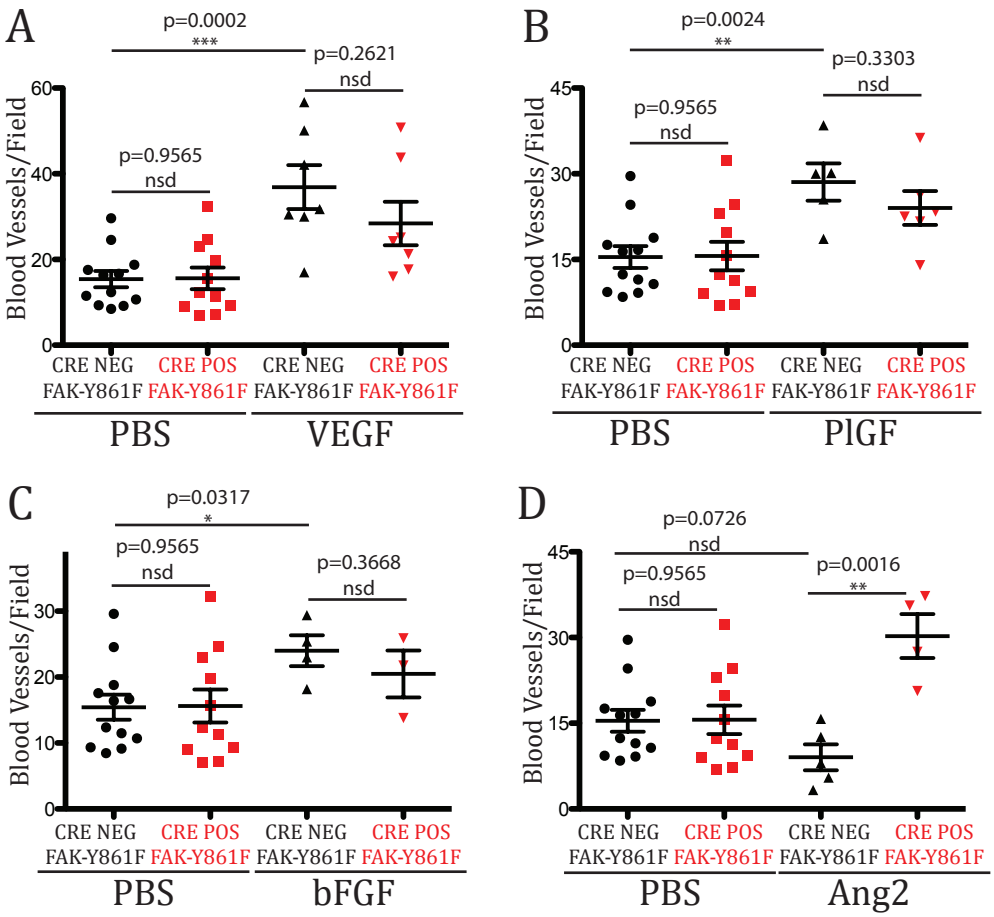

Figure 3.24: Endothelial-specific inactivation of FAK-Y861 phosphorylation does not affect VEGF-, PlGF- or bFGF-driven angiogenesis and allows Ang2 to act as a pro-angiogenic growth factor.

Cre-neg; FAK-Y861F^{KI} and Cre-pos; FAK-Y861F^{KI} mice were given subcutaneous sponge implants, two days after tamoxifen administration. The sponges were injected with PBS, VEGF (**A**), PlGF (**B**), bFGF (**C**) or Ang2 (**D**) every other day starting with Day 2 postimplantation. At Day 14 postimplantation, sponges were harvested, fixed in formalin and the cut sections were stained for endomucin. Angiogenesis was quantified by counting the endomucin-positive blood vessels across the sponge width at 30X magnification and normalized to the number of counted fields. VEGF-, PlGF- or bFGF-triggered microvessel infiltration was not affected by the endothelial specific FAK-Y861F mutation. Ang2 was able to trigger microvessel infiltration in Cre-pos; FAK-Y861F^{KI} sponges. Scatter plots show mean ± s.e.m; * $p<0.05$, ** $p<0.01$, *** $p<0.005$; nsd no significant difference. n=4-12 mice per condition per genotype.

3. Elucidating the effect of endothelial FAK-Y397F and FAK-Y861F mutations on growth factor driven angiogenesis ex vivo

Aortic ring assay was performed in order to further investigate the effect of FAK-Y397F and FAK-Y861F mutations in endothelial cells on VEGF-driven sprouting angiogenesis, as well as on VEGF+Ang2 signalling. This assay allows investigating the effect of one or several growth factors on sprouting angiogenesis. The source of growth factors in this assay is primarily exogenous (added and controlled during the experiment) and the only other source of growth factors might be the aorta itself. This is an advantage compared to the sponge assay, where growth factors can be secreted by a large variety of cell types present in the sponge as well as produced by cells elsewhere in the body and then delivered systemically into the sponge.

The next sections will present data generated with Cre-neg; FAK-WT^{KI} and Cre-pos; FAK-WT^{KI} mice to validate the mouse model in this experimental setting; the effect of the endothelial FAK-397F and FAK-861F mutation will be presented in two different sections[1].

3.1. Validation of the KO/KI system in the ex vivo aortic ring assay

Cre-neg; FAK-WT^{KI} and Cre-pos; FAK-WT^{KI} mice were given tamoxifen 5 days prior to aorta harvesting. The aortas were cut into rings, starved overnight and embedded into 3-dimentional collagen matrix. VEGF or PBS was administered

[1] Each aortic ring assay was done with 3 mice per genotype and the aortic ring assays were performed in duplicates: one duplicate was performed by Dr. Tanguy Lechertier, former postdoctoral research assistant in our group, and the other one by me. The data is presented as a pool of the two duplicates and was therefore generated using 6 mice per genotype.

every other day and the number of sprouts was counted for each aortic ring starting from Day 4. Results presented in **Figure 3.25** show that the average number of spouts per aortic ring from Cre-neg; FAK-WT^{KI} is statistically increased upon VEGF treatment when compared to PBS treatment. This indicates that VEGF is able to trigger aortic ring sprouting in control mice. The same effect is seen in Cre-pos; FAK-WT^{KI} mice, indicating that knocking in WT FAK allows similar level of aortic ring sprouting and validating our KO/KI strategy for this experimental approach.

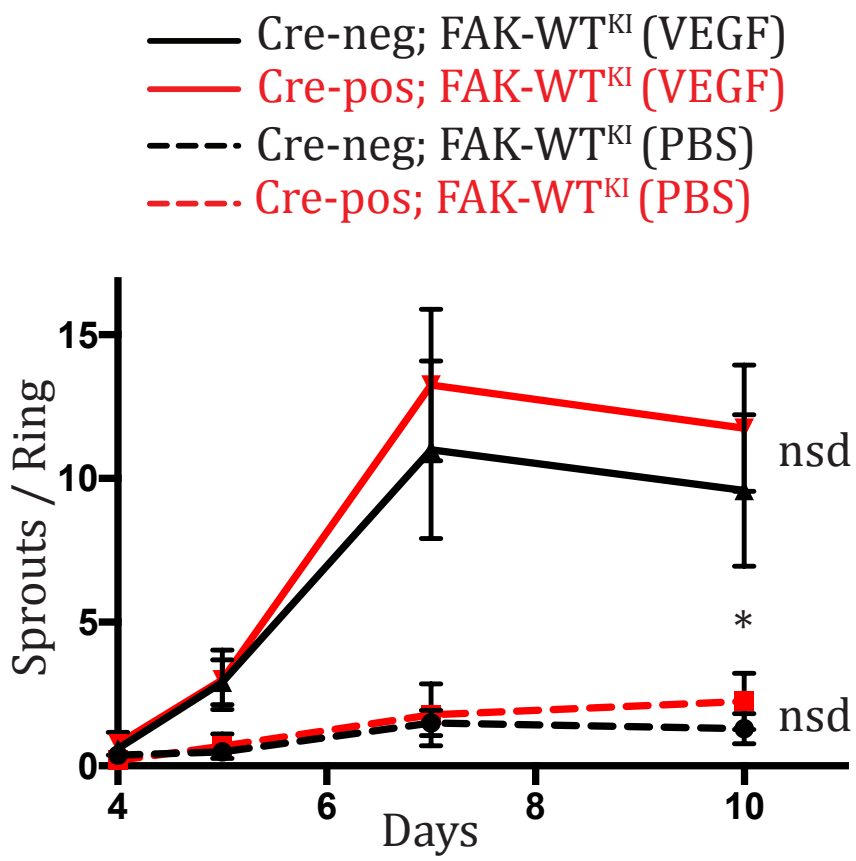

Figure 3.25: Reintroducting a WT version of FAK in endothelial cells does not affect VEGF-driven sprouting angiogenesis.

Cre-neg; FAK-WT^{KI} and Cre-pos; FAK-WT^{KI} mice were given tamoxifen 5 days prior to sacrifice. Aortas were dissected and cut into rings. Rings were starved overnight and then embedded in collagen matrix and treated with VEGF or PBS as a control. The number of sprouts/ring was counted at Day 4, Day 5, Day 7 and Day 10 and averaged at each time point. Statistical analysis indicates that, when compared to PBS control group, VEGF treatment lead to an increase in the number of sprouts/ring for rings dissected from Cre-neg; FAK-WT^{KI} and Cre-pos; FAK-WT^{KI} mice. This indicates that reintroducing FAK-WT in endothelial cells restores the VEGF signalling defect observed in FAK-KO endothelial cells. Data are shown as mean ± s.e.m; * $p<0.05$; nsd no significant difference. n=29-32 rings (dissected from 6 mice per genotype).

3.2. Endothelial-specific inactivation of FAK-Y397 phosphorylation impairs VEGF-driven sprouting

The same experimental procedure was used for aortic rings from Cre-neg; FAK-Y397F^{KI} and Cre-pos; FAK-Y397F^{KI} mice. As previously, VEGF was able to trigger aortic ring sprouting in rings from Cre-neg; FAK-Y397F^{KI} mice (when compared to PBS treatment of rings from Cre-neg; FAK-Y397F^{KI} mice) and, at day 10, the number of spouts for VEGF treated rings from Cre-pos; FAK-Y397F^{KI} mice was statistically decreased (**Figure 3.26 A**). This result indicates that endothelial specific inactivation of FAK-Y397 phosphorylation leads to impaired VEGF-driven aortic ring sprouting. This result is in line with the data obtained in the sponge assay and for tumour blood vessel quantification in the three studied subcutaneous tumour models.

ANG2 alone does not trigger sprouting in Cre-neg; FAK-Y397F^{KI} or Cre-pos; FAK-Y397F^{KI} mice, indicating that ANG2 alone is not a pro-angiogenic factor (**Figure 3.26 B**) and this finding is in line with the data obtained in the sponge assay. The ANG2+VEGF combination showed an increase in microvessel sprouting in Cre-pos; FAK-Y397F^{KI} rings (when compared to Cre-neg; FAK-Y397F^{KI} rings) and the previously observed significant difference between the two genotypes after VEGF treatment alone is lost (**Figure 3.26 B**). This finding suggests that the combination of these two growth factors is able to overcome, at least partially, the effect of the endothelial specific FAK-Y397F mutation. This result has to be interpreted with caution as there is no significant increase between the VEGF vs VEGF+Ang2 treated rings from Cre-pos; FAK-Y397F^{KI}, indicating that the addition of Ang2 is not able to fully compensate for the endothelial specific FAK-Y397F mutation (**Figure 3.26 C**).

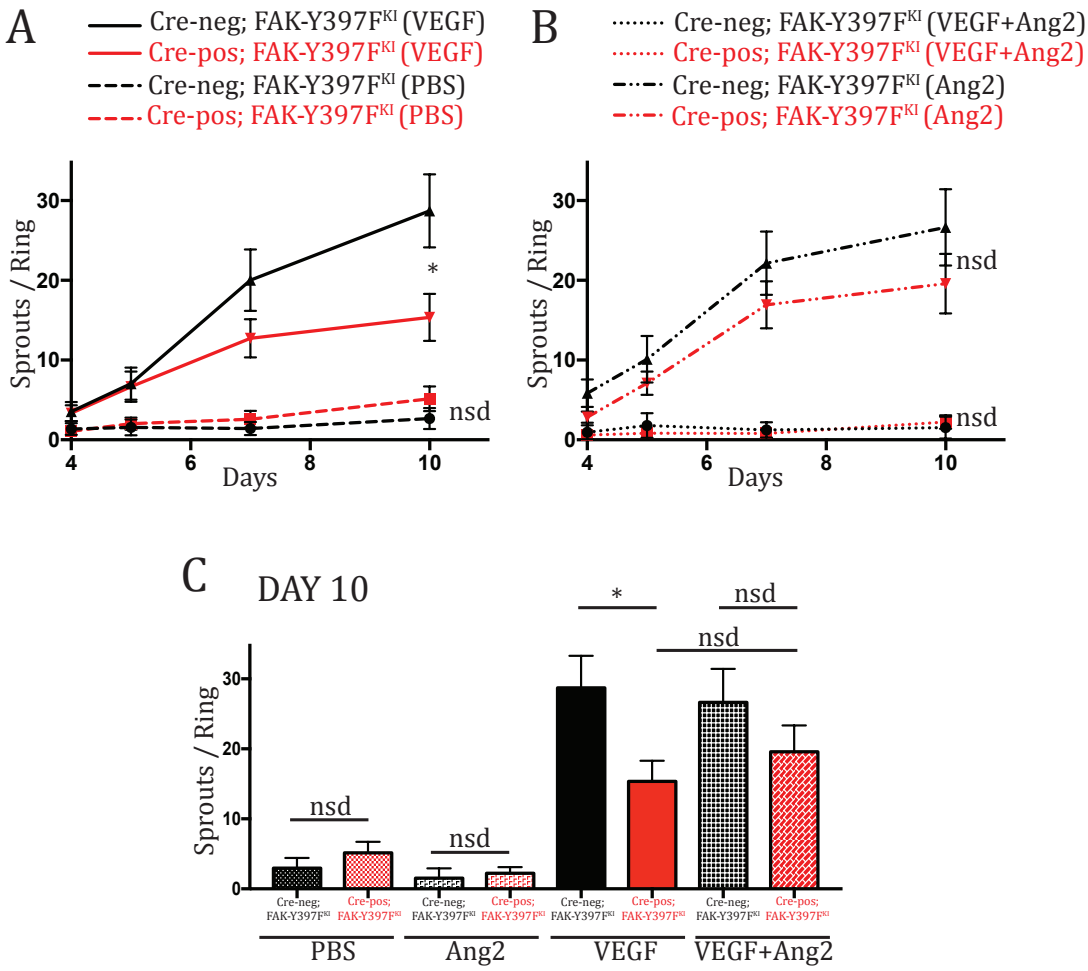

Figure 3.26: Endothelial specific FAK-Y397F mutation impairs VEGF-driven sprouting angiogenesis, but is partially rescued by Ang2 addition.
Cre-neg; FAK-Y397F^{KI} and Cre-pos; FAK-Y397F^{KI} mice were given tamoxifen 5 days prior to sacrifice. Aortas were dissected and cut into rings. Rings were starved overnight and then embedded in collagen matrix and treated with VEGF (**A**), PBS (**A**), Ang2 (**B**) or VEGF+Ang2 (**B**). The number of sprouts/ring was counted at Day 4, Day 5, Day 7 and Day 10 and averaged at each time point. The data from all the treatments at Day 10 are shown in (**C**). Statistical analysis indicates that the number of sprouts per ring was decreased in VEGF-treated rings dissected from Cre-pos; FAK-Y397F^{KI} mice when comparing to VEGF-treated rings from Cre-neg; FAK-Y397F^{KI}, indicating that FAK-Y397 phosphorylation in endothelial cells is essential for VEGF-driven sprouting angiogenesis. This defect is partially rescued when VEGF and Ang2 are administered at the same time to the aortic rings, as no statistical difference is seen between the two genotypes when treated with VEGF+Ang2. Data are shown as mean ± s.e.m; * $p<0.05$; nsd no significant difference. n=24-33 rings (dissected from 6 mice per genotype).

3.3. Endothelial-specific inactivation of FAK-Y861 phosphorylation impairs VEGF-driven sprouting

To study the effect that endothelial specific FAK-Y861F mutation has on growth factor-driven aortic ring sprouting, the aortic ring assay was performed with aortas from Cre-neg; FAK-Y861F^{KI} and Cre-pos; FAK-Y861F^{KI} mice. **Figure 3.27** A shows the obtained results and indicates that VEGF is able to trigger aortic ring sprouting in both Cre-neg; FAK-Y861F^{KI} and Cre-pos; FAK-Y861F^{KI} aortas (when compared to PBS treatment), proving that endothelial specific inactivation of FAK-Y861 phosphorylation does not affect VEGF-driven angiogenesis *in vivo*. These results confirm the previously obtained data on VEGF-driven angiogenesis in sponge assay.

In section 3.2.3 of this chapter, I have shown that ANG2 administration in sponges implanted in Cre-pos; FAK-Y861F^{KI} mice leads to an increase in microvessel density and indicates that ANG2 acts as a pro-angiogenic factor in FAK-Y861F mutated endothelial cells. Aortic ring assay with Cre-neg; FAK-Y861F^{KI} and Cre-pos; FAK-Y861F^{KI} aortas in the presence of ANG2 alone or in combination with VEGF (ANG2+VEGF) was performed to further investigate the effect of the endothelial specific FAK-Y861F mutation on ANG2-driven angiogenesis. Results presented in **Figure 3.27** B show that ANG2 alone is not able to trigger angiogenesis neither in Cre-neg; FAK-Y861F^{KI}, nor in Cre-pos; FAK-Y861F^{KI} aortas, indicating that ANG2 is not pro-angiogenic in FAK-Y861F mutated aortic rings. When treated with ANG2 and VEGF, aortic ring sprouting is triggered to a similar level in Cre-neg; FAK-Y861F^{KI} and Cre-pos; FAK-Y861F^{KI} rings, indicating that the endothelial-specific inactivation of FAK-Y861

phosphorylation has no impact on combined VEGF+ANG2-triggered angiogenesis.

Results from VEGF group were compared to results from ANG2+VEGF group, and this comparison showed that addition of ANG2 did not lead to an increase in the number of sprouting microvessels per aortic ring. This indicates that in this experimental setting ANG2 does not have a cumulative pro-angiogenic effect. Noteworthy is the fact that ANG2 does not have an anti-angiogenic effect either.

These results do not recapitulate the data obtained with the sponge assay where ANG2 administration leads to increased angiogenesis in FAK-Y861F mutated endothelium. One possibility is that a more fine-tuned design of the *ex-vivo* aortic ring assay is necessary to be able to mimic the sponge assay. Another possible explanation is that other components (as for example immune cells) might be involved in the phenotype observed *in vivo* (in the sponge assay) and that cannot be recapitulated *ex vivo* (in the aortic ring assay).

Several *in vivo* models and protocols are available to study the link between FAK-mutated endothelial cells and the immune cells. One way to study this interaction is to determine whether FAK-mutated endothelial cells produce and secrete a different panel of cytokines that will then differentially attract immune cells. As a first step, the *in vitro* cytokine profile of the control and mutated endothelial cells was investigated and is presented in the next section.

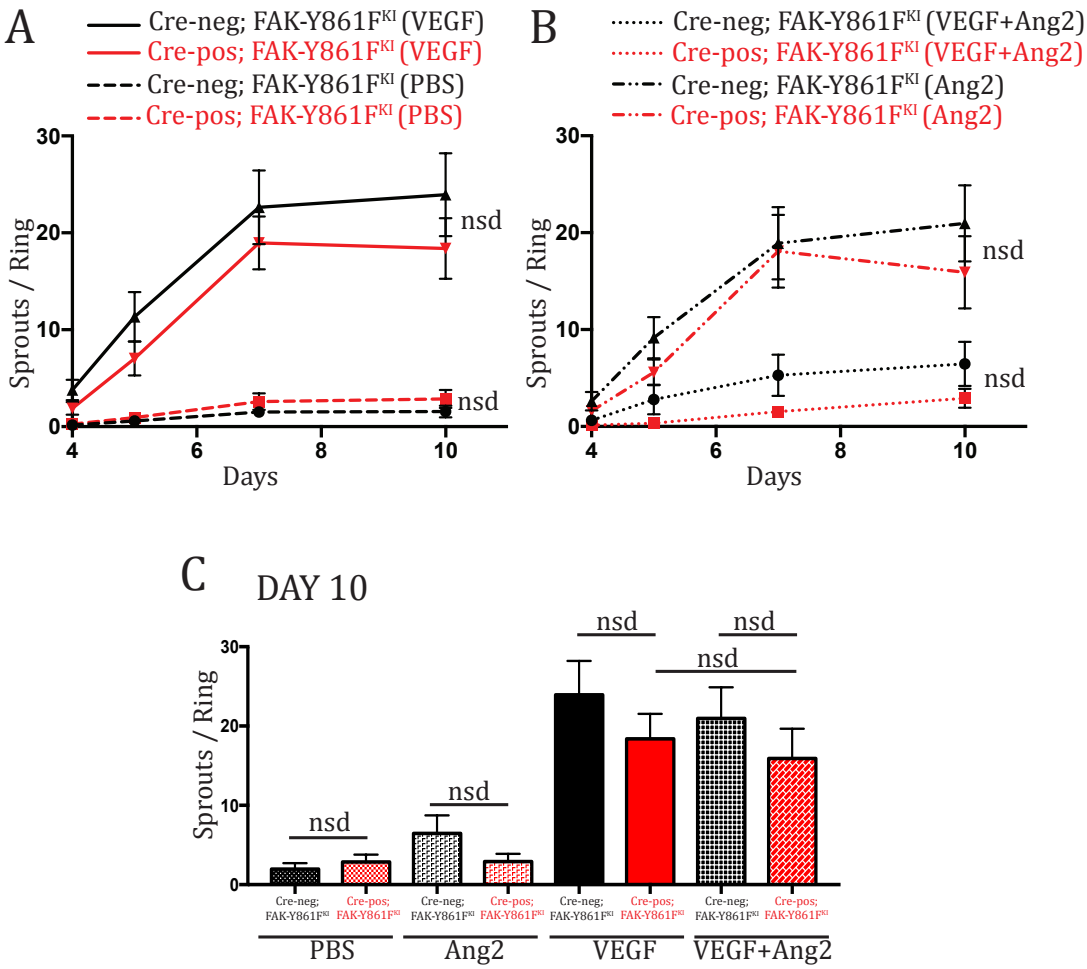

Figure 3.27: Endothelial specific FAK-Y861F mutation does not affect VEGF-driven sprouting angiogenesis, either in the presence, or in the absence of Ang2.

Cre-neg; FAK-Y861F^{KI} and Cre-pos; FAK-Y861F^{KI} mice were given tamoxifen 5 days prior to sacrifice. Aortas were dissected and cut into rings. Rings were starved overnight and then embedded in collagen matrix and treated with VEGF (**A**), PBS (**A**), Ang2 (**B**) or VEGF+Ang2 (**B**). The number of sprouts/ring was counted at Day 4, Day 5, Day 7 and Day 10 and averaged at each time point. The data from all the treatments at Day 10 are shown in (**C**). Statistical analysis indicates that the number of sprouts per ring was not affected in VEGF-treated rings dissected from Cre-pos; FAK-Y861F^{KI} mice when comparing to VEGF-treated rings from Cre-neg; FAK-Y861F^{KI}, indicating that FAK-Y861 phosphorylation in endothelial cells does not impair VEGF-driven sprouting angiogenesis. Ang2 alone did not act as a pro-angiogenic growth factor neither in rings from Cre-neg; FAK-Y861F^{KI} mice, nor in rings from Cre-pos; FAK-Y861F^{KI} mice. When Ang2 was combined with VEGF, sprouting angiogenesis equally triggered in rings from both genotypes indicating that endothelial FAK-Y861F mutation does not affect sprouting angiogenesis either positively, or negatively. Data are shown as mean ± s.e.m; * $p<0.05$; nsd no significant difference. n=26-35 rings (dissected from 6 mice per genotype).

4. Investigating the effect of endothelial FAK-Y397F and FAK-Y861F mutations on endothelial cytokines

Mouse lung endothelial cells were isolated from all the genotypes (Cre-neg; FAK-WT^{KI}, Cre-pos; FAK-WT^{KI}, Cre-neg; FAK-Y397F^{KI}, Cre-pos; FAK-Y397F^{KI}, Cre-neg; FAK-Y861F^{KI} and Cre-pos; FAK-Y861F^{KI} mice) and the induction of the chFAK-myc-tagged gene/protein and deletion of the endogenous mouseFAK gene/protein was confirmed by RT-qPCR and Western blotting in the Cre-pos cell lines as presented at the beginning of the Results chapter (**Figure 3.1 D and E**)[1].

Our laboratory has shown previously that loss of endothelial FAK can alter cytokine production and affect angiocrine signalling (Tavora, 2014b). Here I sought to ask whether endothelial FAK-Y397F and FAK-Y861F mutations have similar effects or not and if a differential cytokine profile could help explain some of the phenotypes observed *in vivo* and the discrepancies between the *in vivo* and the *ex-vivo* phenotypes, especially in regards to Ang2.

For this purpose the 6 cell lines were plated in 6cm dishes, in duplicates, left to grow for 24 hours and lysed. Mouse Cytokine Array panel A (R&D) was performed according to the manufacturer's instructions using the previously prepared lysates to determine whether cytokine production was differentially modulated in FAK-Y397F and FAK-Y861F mutated endothelial cells or if both mutations affected the cytokine profile in a similar way.

[1] Cre-neg; FAK-WT^{KI} and Cre-pos; FAK-WT^{KI} cell lines were isolated and immortalized by Dr. Annika Alexopoulou, former postdoctoral research assistant in our group. Cre-neg; FAK-WT^{KI}, Cre-pos; FAK-WT^{KI}, Cre-neg; FAK-Y397F^{KI} and Cre-pos; FAK-Y397F^{KI} cell lines were transfected by Dr. Isabelle Fernandez, former postdoctoral research assistant in our group. The remaining *in vitro* work presented in this section was performed by me.

The results presented in the following sections were generated using one cell line per genotype and are only a first preliminary study. I have isolated at least two other cell lines per genotype that will be used to confirm these first observations in the future.

4.1. Validation of the KO/KI system for in vitro cytokine arrays

Firstly the cytokine profile was compared between Cre-neg; FAK-WT^{KI} and Cre-pos; FAK-WT^{KI} and no difference was observed between these two cell lines, as shown on the cytokine dot-blot presented in **Figure 3.28**. A few cytokines were produced in large quantities and could be detected after 30 seconds of exposure (sICAM-1 and CCL2) or after 5 minutes of exposure (M-CSF, TIMP-1, and TNF-alpha); therefore, for these cytokines the measurements were taken at the cited exposure times. For the rest of cytokines, measurements were taken after 30 minutes of exposure and the Cre-pos/Cre neg ratio is presented for all the cytokines in **Figure 3.28**. Apart from the already cited cytokines that could be detected after short exposure times, very few other cytokines could be detected after 30 minutes exposure in both Cre-neg; FAK-WT^{KI} and Cre-pos; FAK-WT^{KI} cell lines, indicating that Cre-neg control and Cre-pos; FAK-WT^{KI} endothelial cells do not produce large amounts of any other cytokines and, more importantly, that the chFAK-WT-myc-tagged protein does not influence cytokine production.

4.2. Endothelial-specific FAK-Y397F mutation leads to an increase of a limited number of cytokines

The cytokine level in Cre pos; FAK-Y397F^{KI} was normalised to Cre neg; FAK-Y397F^{KI} and the fold-increase was calculated to determine the effect of FAK-Y397F^{KI} on the level of cytokines present in endothelial cell (**Figure 3.29**). Amongst the thirty-seven analysed targets, two cytokines - CCL1 and CCL2 - had their production 100-fold, and respectively, 350-fold increased.

Five other cytokines, namely CxCL10, CCL11, IL-10, IL-1F2 and IL-7 had their level increased more than 15- and up to 25-fold in the presence of FAK-Y397F mutation, but the biological reference of these results will need to be confirmed with biological repeats or by exploring these targets using other techniques.

4.3. Endothelial-specific FAK-Y861F mutation leads to an increase of a substantial number of cytokines

In a similar way the cytokine level in Cre-pos; FAK-Y861F^{KI} was normalised to Cre-neg; FAK-Y861F^{KI} and the fold-increase was used to determine which cytokines were more abundant in FAK-Y861F mutated endothelial cells. **Figure 3.30** shows that a larger panel of cytokines was affected by the FAK-Y861F mutation (as opposed to the FAK-Y397F mutation) and amongst these IL-12 p70, CXCL12, IL-23, IL-2, IL-1F2, IL-17, IL-16, IL-13, IL-1F3 have their levels increased more than 20- and up to 70-fold. CCL4 and IL-1F1 and CCL2 were more than 100-fold, 600-fold, and respectively 1150-fold more abundant in endothelial cells bearing the FAK-Y861F mutation. These

results highlight the potency of FAK-Y861F mutation to increase the level of cytokine production to a wider extend than the FAK-Y397F mutation, in endothelial cells; and more importantly, that most of these cytokines are differentially up-regulated by the two FAK mutations.

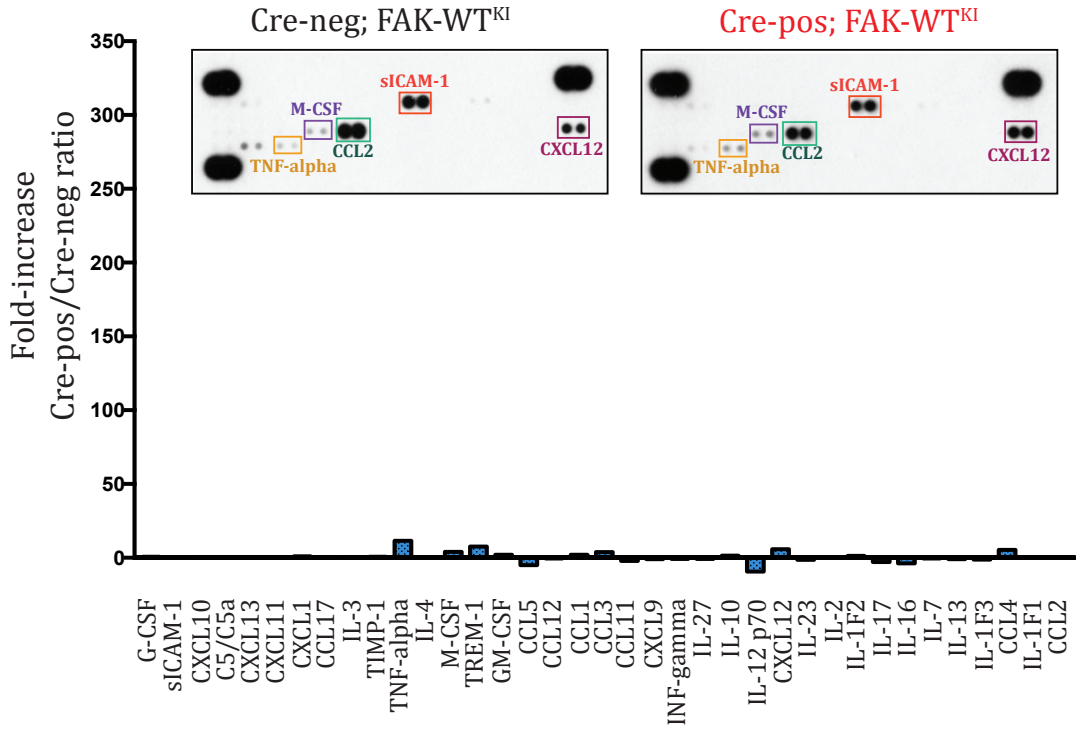

Figure 3.28: Endothelial cells isolated from Cre-neg; FAK-WT^{KI} and Cre-pos; FAK-WT^{KI} mice present with a similar cytokine profile *in vitro*

Endothelial cells were isolated from Cre-neg; FAK-WT^{KI} and Cre-pos; FAK-WT^{KI} mice, plated in 6 cm dishes in duplicates, left to grow overnight and lysed. Protein concentration was adjusted amongst the cell lysates and cell lysates were subsequently used to perform a cytokine array, according to the manufacturer's instructions. Both duplicates were used and were incubated with a membrane each. Pictures from one of each duplicate after 30 minutes of exposure per genotype are shown. CXCL12, sICAM-1, CCL2, M-CSF and TNF-alpha were produced by endothelial cells of both genotypes. Each membrane contains two dots per cytokine; therefore four measurements were available per cytokine and per genotype. The four measurements were averaged and the Cre-pos/Cre-neg ratio was calculated and is presented as fold-increase. The obtained data indicate the cytokine profile is similar between that endothelial cells isolated from Cre-neg; FAK-WT^{KI} and cells isolated from Cre-pos; FAK-WT^{KI} mice.

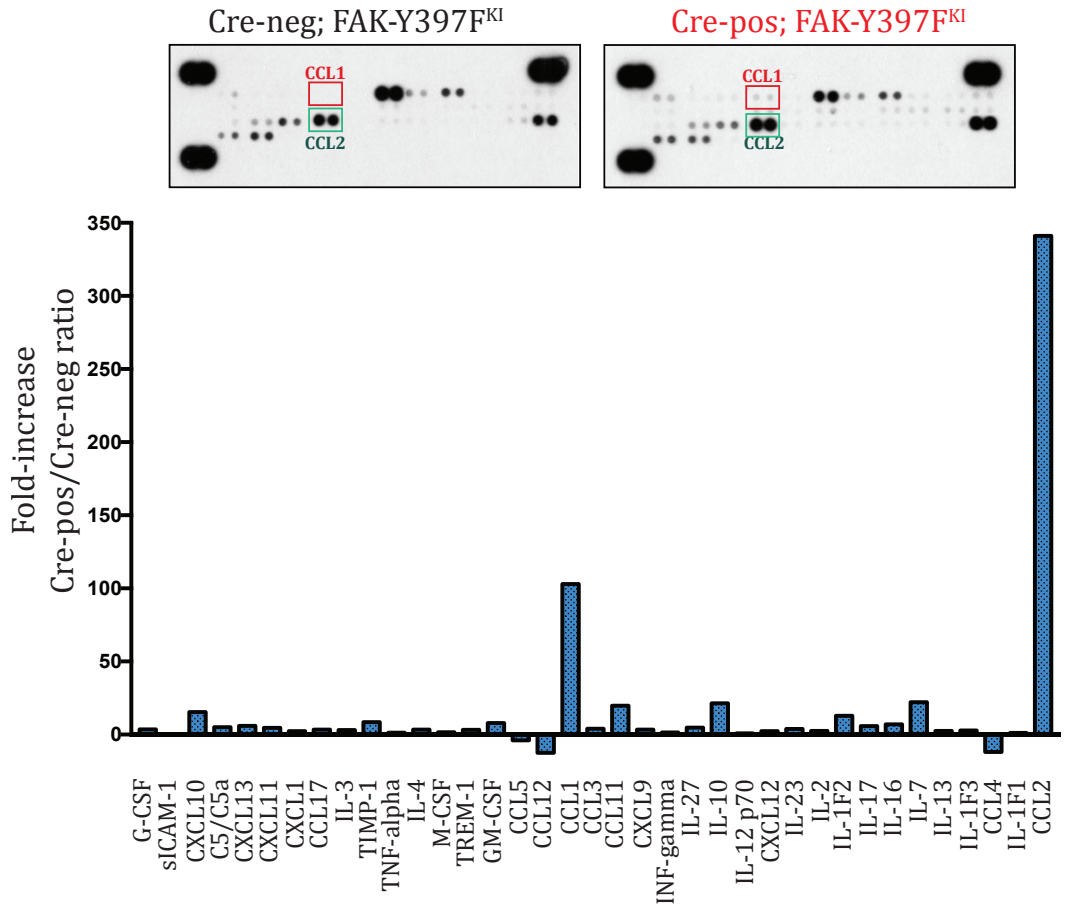

Figure 3.29: Endothelial cells isolated from Cre-pos; FAK-Y397F^{KI} mice produce particularly high levels of CCL1 and CCL2 cytokines *in vitro*

Endothelial cells were isolated from Cre-neg; FAK-Y397F^{KI} and Cre-pos; FAK-Y397F^{KI} mice, plated in 6 cm dishes in duplicates, left to grow overnight and lysed. Protein concentration was adjusted amongst the cell lysates and cell lysates were subsequently used to perform a cytokine array, according to the manufacturer's instructions. Both duplicates were used and were incubated with a membrane each. Pictures from one of each duplicate per genotype after 30 minutes of exposure are shown. Each membrane contains two dots per cytokine; therefore four measurements were available per cytokine and per genotype. The four measurements were averaged and the Cre-pos/Cre-neg ratio was calculated and is presented as fold-increase. The obtained data show a 100-fold and 350-fold increase in CCL1, and respectively CCL2 production when endothelial cells bear the FAK-Y397F mutation.

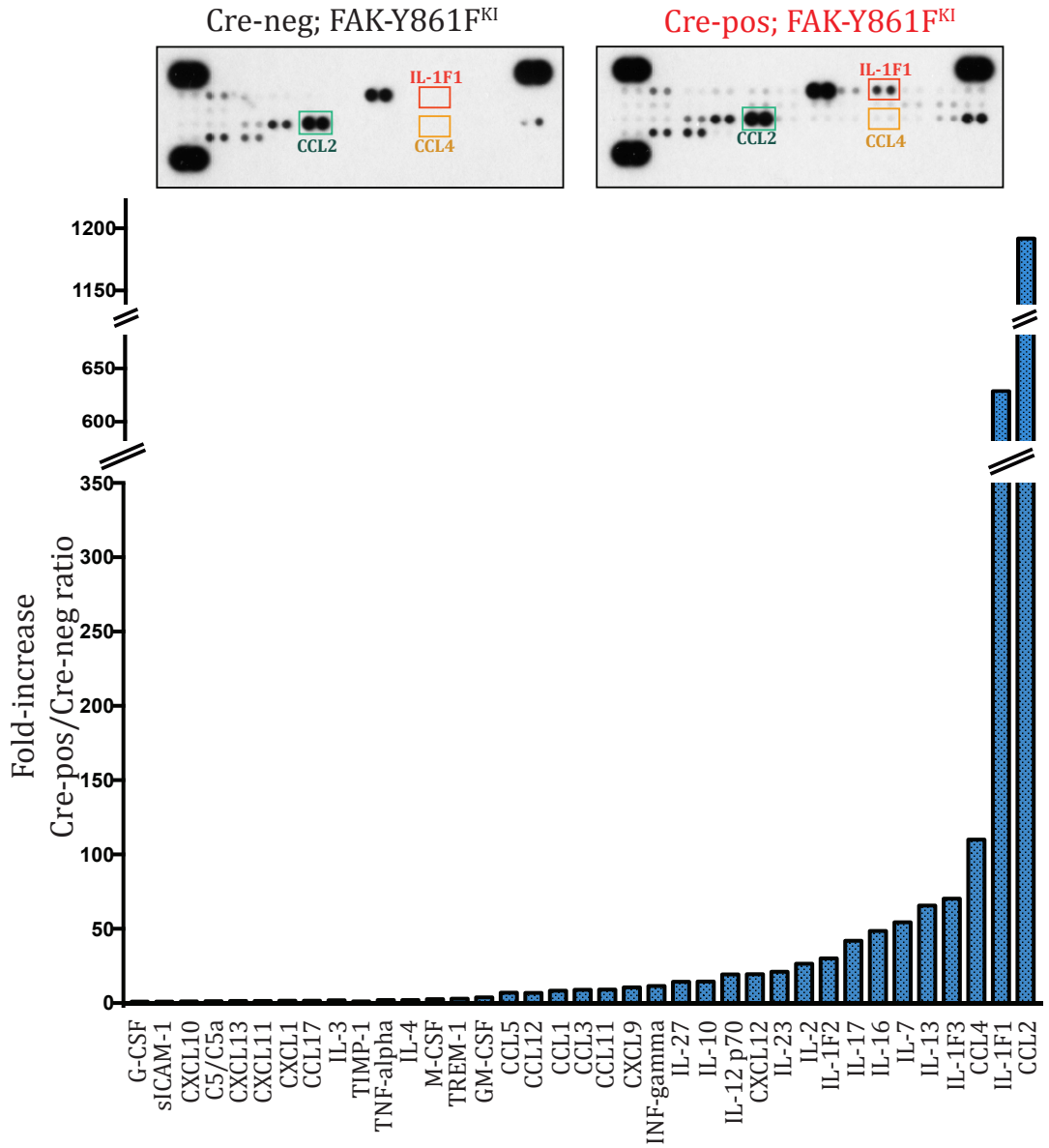

Figure 3.30: Endothelial cells isolated from Cre-pos; FAK-Y861F^{KI} mice produce particularly high levels of several cytokines, including CCL2, IL-1F1 and CCL4 *in vitro*

Endothelial cells were isolated from Cre-neg; FAK-Y861F^{KI} and Cre-pos; FAK-Y861F^{KI} mice, plated in 6 cm dishes in duplicates, left to grow overnight and lysed. Protein concentration was adjusted amongst the cell lysates and cell lysates were subsequently used to perform a cytokine array, according to the manufacturer's instructions. Both duplicates were used and were incubated with a membrane each. Pictures from one of each duplicate per genotype after 30 minutes of exposure are shown. Each membrane contains two dots per cytokine; therefore four measurements were available per cytokine and per genotype. The four measurements were averaged and the Cre-pos/Cre-neg ratio was calculated and is presented as fold-increase. The obtained data show a 100-fold, a 600-fold and a 1150-fold increase in the production of the CCL4, IL-1F1 and respectively CCL2, when endothelial cells bear the FAK-Y861F mutation.

4.4. *Differentially modified cytokines*

Table 3.2 presents the previously cited cytokines' fold-increase in the FAK-Y397F and FAK-Y861F mutated endothelial cells and highlights that CCL2 is the strongest up-regulated cytokine for both mutations. CCL2 was detected in Cre-neg; FAK-WT^{KI} and Cre-pos; FAK-WT^{KI} endothelial cells after very short exposure times and is therefore a cytokine that is constitutively produced by endothelial cells. Nevertheless, its production is increased more than 340-fold and 1150-fold when endothelial cells bear the FAK-Y397F, and respectively, the FAK-Y861F mutation.

Cytokine	Fold-increase in FAK-Y397F endothelial cells	Fold-increase in FAK-Y861F mutated endothelial cells
CCL2	341	1191
IL-1F1	1	628
CCL4	-11	109
IL-1F3	2	70
IL-13	2	65
IL-7	22	54
IL-16	6	48
IL-17	5	42
IL-1F2	12	30
IL-2	2	26
IL-23	3	21
CXCL12	2	19
IL-12 p70	0.8	19
IL-10	21	14
CCL11	19	9
CCL1	103	8

Table 3.2: Differential fold increase in cytokine production between FAK-Y397F and FAK-861F mutated endothelial cells.
The name of the cytokines specifically up-regulated in FAK-Y397F mutated endothelial cells are in red; in blue – the cytokines up-regulated in FAK-Y861F mutated endothelial cells; in purple is CCL2 - strongly up-regulated for both mutations.

CXCL12 is another cytokine that appeared to be constitutively produced by endothelial cells and that is 19-fold increased in Cre-pos; FAK-Y861F^{KI} endothelial cells specifically.

Most of the up-regulated cytokines are specifically up-regulated in Cre-pos; FAK-Y861F^{KI} endothelial cells and are presented in blue in **Table3.2**. The production of IL-7 and IL-1F2 are increased in both Cre-pos; FAK-Y397F^{KI} and Cre-pos; FAK-Y861F^{KI} endothelial cells, but the fold increase is at least twice high in Cre-pos; FAK-Y861F^{KI} endothelial cells, when compared to Cre-pos; FAK-Y397F^{KI} endothelial cells.

CCL1 is the only cytokine strongly up-regulated in Cre-pos; FAK-Y397F^{KI} endothelial cells specifically. The upregulation of CCL11 and IL-10 is stronger in Cre-pos; FAK-Y397F^{KI} endothelial cells, when compared to Cre-pos; FAK-Y861F^{KI} endothelial cells. But biological and technical repeats will be necessary to confirm these initial observations.

Summary: Cytokine production by FAK-Y397F and FAK-Y861F mutated endothelial cells in vitro

These preliminary results show that FAK-Y397F mutated endothelial cells are able to up-regulate only a limited number of the studied cytokines, such as CCL11, IL-10, CCL1 and CCL2. These cytokines are specific to Cre-pos; FAK-Y397F^{KI} endothelial cells, with the exception of CCL2, which is also up-regulated in Cre-pos; FAK-Y861F^{KI} endothelial cells. FAK-Y861F mutated endothelial cells are able to up-regulate a larger number of cytokines and to higher levels. In addition to CCL2, the following cytokines have their production increased - IL-1F1, CCL4, IL-1F3 and IL-13.

Whether FAK-Y397F and FAK-Y861F mutated tumour endothelial cells are up-regulating the same cytokines *in vivo* as the ones highlighted using endothelial cells *in vitro* and whether differential cytokine up-regulation in FAK-Y397F and FAK-Y861F mutated endothelial cells can explain the differential B16F0, CMT19T and LLC tumour phenotypes needs further investigation.

CHAPTER IV: DISCUSSION

Focal adhesion kinase (FAK) is a protein tyrosine kinase, found in the cell cytoplasm, that is expressed ubiquitously. It is activated and overexpressed in many solid cancers at advanced stages. FAK is known to promote tumour progression and metastasis through effects within the malignant cell compartment, as well as within the stromal cell compartment (Gabarra-Niecko, 2003). FAK controls cell migration, cell survival and gene expression. Within the tumour microenvironment FAK is a multifunctional regulator of cell signaling (Parsons, 2003; Zhao and Guan, 2009; Schaller, 2010; Lechertier and Hodivala-Dilke, 2012; Sulzmaier, Jean and Schlaepfer, 2014). In many tumour types, FAK promotes cell motility, survival and proliferation through both kinase-dependent and kinase-independent mechanisms and in the past few years, Phase I and II clinical trials have been initiated with FAK inhibitors (Brunton and Frame, 2008; Roy-Luzarraga and Hodivala-Dilke, 2016); however, some of the functions of FAK in tumorigenesis remain under investigation. Despite the vast amounts of data, the *in vivo* role of FAK in endothelial cells specifically, and in particular how its phosphorylation sites regulate tumour angiogenesis, is poorly understood. Although many studies *in vitro* have demonstrated roles for tyrosine phosphorylation sites of FAK in cell behavior in culture (Brunton, 2005; Serrels, 2012), almost nothing is known about the role of FAK-Y397 and FAK-Y861 phosphorylation in endothelial cells *in vivo*. Here I present data that I have accumulated during my PhD that shows, for the first time, that the unphosphorylatable mutant of FAK-Y397F is sufficient to affect tumour angiogenesis whereas the unphosphorylatable mutant of FAK-Y861F has much

less effect. The data from my thesis demonstrate that by making novel *in vivo* models of mutant FAK we can start to really understand how FAK regulates tumour angiogenesis *in vivo*.

Phosphorylation of FAK-Y397 allows Src to bind FAK via the revealed SH2-binding site. This initiates Src to transphosphorylate FAK on a number of tyrosine residues, including Y861. FAK–Y861 phosphorylation stimulates p130Cas binding, thus activating downstream PI3-kinase signaling (Mitra, 2005; Lechertier and Hodivala-Dilke, 2012; Schlaepfer 2014). Although FAK signaling appears to be straight-forward, some studies have shown that FAK can be upstream of unexpected pathways. For example, VEGF-stimulation can induce a Src-dependent increase in Y861 phosphorlyation, without an increase in Y397 phosphorylation (Abu-Ghazaleh, 2001). The deletion or depletion of *FAK* can enhance invadopodia formation, but cell migration is still inhibited (Ilic, 1995; Shen, 2005); and the re-expression of the FAK (K454R) kinase dead mutant allows for normal invadopodia formation whilst re-expression of FAK-Y397F mutant does not. Together these data highlight that understanding how different residues of FAK control cell behaviour *in vivo* becomes critical.

Endothelial-specific FAK-null mice have been developed using different inducible Cre drivers: PDGFB-CreERT (Tavora, 2010), SCL-CreERT (Weis, 2008; Schmidt, 2013) and Tie2-CreERT (Braren, 2006) and all show an impact on neovascularization. These data indicate that FAK is involved in angiogenesis, but how different tyrosine motifs of FAK regulate processes *in vivo* is still unexplained. One of the first FAK-point mutant knock-in mouse models was the FAK-kinase dead knockin, generated using SCL-CreERT–driven induction of the mutant FAK on one allele of FAK null mice (Zhao, 2010; Chen, 2012). This

strategy induces the one copy of the mutant FAK-kinase dead as a hemizygous and controls were hemizygous wild types. Our laboratory has shown that the global FAK-heterozygous mice display enhanced tumour growth and angiogenesis and thus these data suggest that half the expression levels of FAK can give an elevated tumour angiogenic response (Kostourou, 2013).

We were particularly interested in examining the role of phosphorylation of Y397 and Y861 specifically *in vivo*. But given that hemizygous FAK-mutants might lead results different from homozygous FAK mutants, we used mice where FAK could be knocked-out on both alleles and mutated FAK knocked-in on both alleles as well. Therefore we developed a series of endothelial cell-specific PDGFb-Cre^{ERT2} inducible mutant FAK-knockin mice which, when crossed with FAK-floxed mice, generate mice where endogenous FAK is knocked-out and mutant FAK, either WT, Y397F or Y861F, is simultaneously knocked-in driven by the ROSA 26 promoter, and where the knocked-in FAK is expressed in a homozygous and not hemizygous fashion (Claxton, 2008; Tavora, 2014a).

1. *Role of endothelial specific FAK-Y397 and FAK-Y861 phosphorylation in tumour growth and angiogenesis in vivo*

To study the role of endothelial specific FAK-Y397 and FAK-Y861 phosphorylation in tumour growth and angiogenesis *in vivo*, Cre-pos; FAK-Y397F^{KI} and Cre-neg; FAK-Y397F^{KI}; Cre-pos; FAK-Y861F^{KI} and Cre-neg; FAK-Y861F^{KI} mice were given melanoma (B16F0) or lung carcinoma (CMT19T or LLC) subcutaneous tumour cell injections. Subsequent tumour growth and angiogenesis was examined. The endothelial-specific FAK-Y397F mutation

resulted in delayed angiogenesis for all the studied subcutaneous models, suggesting that FAK-Y397 autophosphorylation in endothelial cells is essential for tumour angiogenesis. Previous work on FAK-kinase dead mutant mice actually showed no difference in tumour angiogenesis (Chen, 2012; Jean, 2014). In those studies the kinase dead mutation induces a reduction in phosphorylation of Y397 implying that this effect was not involved in tumour angiogenesis. However, our results suggest that phosphorylation of endothelial cell Y397 is indeed required for tumour angiogenesis. What could explain this apparent discrepancy is that in my study I have induced the endothelial mutation before the injection of tumour cells, where as in the kinase dead studies the FAK-kinase dead mutation was induced after tumour growth and presumably angiogenesis had been initiated (Jean, 2014). This implies that loss of Y397 phosphorylation may be important in the initiation of angiogenesis rather than the maintenance of established vessels. To test this hypothesis, it could be possible to perform tumour growth experiments and to administer tamoxifen after tumour cell injection. If tumour growth is not impaired, than this would confirm that FAK-Y397 phosphorylation is important in angiogenesis initiation, rather than in tumour vasculature maintenance and/or remodelling.

In addition, other studies have examined the effect of loss of the Y397 motif in developmental angiogenesis, where the mice have been mutated to induce a deletion of Y397 at exon 15 (Corsi, 2009). This exon 15 deletion mutation totally removes the Y397 motif from FAK, maintains kinase activity but was a constitutive, global mutant that caused embryonic lethality at around E12.5 onwards. These *FAK* exon 15 deleted embryos displayed hemorrhage, edema,

delayed artery formation and various vascular remodeling defects demonstrating that FAK-Y397 is required for normal development (Corsi, 2009). Although this was not an endothelial-specific knockout it does suggest that Y397 is required for at least some stages of developmental angiogenesis and in this regard correlates with our tumour angiogenesis defect in our Cre-pos; FAK-Y397F^{KI} mice. Our data suggest that targeting endothelial-specific FAK-Y397 phosphorylation is sufficient to affect tumour growth and may be worth pursuing clinically. Several papers have demonstrated that the scaffolding function of Y397 is important in FAK function and that inhibiting this scaffold function could provide pharmacologically relevant agents that may indeed be more effective than inhibiting FAK-kinase function alone (Cance, 2013). Inhibitors of scaffold function to Y397 have been tested and do show promise, but they are not specific for FAK-Y397 and thus there is some resistance in the field to take these into general clinical practice.

As tumour blood vessels develop they go through various stages of morphological changes that affect their function. Tumour blood vessels need to be well perfused but many reports have highlighted that their perfusion can be erratic and that this can affect tumour growth (Carmeliet, 2011). In addition tumour blood vessels are notoriously leaky with large intercellular gaps (Carmeliet, 2011). Lastly, supporting cell pericyte coverage can affect the stability of the vessels and their diameter that in-turn affect flow through the vessel (Carmeliet, 2011). In global FAK heterozygous mice in addition to the increased tumour vascularization, increased tumour blood vessel perfusion and increased associated VEGF-induced pAkt:Akt signaling with an rebalance in phosphorylation at Y397 vs Y861 residues was reported indicating that FAK

can affect these parameters (Kostourou, 2013). In contrast, in PDGFb-Cre^{ERT};FAKfl/fl mice, in addition to reduced tumour blood vessel density, there was an associated increase in tumour hypoxia and decreased VEGF-induced pAkt;Akt ration (Tavora, 2010). Thus I investigated these features in the tumour blood vessels in Cre-pos; FAK-Y397F^{KI} mutant mice. Tumour blood vessel perfusion, tumour blood vessel perimeter, Hoechst leakage and pericyte coverage were unaffected by the endothelial specific FAK-Y397F mutation. These data indicate that this mutation is able to delay tumour angiogenesis, but does not cause a perfusion or leakage defect, and does not lead to dilated tumour blood vessels or a impair maturation. In the case of B16F0 melanoma and CMT19T carcinoma, the delayed tumour angiogenesis observed in the Cre pos; FAK-Y397F^{KI} mice was accompanied by delayed tumour growth. It is therefore likely that the delayed tumour growth is a consequence of delayed tumour angiogenesis and that endothelial specific FAK-Y397F mutation affects tumour growth by quantitatively, rather that qualitatively, affecting tumour endothelium. Two supplementary observations support this hypothesis: delayed tumour angiogenesis at an early time point (Day 8) and increased tumour hypoxia (Day 17). Indeed, the delayed tumour angiogenesis was observed in 8-day old tumours before the difference in tumour volumes was apparent, suggesting that delay in tumour angiogenesis precedes, if not causes, delayed tumour growth. The endothelial cell-specific FAK-Y397F mutation leads to increased tumour hypoxia in 17-day old tumours, indicating that tumour cells lack oxygen in tumours irrigated by a reduced number of FAK-Y397F mutated blood vessels. This evidence suggests strongly that FAK-Y397F endothelial mutation, via reduced angiogenesis, affects oxygen availability as

demonstrated by the increased in tumour hypoxia, and leads to delayed tumour growth.

In contrast to these findings, the growth of LLC carcinoma tumours was not delayed by the endothelial-specific FAK-Y397F mutation. Interestingly this lack of a tumour growth phenotype was actually accompanied by reduced tumour angiogenesis in the Cre-pos; FAK-Y397F^{KI} mice. This suggests that the previously described hypothesis/conclusion – that delayed tumour growth is a consequence of delayed tumour angiogenesis – does not apply to the LLC tumour model, where the delayed tumour angiogenesis observed in 24-day old tumours does not affect tumour volumes and raises the question about the differences that exist between the three tumour models, about the parameters that drive/allow their growth and about the possibility that LLC carcinoma cells might require less oxygen. Tumour hypoxia has not yet been assessed in LLC tumours and it will be important to determine if decreased tumour angiogenesis leads to increased tumour hypoxia in a situation where tumour volumes are not affected by the endothelial specific FAK-Y397F mutation. Some studies have highlighted that tumour growth and angiogenesis are not always related (Adighibe, 2016). Indeed knowing that different tumour cell lines can produce different amounts and signatures of growth factors may well be a reason why the LLC tumour growth was not affected in the same way as the B16F0 or CMT19T tumour growth in the Cre-pos; FAK-Y397F^{KI} mice (Zhang, 2008).

Indeed, the results obtained for LLC tumour model in the Cre-pos; FAK-Y397F^{KI} mice raise several questions. For example, is the inefficiency of the anti-angiogenic affect of the endothelial FAK-Y397F mutation on tumour

volumes specific to the LLC tumour model? And, in the B16F0 and the CMT19T tumour models, is the anti-angiogenic effect of the endothelial FAK-Y397F mutation that leads to delayed tumour growth or is it a different parameter, not yet investigated, that is able to reduce tumour volumes in B16F0 and CMT19T, but not in LLC model?

The observation that the three studied tumour models do not present the same phenotype for the same endothelial FAK-Y397F mutation could be indicative that the anti-angiogenic effect of the mutation might not be the cause for delayed tumour growth. It raises the notion that there is a possibility that even for the B16F0 and CMT19T tumour models, the observed effect on tumour volumes, might not be completely attributable to reduced vasculature. Although against the dogma, this idea should not be ruled out. Indeed the endothelial FAK-Y397F mutation might have a paracrine effect on other stromal elements such as immune infiltrate or directly tumour cells, that collectively affect tumour growth. I will come back to this idea nearer the end of this chapter but others have shown that paracrine factors generated by endothelial cells can affect immune cell infiltrate and tumour cells directly, so this may well be an interesting idea to follow up in future experiments.

The observation that delayed angiogenesis does not necessarily lead to delayed tumour growth is either restricted to FAK-Y397F mutated endothelium, or to the LLC tumour model. Indeed, delayed tumour angiogenesis was also observed in 7- and 17-day old B16F0 tumours growth in Cre-pos; FAK-Y861F^{KI} mice. Nevertheless, quantification of tumour angiogenesis at Day 21 shows that there is no difference in tumour angiogenesis at this latest time point. Previous work has suggested that

phosphorylation of the FAK-Y861 motif is especially important in VEGF-induced angiogenic processes *in vitro* (Abu-Gazaleh, 2001). Indeed this study suggested that phosphorylation at FAK-Y861 is likely to play a more important role than phosphorylation at FAK-Y397 in the regulation of endothelial cell migration and apoptosis (Abu-Gazaleh, 2001). My data suggest that *in vivo*, it is possible that the inactivation of FAK-Y861 phosphorylation affects the initiation of tumour angiogenesis, but becomes dispensable for tumour endothelium remodeling, thus restoring blood vessel density at time points after day 21 of tumour growth.

Parameters of tumour blood vessel function and integrity were also analysed in the B16F0 tumours grown in Cre-pos; FAK-Y861F^{KI} mice. For all the parameters tested including tumour blood vessel perfusion, tumour blood vessel perimeter, Hoechst leakage and pericyte coverage and no difference was observed between Cre-pos; FAK-Y861F^{KI} and Cre-neg; FAK-Y861F^{KI} mice. Importantly, tumour hypoxia was not increased in B16F0 tumours grown in Cre-pos; FAK-Y861F^{KI} mice indicating that this mutation does not lead to decreased oxygen perfusion through the tumour (as the FAK-Y397F does). To further confirm this hypoxia phenotype, HIF-1α staining could be performed on tumour sections harvested at various time points; this would allow monitoring the relationship between the initially impaired tumour angiogenesis and the hypoxic tumour tissues. It should be noted that I analysed tumour hypoxia at Day 21, when the FAK-Y861F tumour angiogenesis defect was already resolved and blood vessel density was not reduced anymore. In future experiments it would be important to examine tumour hypoxia at earlier stage tumours in Cre-pos; FAK-Y861F^{KI} mice, ie., when the blood vessel density is low, and see if

this correlates with changes in hypoxia. Although it is unclear if similar scenarios have been discovered previously, if the endothelial specific FAK-Y861F mutation fails to induce tumour hypoxia in early time points when delayed tumour angiogenesis is observed, then perhaps the inability to trigger tumour hypoxia might explain why this mutation does not lead to impaired tumour growth. On the other hand, if hypoxia were affected in early time points and then overcome, as delayed angiogenesis is, then this would highlight the ability of FAK-Y861F mutation to overcome not only delayed tumour angiogenesis but also restore the levels of tumour cell hypoxia. Determining the similarities and the differences between the three tumour types in terms of tumour cell hypoxia as a result of endothelial FAK-Y861F mutation will provide clues into potential signalling mechanisms.

In a nutshell, the two FAK mutations in endothelial cells present with different hypoxia phenotype, more precisely endothelial FAK-Y397F mutation increases tumour cell hypoxia, whereas endothelial FAK-Y861F mutation does not have an effect on tumour hypoxia (at the studied time point). This is indicative that two phosphorylation sites of the same protein in endothelial cells might be able to differentially regulate signaling pathways leading to tumour cell hypoxia. This could be due to the differential ability of these endothelial mutations to affect tumour angiogenesis, but also the possibility that secreted factors, controlled by the mutated endothelial cells or other elements of the stroma could play a role.

Permeability through blood vessels is controlled at endothelial cell-cell junctions. VE-cadherin is one of the major cell-cell endothelial-specific adhesion molecules that is known to control vascular permeability (Dejana, 2008). In

human ECs, knockdown of FAK enhances the stability of cell-cell junctions with elevated VE-Cadherin at endothelial cell junctions suggesting further that FAK is directly involved in vessel permeability (Arnold, 2013). In endothelial-specific FAK-kinase dead mutant mice VEGF-induced vascular permeability was also reduced (Chen, 2012). This was demonstrated by injecting mice intradermally with VEGF and then following the 'leakage' of intravenously injected Evans blue dye into the surrounding skin. The suggested underlying mechanism was due to FAK-kinase regulation of VE-cadherin activity (Chen, 2012). Additionally tumour metastasis was shown to be reduced in EC-FAK-kinase dead mice suggesting that FAK inhibition using FAK-kinase-inhibitors may be a good strategy for controlling tumour metastasis (Jean, 2014). In these papers, the authors show that the endothelial cells from the EC-FAK-kinase dead mice have a reduction in levels of FAK-Y397 phosphorylation, implying that phosphorylation of Y397 maybe be involved in this process. In FAK exon 15 mutant mice (where the FAK-Y397 motif is absent) embryos showed heamorrhage (Corsi, 2009). This may be related to vessel leakage or, since these were global mutant mice and not endothelial-specific mutants, they may relate to non endothelial functions such as poor platelet function (Corsi, 2009). In my PhD I have tested tumour vascular leakage using adult endothelial cell-specific mutants and a different method. I waited for tumours to grow in the endothelial FAK-Y397F and endothelial FAK-Y861F mice and in an ante-mortem procedure injected the mice via the tail vein with Hoechst. The Hoechst can then leak out of the vessels in the tumour and is taken up by surrounding tumour cells as a measure of leakage. I found that unphosphorylated endothelial-specific FAK-Y397F or Y861F mutant mice had no apparent defect in tumour vascular

leakage. This means that it is unlikely that phosphorylation at FAK-Y397 and Y861 is involved in tumour vascular leakage. Although the different methods in measuring tumour vascular were employed it is hard to imagine that this could bias our results when we compare with previous studies. Importantly, understanding whether homozygous FAK-kinase dead mice show reduced tumour vessel leakage would be important to determine and our laboratory has developed these mice for this purpose. In future experiments understanding whether tumour metastasis, VE-Cadherin expression and function or responses to VEGF-induced permeability are affected by endothelial-specific FAK-Y397F or endothelial-specific FAK-Y861F mutations would be of interest. Metastasis could be investigated using the B16F10 tumour model, that allows these particular type of melanoma cells to form metastasis in the lungs. Alternatively, spontaneous tumour models (such as Rip-TAG models) could be crosses with the KI colonies to look at the role of tumour angiogenesis in a more physiologically relevant metastasis assay.

2. Role of endothelial specific FAK-Y397 and FAK-Y861 phosphorylation in growth-factor induced angio-genesis in vivo

Several publications have demonstrated that tumour angiogenesis is governed by responses to tumour cell derived growth factors (Ziyad, 2011; Gacche, 2015; Yadav, 2015). In endothelial cells isolated from tumours, the levels of FAK-Y397 phosophorylation are elevated and have been linked, indirectly, with growth factor-stimulated enhanced endothelial cell migration an essential endothelial cell response in tumour angiogenesis (Angelucci, 2007;

Lu, 2007). In whole animals, endothelial-specific FAK-knockout mice have been used previously to test whether specific growth factor induced angiogenesis was altered (Tavora, 2010). In these studies both VEGF and bFGF induced angiogenesis was inhibited in ECFAK-null mice (Tavora, 2010). In contrast VEGF induced angiogenesis was enhanced in global FAK heterozygous mice indicating that somehow, FAK could regulate specific growth factor induced angiogenic responses, in a dose dependent fashion, in a tumour-free environment (Kostourou, 2013). However, understanding the role of phosphorylation at FAK-Y397 or FAK-Y861 was not possible in these mice. In order to test the effect of endothelial-specific FAK-Y397F and endothelial-specific FAK-Y861F in growth factor driven angiogenesis *in vivo*, and because differential responses to tumours may reflect changes in the cocktail of growth factors generated from different tumour cells, sponge assay (an *in vivo* growth factor induced angiogenesis assay) was performed in our endothelial-specific FAK-Y397F and endothelial-specific FAK-Y861F mutant mice. The effects of these mutations on VEGF, PlGF, bFGF and Ang2 stimulated angiogenesis were assessed.

Endothelial specific FAK-Y397F mutation impairs microvessel infiltration in VEGF, PlGF and bFGF stimulated *in vivo* growth factor induced assays. My results indicate that FAK-Y397 auto- phosphorylation site plays a major role in all the studied growth factor initiated pathways. This is not surprising as this mutation presented with a strong tumour angiogenesis phenotype in all the studied tumour models.

Interestingly, endothelial FAK-Y397F mutation also affected microvessel infiltration in PBS control sponges suggesting that this mutation

might be able to impair angiogenesis independently of the growth factor that is triggering it. Indeed, since FAK-deficiency has been related to an increase in endothelial cell apoptosis and decrease in proliferation (Tavora, 2010) endothelial FAK-Y397F mutation may induce baseline changes in endothelial cell apoptosis which would affect the overall survival rate of the endothelial cells and this independently of the growth factor stimulation.

This observation might be important for tumour models as well. For example, when anti-VEGF antibodies were used in animal models of pancreatic cancer, they showed a temporary reduction in tumour blood vessels (Casanovas, 2005). Casanovas *et al.* demonstrated that resistance to anti-VEGF therapy was enabled by compensatory mechanisms involving bFGF. Since both VEGF and bFGF signaling are reduced by the endothelial specific FAK-Y397F mutation, it would be interesting to investigate if delayed angiogenesis would be temporary or more long lasting in a similar model of pancreatic cancer.

In contrast to the endothelial-specific FAK-Y397F mutation, endothelial specific FAK-Y861F mutant mice did not show changes in microvessel infiltration in VEGF, PlGF and bFGF treated sponges. These data indicate that phosphorylation and FAK-Y861 is dispensable for angiogenesis in this experimental setting. The finding that FAK-Y861F mutation does not affect VEGF signaling is surprising, especially since previous *in vitro* work has shown that VEGF-stimulated angiogenesis responses may act predominantly via phosphorylation at FAK-Y861 and not FAK-Y397 (Abu-Ghazaleh, 2001). What this tells us about the differential responses to tumour angiogenesis in early and late stage B16F0 or even in the CMT and LLC tumour still remains a

mystery. It must be noted that the cited study was conducted *in vitro* and in 2D culture conditions and it is possible that the difference in the models and approaches (*in vitro* vs *in vivo/ex-vivo*; 2D model vs 3D model) could explain why the same results are not obtained. Nevertheless, in the area of cancer research and tumour angiogenesis, *in vivo* and 3D models are mostly relevant.

Microvessel infiltration in sponges and tumour angiogenesis can be governed by different mechanisms, and this is not only due to tumour cell presence, but also to tumour stroma, such as cancer associated fibroblasts and tumour infiltrated immune cells. It may be that actually what governs the role of FAK-Y861 phosphorylation is not to do with differential growth factor responses but differential responses to other components of the tumour microenvironment.

In my growth factor-induced angiogenesis assays *in vivo*, Ang2 was not able to trigger microvessel infiltration into the sponges implanted in Cre-negative control mice as strikingly as VEGF did. This is in line with previous work, especially from Helmut Augustin lab that shows that Ang2 needs to work in partnership with other growth factors to control endothelial cell behavior (Felcht, 2012). Nevertheless when endothelial cells bear the FAK-Y397F mutation microvessel infiltration into Ang2 containing sponges is decreased. This might be due to the fact that in all conditions, including control conditions microvessel infiltration was decreased. However microvessel infiltration was increased upon Ang2 treatment in cells bearing the FAK-Y861F mutation, indicating that Ang2 is sensed as a pro-angiogenic factor by FAK-Y861F mutated endothelial cells. This is a very exciting observation and one that will be followed up in future experiments. Ang2 has

been reported to be produced by endothelial cells (Fiedler, 2004). Previous work showed an involvement of FAK-S910 in Tie-2 expressing endothelial cells (Felcht, 2012). However it is not known to date whether loss of FAK-Y861 phosphorylation could affect Ang2 production that in-turn could affect different parameters of tumour cell growth, other tumour micro-environmental elements and endothelial cell behaviour. Indeed it will be very interesting to understand how switching to a non-phosphorylatable version of FAK-Y861 makes the endothelial cells responsive to Ang2 and whether this effect is due to changes in Ang2 receptor expression (Tie1 and Tie2) or activity on these mutant endothelial cells. It would be of interest also to examine whether B16F0, CMT19T and LLC tumour cells all have differential Ang2 expression relative to other growth factors and how the balance of these growth factors might affect angiogenic responses in growth factor induced assays *in vivo*. Another aspect to consider is potential changes in growth factor receptors (VEGFR1, VEGFR2, FGFR2, etc) at the plasma membrane of endothelial cells due to FAK-Y397F or FAK-Y861F mutations.

Lastly, it is clear that these growth factor induced angiogenesis assays will induces changes cytokine production and in immune infiltrate into sponges that may not reflect the cytokine and immune infiltrate within the tumours and might complicate the interpretation of the results (Crusz and Balkwill, 2015). Thus angiogenesis assays *ex vivo*, in controlled micro environments were also employed.

3. Role of endothelial specific FAK-Y397 and FAK-Y861 phosphorylation in growth-factor induced angiogenesis ex vivo

Sprouting angiogenesis was next studied *ex vivo* using the aortic rings assay (Baker, 2011). This method is used extensively to examine growth factor induced angiogenic responses *ex vivo* (Baker, 2011). Using aortic rings isolated from endothelial-specific WT, FAK-Y397F or FAK-Y 861 mice and their controls I studied *ex vivo* angiogenic responses to VEGF, Ang2 or the combination of both (VEGF+Ang2).

As observed in the sponge assay and in line with tumour angiogenesis data, endothelial specific FAK-Y397F mutation impairs VEGF-driven sprouting angiogenesis. Moreover Ang2 does not act as a pro-angiogenic growth factor on the FAK-Y397F mutated sprouts. Nevertheless when Ang2 is given in combination with VEGF, the previously observed impaired sprouting angiogenesis is partially rescued. This is a very surprising observation as endothelial specific FAK-Y397F mutation has presented with a very strong anti- angiogenic phenotype in all the performed assays. There was only one other occasion when this mutation has had a milder effect, and more specifically endothelial FAK-Y397F mutation did not delay tumour growth in the LLC carcinoma model. This suggests that there might be a link between the milder LLC tumour growth phenotype in the endothelial-specific FAK-Y397F mice and the ability of Ang2 to partially rescue the impaired sprouting angiogenesis phenotype. This hypothesis could be investigated by determining if LLC tumours attract a different Ang2-responsive immune cell

infiltrate to that in B16F0 or CMT19T tumours and thus somehow regulate tumour growth.

Endothelial specific FAK-Y861F mutation does not impair VEGF-driven sprouting angiogenesis in aortic rings and this finding is in line with the data obtained in the sponge assay. Ang2 alone does not trigger angiogenesis either in control, or in the endothelial FAK-Y861F mutated sprouts, indicating that in this experimental setting Ang2 does not act as a pro-angiogenic growth factor. When endothelial FAK-Y861F mutated sprouts are treated with the VEGF+Ang2 combination, sprouting angiogenesis is triggered to a level similar to the previously observed VEGF-driven sprouting angiogenesis. This indicates that Ang2 does not act as an anti-angiogenic growth factor either in control, or in the FAK-Y861F mutated endothelial cells, in this experimental setting.

Overall the findings for the FAK-Y861F mutation indicate that Ang2 does not act as a pro-angiogenic factor in the *ex vivo* aortic ring assay, where immune cells do not play a role, whereas it can be sensed as a pro-angiogenic factor by FAK-Y861F mutated endothelial cells in the *in vivo* sponge assay, where immune cells could potentially infiltrate the sponges. This might suggest that Ang2 is able to act as a pro-angiogenic factor in endothelial cells bearing the FAK-Y861F mutation through immune cells.

4 Role of FAK-Y397 and FAK-Y861 phosphorylation in endothelial cell cytokine production in vitro

FAK can regulate transcription via its scaffolding functions in the nucleus (Lim, 2012). In addition to its roles in tumour growth and angiogenesis initiation, endothelial-specific FAK has been shown to regulate cytokine production in response to DNA-damaging agents (Tavora, 2014b). Several studies have implicated endothelial cells as producers of cytokines and have shown that cytokines can control the efficacy of DNA-damaging agents (Gilbert, 2010; Acharyya, 2012; Nakasone, 2012; Sun, 2012; Lu, 2013). These changes in paracrine signals of endothelial cells *in vivo* have been coined angiocrine signals, ie paracrine signals originating from endothelial cells that control the surrounding malignant cell responses. Although the endothelial cell specific loss of FAK in tumour blood vessels was not sufficient to affect baseline cytokine production, treatment of endothelial cells with DNA-damaging agents such as doxorubicin or radiation induced an increase in cytokine production from wild-type, but not FAK-null endothelial cells (Tavora, 2014b).

The regulation of DNA-damage induced cytokine production by FAK was controlled by changes in NF-kB signaling, a known regulator of cytokine production (Funakoshi-Tago, 2003; Zhang, 2006; Petzold, 2009; Tseng, 2010; Ben-Neriah, 2011; DiDonato, 2012; Tavora, 2014b). Although of great interest as a possible regulator of chemosensitisation in cancer therapy this study did not address the roles of endothelial cell FAK-Y397 and FAK-Y861 phosphorylation in cytokine production. In my project I isolated endothelial cells from Cre-neg and Cre-pos; FAK-WT^{KI}, FAK-Y397F^{KI} and FAK-Y861^{KI} mice. Using similar protein profiler arrays to those used in the EC-FAK-knockout

study I showed that the FAK-Y397F mutation induced significant and dramatic increase in CCL1 and CCL2 production. In contrast FAK-Y861F mutations induced much less of a change in CCL1 but an increase in a several other cytokines with a particularly a massive (100 fold or more) increase in IL-13, IL-1F3, CCL4, IL-1F1 and CCL2. Why total deletion of endothelial-cell FAK would not affect cytokine production prior to treatment with DNA-damaging agents, but that non-phosphorylation mutations of FAK-Y397F and FAK-Y861F should induce changes is still unclear and might relate to changes in signalling down stream of FAK-Y397F and FAK-Y861F that are not apparent in the FAK-null endothelial cells. It is of special interest that the FAK-Y861F mutation should induce such a dramatic change in a wide range of cytokines that the FAK-Y397F mutant does not. It is tempting to speculate that these data may relate to differential tumour growth and angiogenesis responses in the Cre-pos; FAK-Y397F^{KI} and Cre-pos; FAK-Y861F^{KI} mice, possibly by changing immune infiltrate responses and thus dependence on endothelial FAK for angiogenic changes. In other words, could it be that the change in the cytokine profiles of these mutant forms of endothelial cells is able to compensate for the quantitative defect in blood vessel density without affecting tumour growth? It should be noted that these experiments are still preliminary and that further repeats and statistical analysis would be required to really confirm them. Nevertheless FAK-KO endothelial cells where shown to have the expression of their cytokines modulated after exposure to doxorubicine and these cytokine variations have been linked to NF-kB signalling (Tavora, 2014b). Therefore understanding how cytokine production is regulated by phosphorylation status of FAK will be of great interest in future studies.

CONCLUDING REMARKS

My PhD studies have demonstrated the *in vivo* roles for phosphorylation of FAK-Y397 and FAK-Y861 in tumour angiogenesis. The growth factor specific angiogenic responses *in vivo* and *ex vivo* reveal differential responses to VEGF, PlGF, bFGF and Ang2 stimulation depending on the FAK-Y397F or FAK-Y861 mutations.

Endothelial cells bearing FAK-Y397F or FAK-Y861F mutation have been isolated from the mutated mice and future work, designed to understand the molecular mechanisms underlying the differential phenotypes observed *in vivo*, will include using these cells to confirm the cytokine array findings, to perform adhesion assays, growth factor induced migration assays, proliferation and apoptosis assays. Importantly examining integrin expression and activity as well as growth factor receptor expression levels and regulation may shed light on the differential responses to the different growth factors and explain how these might relate back to angiogenesis control *in vivo*. Obviously determining the effect of Y397F and Y861F mutations on downstream signaling such as ERK, Akt and JNK signaling pathways will be essential. Lastly, how differential cytokine production actually affect tumour growth and angiogenesis will be a study that opens a new field of research in the arena of FAK, angiogenesis and angiocrine signaling.

When I started this PhD project it was my intention to report whether or not non-phosphorylatable forms of FAK-Y397 and FAK-Y861 can actually inhibit tumour angiogenesis and tumour growth. Previous *in vitro* studies suggested that the story might be straight-forward. However, it is clear that the

power of using the endothelial cell-specific FAK-mutant mice in *in vivo* studies means that we can learn a lot more than we ever envisaged. The future will hold more opportunities for us to learn even more about how this non-receptor protein tyrosine kinase, that has been studied for over 25 years, fulfills its functions in physiological and pathological conditions *in vivo*.

Appendix I

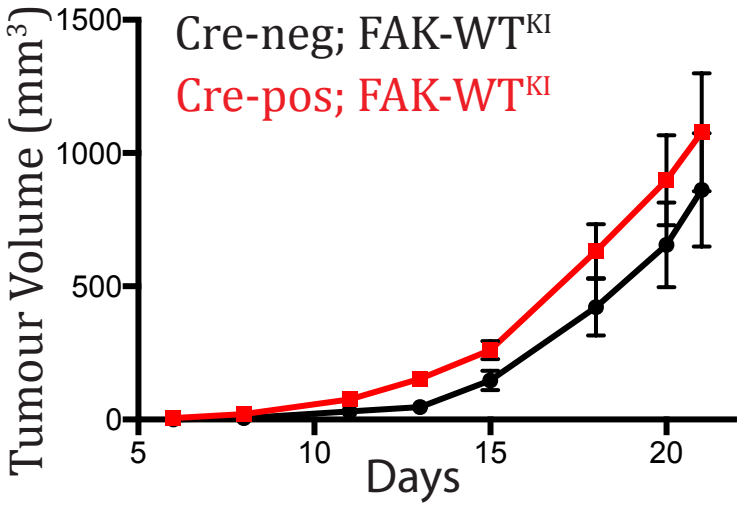

Appendix Figure A3.1: Reintroducing a WT version of FAK in endothelial cells does not affect B16F0 tumour growth *in vivo*

Cre-neg; FAK-WT^{KI} and Cre-pos; FAK-WT^{KI} mice were given subcutaneous injections of syngeneic B16F0 melanoma cells, 5-7 days after tamoxifen injection. Tumour dimensions were measured from day 6 to day 21 and tumour volumes calculated (Volume = 0.52 x Length x Width^2). At day 21 tumours were dissected. Statistical t-Student test was performed and no significant difference in tumour growth was determined between Cre-neg; FAK-WT^{KI} and Cre-pos; FAK-WT^{KI} mice indicating that knocking-in a WT version of FAK does not affect B16F0 melanoma tumour growth. n=8-11 mice/genotype.

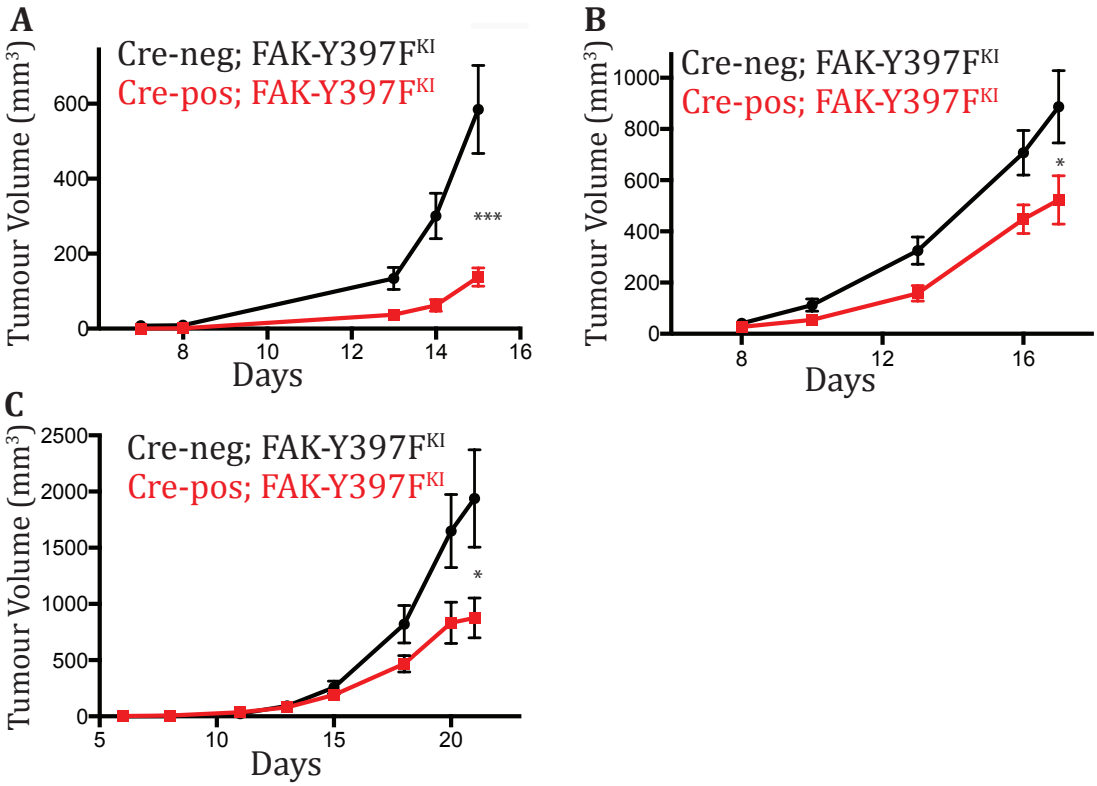

Appendix Figure A3.2: Endothelial-specific inactivation of FAK-Y397 phosphorylation inhibits B16F0 tumour growth.

Cre-neg; FAK-Y397F^{KI} and Cre-pos; FAK-Y397F^{KI} mice were given subcutaneous injections of syngeneic B16F0 melanoma cells, 5-7 days after tamoxifen injection. Tumour dimensions were measured from day 6 and up to day 21 and tumour volumes calculated (Volume = 0.52 x Length x Width^2). (**A**), (**B**) and (**C**) represent three independent experimental repeats and indicate that tumour growth was significantly retarded in Cre-pos; FAK-Y397F^{KI} mice when compared to Cre-neg; FAK-Y397F^{KI}. * P<0.05. *** P<0.005. n=6-13 mice/genotype.

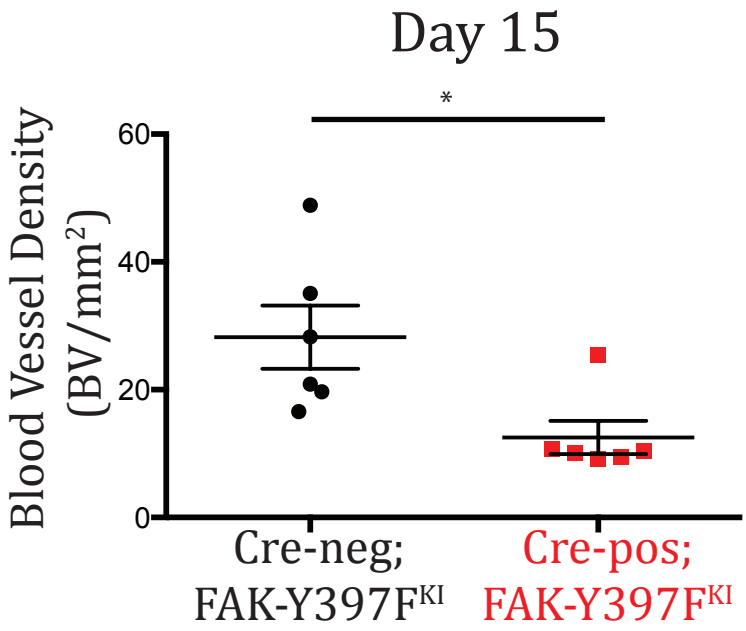

Appendix Figure A3.3: Endothelial-specific inactivation of FAK-Y397 phosphorylation is sufficient to reduce B16F0 tumour angiogenesis *in vivo*

B16F0 tumour blood vessel density was calculated by counting all the endomucin-positive blood vessels across the entire midline tumour section from size-matched 15-day-old tumours. Blood vessel density quantification indicated that FAK-Y397F mutation in endothelial cells delays B16F0 tumour angiogenesis. Values are given as means + s.e.m. * $P<0.05$. n=6 mice/genotype.

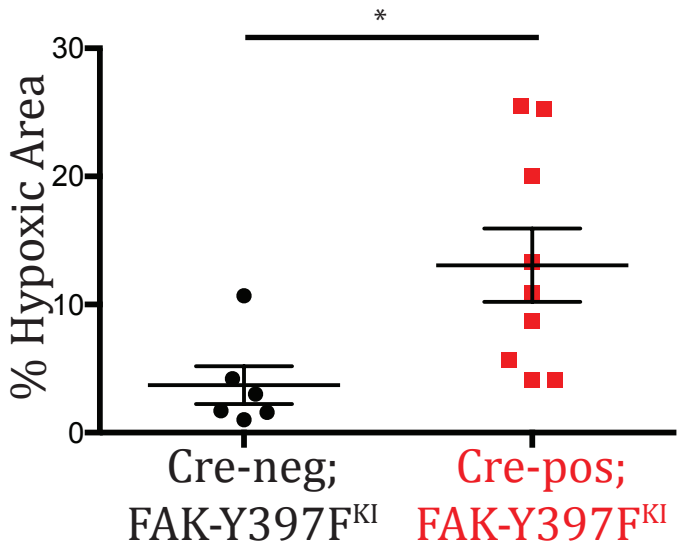

Appendix Figure A3.4: Endothelial-specific inactivation of FAK-Y397 phosphorylation leads to increased B16F0 tumour hypoxia *in vivo*

B16F0 tumour-burdened Cre-neg; FAK-Y397F^{KI} and Cre-pos; FAK-Y397F^{KI} were given intraperitoneal injections of Pimonidazole probe. FITC-anti-Pimonidazole antibody was used to detect hypoxic regions. The percentage of hypoxic area was determined by dividing the Pimonidazole stained area by the total field area. This data indicates that endothelial specific inactivation of FAK-Y397 phosphorylation leads to an increase in tumour hypoxia. Values are given as means + s.e.m. * $p<0.05$. n=6-9 mice/genotype.

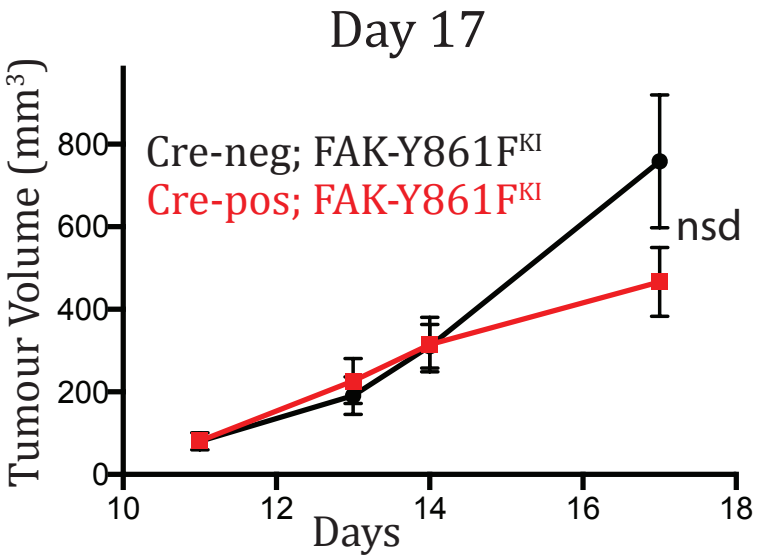

Appendix Figure A3.5: Endothelial-specific inactivation of FAK-Y861 phosphorylation does not affect B16F0 tumour growth.

Cre-neg; FAK-Y861F^{KI} and Cre-pos; FAK-Y861F^{KI} mice were given subcutaneous injections of syngeneic B16F0 melanoma cells, 5-7 days after tamoxifen injection. Tumour dimensions were measured from day 11 to day 17 and tumour volumes calculated (Volume = 0.52 x Length x Width^2). At day 17 tumours were dissected. No significant difference in tumour growth was determined between Cre-neg; FAK-Y861F^{KI} and Cre-pos; FAK-Y861F^{KI} mice. Values are given as means + s.e.m. n=8-11 mice/genotype.

AKNOWLEDGEMENTS

I want to thank my primary supervisor Professor Kairbaan Hodivala-Dilke for her support, advice and encouragement during my 4 years. Thank you for your patience and understanding. I want to thank my secondary supervisor Professor Hemant Kocher for advice and support. I am also grateful to Cancer Research-UK for funding this work.

I also want to thank Dr. Isabelle Fernandez and Dr. Silvia Batista for their teaching and friendship. I know I can always count on you! I want to thank Dr. Tanguy Lechertier for his help with experimental work and friendships. I am very grateful to Julie Holdsworth for the technical teaching, support and friendship and to Bruce Williams for his help with experimental procedures.

I am thankful to all the members of Cell Adhesion and Angiogenesis Laboratory: Dr. Annika Alexopoulou, Dr. Gabriela D'Amico-Lago, Fevzi Demircioglu, Dr. Delphine Lees, Dr. Louise Reynolds, Dr. Bernardo Tavora and Dr. Ping Pui Wong as well as to the more recent recruits: Matthew Scott Dukinfield, Dr. Jose Munoz-Felix, Marina Elena Roy Luzarraga and Dr. Ana Rita Pedrosa.

I want to thank all the members of Tumour Biology Department for the fun and support. Thank you Ami, Beta, Caroline, Ed, Francesca, Ivan and Zareen for helping me combine work and fun.

A special thank you for my dear friends Arina, Claire, Letitia, Marina and Misha, Adrien and Michele for being understanding and always there for me.

I want to thank my parents, grandparents and my sister Alexandrina for always believing in me and a special thank you goes to Romain for his endless patience and kindness.

BIBLIOGRAPHY

Abedi, H. and I. Zachary (1997). "Vascular endothelial growth factor stimulates tyrosine phosphorylation and recruitment to new focal adhesions of focal adhesion kinase and paxillin in endothelial cells." J Biol Chem 272(24): 15442-15451.

Abu-Ghazaleh, R., J. Kabir, H. Jia, M. Lobo and I. Zachary (2001). "Src mediates stimulation by vascular endothelial growth factor of the phosphorylation of focal adhesion kinase at tyrosine 861, and migration and anti-apoptosis in endothelial cells." Biochem J 360(Pt 1): 255-264.

Acharyya, S., T. Oskarsson, S. Vanharanta, S. Malladi, J. Kim, P. G. Morris, K. Manova-Todorova, M. Leversha, N. Hogg, V. E. Seshan, L. Norton, E. Brogi and J. Massague (2012). "A CXCL1 paracrine network links cancer chemoresistance and metastasis." Cell 150(1): 165-178.

Adighibe, O., R. D. Leek, M. Fernandez-Mercado, J. Hu, C. Snell, K. C. Gatter, A. L. Harris and F. Pezzella (2016). "Why some tumours trigger neovascularisation and others don't: the story thus far." Chin J Cancer 35: 18.

Allen, E., I. B. Walters and D. Hanahan (2011). "Brivanib, a dual FGF/VEGF inhibitor, is active both first and second line against mouse pancreatic neuroendocrine tumors developing adaptive/evasive resistance to VEGF inhibition." Clin Cancer Res 17(16): 5299-5310.

Angelucci, A. and M. Bologna (2007). "Targeting vascular cell migration as a strategy for blocking angiogenesis: the central role of focal adhesion protein tyrosine kinase family." Curr Pharm Des 13(21): 2129-2145.

Armulik, A., A. Abramsson and C. Betsholtz (2005). "Endothelial/pericyte interactions." Circ Res 97(6): 512-523.

Arnold, K. M., Z. M. Goeckeler and R. B. Wysolmerski (2013). "Loss of focal adhesion kinase enhances endothelial barrier function and increases focal adhesions." Microcirculation 20(7): 637-649.

Baker, M., S. D. Robinson, T. Lechertier, P. R. Barber, B. Tavora, G. D'Amico, D. T. Jones, B. Vojnovic and K. Hodivala-Dilke (2012). "Use of the mouse aortic ring assay to study angiogenesis." Nat Protoc 7(1): 89-104.

Ben-Neriah, Y. and M. Karin (2011). "Inflammation meets cancer, with NF-kappaB as the matchmaker." Nat Immunol 12(8): 715-723.

Bergers, G. and L. E. Benjamin (2003). "Tumorigenesis and the angiogenic switch." Nat Rev Cancer 3(6): 401-410.

Braren, R., H. Hu, Y. H. Kim, H. E. Beggs, L. F. Reichardt and R. Wang (2006). "Endothelial FAK is essential for vascular network stability, cell survival, and lamellipodial formation." J Cell Biol 172(1): 151-162.

Brooks, P. C., R. A. Clark and D. A. Cheresh (1994). "Requirement of vascular integrin alpha v beta 3 for angiogenesis." Science 264(5158): 569-571.

Brooks, P. C., A. M. Montgomery, M. Rosenfeld, R. A. Reisfeld, T. Hu, G. Klier and D. A. Cheresh (1994). "Integrin alpha v beta 3 antagonists promote tumor regression by inducing apoptosis of angiogenic blood vessels." Cell 79(7): 1157-1164.

Brunton, V. G., E. Avizienyte, V. J. Fincham, B. Serrels, C. A. Metcalf, 3rd, T. K. Sawyer and M. C. Frame (2005). "Identification of Src-specific phosphorylation site on focal adhesion kinase: dissection of the role of Src SH2 and catalytic functions and their consequences for tumor cell behavior." Cancer Res 65(4): 1335-1342.

Brunton, V. G. and M. C. Frame (2008). "Src and focal adhesion kinase as therapeutic targets in cancer." Curr Opin Pharmacol 8(4): 427-432.

Calalb, M. B., X. Zhang, T. R. Polte and S. K. Hanks (1996). "Focal adhesion kinase tyrosine-861 is a major site of phosphorylation by Src." Biochem Biophys Res Commun 228(3): 662-668.

Cance, W. G., E. Kurenova, T. Marlowe and V. Golubovskaya (2013). "Disrupting the scaffold to improve focal adhesion kinase-targeted cancer therapeutics." Sci Signal 6(268): pe10.

Carmeliet, P. (2000). "Mechanisms of angiogenesis and arteriogenesis." Nat Med 6(4): 389-395.

Carmeliet, P. (2003). "Angiogenesis in health and disease." Nat Med 9(6): 653-660.

Carmeliet, P. (2005). "VEGF as a key mediator of angiogenesis in cancer." Oncology 69 Suppl 3: 4-10.

Carmeliet, P., V. Ferreira, G. Breier, S. Pollefeyt, L. Kieckens, M. Gertsenstein, M. Fahrig, A. Vandenhoeck, K. Harpal, C. Eberhardt, C. Declercq, J. Pawling, L. Moons, D. Collen, W. Risau and A. Nagy (1996). "Abnormal blood vessel development and lethality in embryos lacking a single VEGF allele." Nature 380(6573): 435-439.

Carmeliet, P. and R. K. Jain (2000). "Angiogenesis in cancer and other diseases." Nature 407(6801): 249-257.

Carmeliet, P. and R. K. Jain (2011). "Principles and mechanisms of vessel normalization for cancer and other angiogenic diseases." Nat Rev Drug Discov 10(6): 417-427.

Casanovas, O., D. J. Hicklin, G. Bergers and D. Hanahan (2005). "Drug resistance by evasion of antiangiogenic targeting of VEGF signaling in late-stage pancreatic islet tumors." Cancer Cell 8(4): 299-309.

Cascone, I., L. Napione, F. Maniero, G. Serini and F. Bussolino (2005). "Stable interaction between alpha5beta1 integrin and Tie2 tyrosine kinase receptor regulates endothelial cell response to Ang-1." J Cell Biol 170(6): 993-1004.

Caswell, P. T., M. Chan, A. J. Lindsay, M. W. McCaffrey, D. Boettiger and J. C. Norman (2008). "Rab-coupling protein coordinates recycling of alpha5beta1 integrin and EGFR1 to promote cell migration in 3D microenvironments." J Cell Biol 183(1): 143-155.

Cebe Suarez, S., M. Pieren, L. Cariolato, S. Arn, U. Hoffmann, A. Bogucki, C. Manlius, J. Wood and K. Ballmer-Hofer (2006). "A VEGF-A splice variant defective for heparan sulfate and neuropilin-1 binding shows attenuated signaling through VEGFR-2." Cell Mol Life Sci 63(17): 2067-2077.

Chen, X. L., J. O. Nam, C. Jean, C. Lawson, C. T. Walsh, E. Goka, S. T. Lim, A. Tomar, I. Tancioni, S. Uryu, J. L. Guan, L. M. Acevedo, S. M. Weis, D. A. Cheresh and D. D. Schlaepfer (2012). "VEGF-induced vascular permeability is mediated by FAK." Dev Cell 22(1): 146-157.

Chodniewicz, D. and R. L. Klemke (2004). "Guiding cell migration through directed extension and stabilization of pseudopodia." Exp Cell Res 301(1): 31-37.

Choi, K., M. Kennedy, A. Kazarov, J. C. Papadimitriou and G. Keller (1998). "A common precursor for hematopoietic and endothelial cells." Development 125(4): 725-732.

Claxton, S., V. Kostourou, S. Jadeja, P. Chambon, K. Hodivala-Dilke and M. Fruttiger (2008). "Efficient, inducible Cre-recombinase activation in vascular endothelium." Genesis 46(2): 74-80.

Cobb, B. S., M. D. Schaller, T. H. Leu and J. T. Parsons (1994). "Stable association of pp60src and pp59fyn with the focal adhesion-associated protein tyrosine kinase, pp125FAK." Mol Cell Biol 14(1): 147-155.

Conway, E. M., D. Collen and P. Carmeliet (2001). "Molecular mechanisms of blood vessel growth." Cardiovasc Res 49(3): 507-521.

Cooper, L. A., T. L. Shen and J. L. Guan (2003). "Regulation of focal adhesion kinase by its amino-terminal domain through an autoinhibitory interaction." Mol Cell Biol 23(22): 8030-8041.

Corsi, J. M., C. Houbron, P. Billuart, I. Brunet, K. Bouvree, A. Eichmann, J. A. Girault and H. Enslen (2009). "Autophosphorylation-independent and -dependent functions of focal adhesion kinase during development." J Biol Chem 284(50): 34769-34776.

Crusz, S. M. and F. R. Balkwill (2015). "Inflammation and cancer: advances and new agents." Nat Rev Clin Oncol 12(10): 584-596.

da Silva, R. G., B. Tavora, S. D. Robinson, L. E. Reynolds, C. Szekeres, J. Lamar, S. Batista, V. Kostourou, M. A. Germain, A. R. Reynolds, D. T. Jones, A. R. Watson, J. L. Jones, A. Harris, I. R. Hart, M. L. Iruela-Arispe, C. M. Dipersio, J. A. Kreidberg and K. M. Hodivala-Dilke (2010). "Endothelial alpha3beta1-integrin represses pathological angiogenesis and sustains endothelial-VEGF." Am J Pathol 177(3): 1534-1548.

Dejana, E., F. Orsenigo and M. G. Lampugnani (2008). "The role of adherens junctions and VE-cadherin in the control of vascular permeability." J Cell Sci 121(Pt 13): 2115-2122.

Deramaudt, T. B., D. Dujardin, A. Hamadi, F. Noulet, K. Kolli, J. De Mey, K. Takeda and P. Ronde (2011). "FAK phosphorylation at Tyr-925 regulates cross-talk between focal adhesion turnover and cell protrusion." Mol Biol Cell 22(7): 964-975.

DiDonato, J. A., F. Mercurio and M. Karin (2012). "NF-kappaB and the link between inflammation and cancer." Immunol Rev 246(1): 379-400.

Djonov, V., M. Schmid, S. A. Tschanz and P. H. Burri (2000). "Intussusceptive angiogenesis: its role in embryonic vascular network formation." Circ Res 86(3): 286-292.

Djordjevic, S. and P. C. Driscoll (2012). "Targeting VEGF signalling via the neuropilin co-receptor." Drug Discov Today.

Dunty, J. M. and M. D. Schaller (2002). "The N termini of focal adhesion kinase family members regulate substrate phosphorylation, localization, and cell morphology." J Biol Chem 277(47): 45644-45654.

Eliceiri, B. P. and D. A. Cheresh (1999). "The role of alphav integrins during angiogenesis: insights into potential mechanisms of action and clinical development." J Clin Invest 103(9): 1227-1230.

Eliceiri, B. P., X. S. Puente, J. D. Hood, D. G. Stupack, D. D. Schlaepfer, X. Z. Huang, D. Sheppard and D. A. Cheresh (2002). "Src-mediated coupling of focal adhesion kinase to integrin alpha(v)beta5 in vascular endothelial growth factor signaling." J Cell Biol 157(1): 149-160.

Ellis, L. M. (2006). "The role of neuropilins in cancer." Mol Cancer Ther 5(5): 1099-1107.

Felcht, M., R. Luck, A. Schering, P. Seidel, K. Srivastava, J. Hu, A. Bartol, Y. Kienast, C. Vettel, E. K. Loos, S. Kutschera, S. Bartels, S. Appak, E. Besemfelder, D. Terhardt, E. Chavakis, T. Wieland, C. Klein, M. Thomas, A. Uemura, S. Goerdt and H. G. Augustin (2012). "Angiopoietin-2 differentially regulates angiogenesis through TIE2 and integrin signaling." J Clin Invest 122(6): 1991-2005.

Ferrara, N., K. Carver-Moore, H. Chen, M. Dowd, L. Lu, K. S. O'Shea, L. Powell-Braxton, K. J. Hillan and M. W. Moore (1996). "Heterozygous embryonic lethality induced by targeted inactivation of the VEGF gene." Nature 380(6573): 439-442.

Fiedler, U., M. Scharpfenecker, S. Koidl, A. Hegen, V. Grunow, J. M. Schmidt, W. Kriz, G. Thurston and H. G. Augustin (2004). "The Tie-2 ligand angiopoietin-2 is stored in and rapidly released upon stimulation from endothelial cell Weibel-Palade bodies." Blood 103(11): 4150-4156.

Folkman, J. (2006). "Angiogenesis." Annu Rev Med 57: 1-18.

Fong, G. H., J. Rossant, M. Gertsenstein and M. L. Breitman (1995). "Role of the Flt-1 receptor tyrosine kinase in regulating the assembly of vascular endothelium." Nature 376(6535): 66-70.

Fontanini, G., M. Lucchi, S. Vignati, A. Mussi, F. Ciardiello, M. De Laurentiis, S. De Placido, F. Basolo, C. A. Angeletti and G. Bevilacqua (1997). "Angiogenesis as a prognostic indicator of survival in non-small-cell lung carcinoma: a prospective study." J Natl Cancer Inst 89(12): 881-886.

Friedlander, M., P. C. Brooks, R. W. Shaffer, C. M. Kincaid, J. A. Varner and D. A. Cheresh (1995). "Definition of two angiogenic pathways by distinct alpha v integrins." Science 270(5241): 1500-1502.

Fruttiger, M. (2002). "Development of the mouse retinal vasculature: angiogenesis versus vasculogenesis." Invest Ophthalmol Vis Sci 43(2): 522-527.

Funakoshi-Tago, M., Y. Sonoda, S. Tanaka, K. Hashimoto, K. Tago, S. Tominaga and T. Kasahara (2003). "Tumor necrosis factor-induced nuclear factor kappaB activation is impaired in focal adhesion kinase-deficient fibroblasts." J Biol Chem 278(31): 29359-29365.

Gabarra-Niecko, V., M. D. Schaller and J. M. Dunty (2003). "FAK regulates biological processes important for the pathogenesis of cancer." Cancer Metastasis Rev 22(4): 359-374.

Gacche, R. N. (2015). "Compensatory angiogenesis and tumor refractoriness." Oncogenesis 4: e153.

Gale, N. W. and G. D. Yancopoulos (1999). "Growth factors acting via endothelial cell-specific receptor tyrosine kinases: VEGFs, angiopoietins, and ephrins in vascular development." Genes Dev 13(9): 1055-1066.

Gaya, A. and V. Tse (2012). "A preclinical and clinical review of aflibercept for the management of cancer." Cancer Treat Rev 38(5): 484-493.

George, D. J., S. Halabi, T. F. Shepard, N. J. Vogelzang, D. F. Hayes, E. J. Small and P. W. Kantoff (2001). "Prognostic significance of plasma vascular endothelial growth factor levels in patients with hormone-refractory prostate cancer treated on Cancer and Leukemia Group B 9480." Clin Cancer Res 7(7): 1932-1936.

George, E. L., E. N. Georges-Labouesse, R. S. Patel-King, H. Rayburn and R. O. Hynes (1993). "Defects in mesoderm, neural tube and vascular development in mouse embryos lacking fibronectin." Development 119(4): 1079-1091.

Gerber, H. P., A. McMurtrey, J. Kowalski, M. Yan, B. A. Keyt, V. Dixit and N. Ferrara (1998). "Vascular endothelial growth factor regulates endothelial cell survival through the phosphatidylinositol 3'-kinase/Akt signal transduction pathway. Requirement for Flk-1/KDR activation." J Biol Chem 273(46): 30336-30343.

Gerhardt, H. (2008). "VEGF and endothelial guidance in angiogenic sprouting." Organogenesis 4(4): 241-246.

Gerhardt, H. and C. Betsholtz (2003). "Endothelial-pericyte interactions in angiogenesis." Cell Tissue Res 314(1): 15-23.

Gilbert, L. A. and M. T. Hemann (2010). "DNA damage-mediated induction of a chemoresistant niche." Cell 143(3): 355-366.

Girault, J. A., G. Labesse, J. P. Mornon and I. Callebaut (1999). "The N-termini of FAK and JAKs contain divergent band 4.1 domains." Trends Biochem Sci 24(2): 54-57.

Golubovskaya, V. M., F. A. Kweh and W. G. Cance (2009). "Focal adhesion kinase and cancer." Histol Histopathol 24(4): 503-510.

Hammes, H. P., M. Brownlee, A. Jonczyk, A. Sutter and K. T. Preissner (1996). "Subcutaneous injection of a cyclic peptide antagonist of vitronectin receptor-type integrins inhibits retinal neovascularization." Nat Med 2(5): 529-533.

Hanks, S. K., L. Ryzhova, N. Y. Shin and J. Brabek (2003). "Focal adhesion kinase signaling activities and their implications in the control of cell survival and motility." Front Biosci 8: d982-996.

Hicklin, D. J. and L. M. Ellis (2005). "Role of the vascular endothelial growth factor pathway in tumor growth and angiogenesis." J Clin Oncol 23(5): 1011-1027.

Hildebrand, J. D., M. D. Schaller and J. T. Parsons (1993). "Identification of sequences required for the efficient localization of the focal adhesion kinase, pp125FAK, to cellular focal adhesions." J Cell Biol 123(4): 993-1005.

Hodivala-Dilke, K. M., K. P. McHugh, D. A. Tsakiris, H. Rayburn, D. Crowley, M. Ullman-Cullere, F. P. Ross, B. S. Coller, S. Teitelbaum and R. O. Hynes (1999). "Beta3-integrin-deficient mice are a model for Glanzmann thrombasthenia showing placental defects and reduced survival." J Clin Invest 103(2): 229-238.

Hodivala-Dilke, K. M., A. R. Reynolds and L. E. Reynolds (2003). "Integrins in angiogenesis: multitalented molecules in a balancing act." Cell Tissue Res 314(1): 131-144.

Hood, J. D., R. Frausto, W. B. Kiosses, M. A. Schwartz and D. A. Cheresh (2003). "Differential alphav integrin-mediated Ras-ERK signaling during two pathways of angiogenesis." J Cell Biol 162(5): 933-943.

Hua, H., M. Li, T. Luo, Y. Yin and Y. Jiang (2011). "Matrix metalloproteinases in tumorigenesis: an evolving paradigm." Cell Mol Life Sci 68(23): 3853-3868.

Huang, D., M. Khoe, M. Befekadu, S. Chung, Y. Takata, D. Ilic and M. Bryer-Ash (2007). "Focal adhesion kinase mediates cell survival via NF-kappaB and ERK signaling pathways." Am J Physiol Cell Physiol 292(4): C1339-1352.

Hurwitz, H., L. Fehrenbacher, W. Novotny, T. Cartwright, J. Hainsworth, W. Heim, J. Berlin, A. Baron, S. Griffing, E. Holmgren, N. Ferrara, G. Fyfe, B. Rogers, R. Ross and F. Kabbinavar (2004). "Bevacizumab plus irinotecan, fluorouracil, and leucovorin for metastatic colorectal cancer." N Engl J Med 350(23): 2335-2342.

Hutchings, H., N. Ortega and J. Plouet (2003). "Extracellular matrix-bound vascular endothelial growth factor promotes endothelial cell adhesion, migration, and survival through integrin ligation." FASEB J 17(11): 1520-1522.

Ikeda, N., M. Adachi, T. Taki, C. Huang, H. Hashida, A. Takabayashi, M. Sho, Y. Nakajima, H. Kanehiro, M. Hisanaga, H. Nakano and M. Miyake (1999). "Prognostic significance of angiogenesis in human pancreatic cancer." Br J Cancer 79(9-10): 1553-1563.

Ilic, D., Y. Furuta, S. Kanazawa, N. Takeda, K. Sobue, N. Nakatsuji, S. Nomura, J. Fujimoto, M. Okada and T. Yamamoto (1995). "Reduced cell motility and enhanced focal adhesion contact formation in cells from FAK-deficient mice." Nature 377(6549): 539-544.

Itoh, N., S. Semba, M. Ito, H. Takeda, S. Kawata and M. Yamakawa (2002). "Phosphorylation of Akt/PKB is required for suppression of cancer cell

apoptosis and tumor progression in human colorectal carcinoma." Cancer 94(12): 3127-3134.

Jean, C., X. L. Chen, J. O. Nam, I. Tancioni, S. Uryu, C. Lawson, K. K. Ward, C. T. Walsh, N. L. Miller, M. Ghassemian, P. Turowski, E. Dejana, S. Weis, D. A. Cheresh and D. D. Schlaepfer (2014). "Inhibition of endothelial FAK activity prevents tumor metastasis by enhancing barrier function." J Cell Biol 204(2): 247-263.

Kanner, S. B., A. B. Reynolds, R. R. Vines and J. T. Parsons (1990). "Monoclonal antibodies to individual tyrosine-phosphorylated protein substrates of oncogene-encoded tyrosine kinases." Proc Natl Acad Sci U S A 87(9): 3328-3332.

Kawasaki, K., R. S. Smith, Jr., C. M. Hsieh, J. Sun, J. Chao and J. K. Liao (2003). "Activation of the phosphatidylinositol 3-kinase/protein kinase Akt pathway mediates nitric oxide-induced endothelial cell migration and angiogenesis." Mol Cell Biol 23(16): 5726-5737.

Kim, S., K. Bell, S. A. Mousa and J. A. Varner (2000). "Regulation of angiogenesis in vivo by ligation of integrin alpha5beta1 with the central cell-binding domain of fibronectin." Am J Pathol 156(4): 1345-1362.

Kostourou, V., T. Lechertier, L. E. Reynolds, D. M. Lees, M. Baker, D. T. Jones, B. Tavora, A. R. Ramjaun, G. M. Birdsey, S. D. Robinson, M. Parsons, A. M. Randi, I. R. Hart and K. Hodivala-Dilke (2013). "FAK-heterozygous mice display enhanced tumour angiogenesis." Nat Commun 4: 2020.

Laakkonen, P., M. Waltari, T. Holopainen, T. Takahashi, B. Pytowski, P. Steiner, D. Hicklin, K. Persaud, J. R. Tonra, L. Witte and K. Alitalo (2007). "Vascular endothelial growth factor receptor 3 is involved in tumor angiogenesis and growth." Cancer Res 67(2): 593-599.

Lamalice, L., F. Le Boeuf and J. Huot (2007). "Endothelial cell migration during angiogenesis." Circ Res 100(6): 782-794.

Lechertier, T. and K. Hodivala-Dilke (2012). "Focal adhesion kinase and tumour angiogenesis." J Pathol 226(2): 404-412.

Lee, J., A. K. Borboa, H. B. Chun, A. Baird and B. P. Eliceiri (2010). "Conditional deletion of the focal adhesion kinase FAK alters remodeling of the blood-brain barrier in glioma." Cancer Res 70(24): 10131-10140.

Lee, J. C., N. H. Chow, S. T. Wang and S. M. Huang (2000). "Prognostic value of vascular endothelial growth factor expression in colorectal cancer patients." Eur J Cancer 36(6): 748-753.

Lietha, D., X. Cai, D. F. Ceccarelli, Y. Li, M. D. Schaller and M. J. Eck (2007). "Structural basis for the autoinhibition of focal adhesion kinase." Cell 129(6): 1177-1187.

Lim, S. T., X. L. Chen, Y. Lim, D. A. Hanson, T. T. Vo, K. Howerton, N. Larocque, S. J. Fisher, D. D. Schlaepfer and D. Ilic (2008). "Nuclear FAK promotes cell proliferation and survival through FERM-enhanced p53 degradation." Mol Cell 29(1): 9-22.

Lim, S. T., X. L. Chen, A. Tomar, N. L. Miller, J. Yoo and D. D. Schlaepfer (2010). "Knock-in mutation reveals an essential role for focal adhesion kinase activity in blood vessel morphogenesis and cell motility-polarity but not cell proliferation." J Biol Chem 285(28): 21526-21536.

Lim, S. T., N. L. Miller, X. L. Chen, I. Tancioni, C. T. Walsh, C. Lawson, S. Uryu, S. M. Weis, D. A. Cheresh and D. D. Schlaepfer (2012). "Nuclear-localized focal adhesion kinase regulates inflammatory VCAM-1 expression." J Cell Biol 197(7): 907-919.

Lim, Y., I. Han, J. Jeon, H. Park, Y. Y. Bahk and E. S. Oh (2004). "Phosphorylation of focal adhesion kinase at tyrosine 861 is crucial for Ras transformation of fibroblasts." J Biol Chem 279(28): 29060-29065.

Lu, C., T. Bonome, Y. Li, A. A. Kamat, L. Y. Han, R. Schmandt, R. L. Coleman, D. M. Gershenson, R. B. Jaffe, M. J. Birrer and A. K. Sood (2007). "Gene alterations identified by expression profiling in tumor-associated endothelial cells from invasive ovarian carcinoma." Cancer Res 67(4): 1757-1768.

Lu, J., X. Ye, F. Fan, L. Xia, R. Bhattacharya, S. Bellister, F. Tozzi, E. Sceusi, Y. Zhou, I. Tachibana, D. M. Maru, D. H. Hawke, J. Rak, S. A. Mani, P. Zweidler-McKay and L. M. Ellis (2013). "Endothelial cells promote the colorectal cancer stem cell phenotype through a soluble form of Jagged-1." Cancer Cell 23(2): 171-185.

Madan, R., M. B. Smolkin, R. Cocker, R. Fayyad and M. H. Oktay (2006). "Focal adhesion proteins as markers of malignant transformation and prognostic indicators in breast carcinoma." Hum Pathol 37(1): 9-15.

Mahabeleshwar, G. H., W. Feng, K. Reddy, E. F. Plow and T. V. Byzova (2007). "Mechanisms of integrin-vascular endothelial growth factor receptor cross-activation in angiogenesis." Circ Res 101(6): 570-580.

Marlowe, T. A., F. L. Lenzo, S. A. Figel, A. T. Grapes and W. G. Cance (2016). "Oncogenic Receptor Tyrosine Kinases Directly Phosphorylate Focal Adhesion Kinase (FAK) as a Resistance Mechanism to FAK-kinase Inhibitors." Mol Cancer Ther.

McLean, G. W., N. H. Komiyama, B. Serrels, H. Asano, L. Reynolds, F. Conti, K. Hodivala-Dilke, D. Metzger, P. Chambon, S. G. Grant and M. C. Frame (2004). "Specific deletion of focal adhesion kinase suppresses tumor formation and blocks malignant progression." Genes Dev 18(24): 2998-3003.

Mitra, S. K., D. A. Hanson and D. D. Schlaepfer (2005). "Focal adhesion kinase: in command and control of cell motility." Nat Rev Mol Cell Biol 6(1): 56-68.

Morgan, E. A., J. G. Schneider, T. E. Baroni, O. Uluckan, E. Heller, M. A. Hurchla, H. Deng, D. Floyd, A. Berdy, J. L. Prior, D. Piwnica-Worms, S. L. Teitelbaum, F. P. Ross and K. N. Weilbaecher (2010). "Dissection of platelet and myeloid cell defects by conditional targeting of the beta3-integrin subunit." FASEB J 24(4): 1117-1127.

Nakasone, E. S., H. A. Askautrud, T. Kees, J. H. Park, V. Plaks, A. J. Ewald, M. Fein, M. G. Rasch, Y. X. Tan, J. Qiu, J. Park, P. Sinha, M. J. Bissell, E. Frengen, Z. Werb and M. Egeblad (2012). "Imaging tumor-stroma interactions during chemotherapy reveals contributions of the microenvironment to resistance." Cancer Cell 21(4): 488-503.

Neufeld, G., O. Kessler and Y. Herzog (2002). "The interaction of Neuropilin-1 and Neuropilin-2 with tyrosine-kinase receptors for VEGF." Adv Exp Med Biol 515: 81-90.

Ossovskaya, V., S. T. Lim, N. Ota, D. D. Schlaepfer and D. Ilic (2008). "FAK nuclear export signal sequences." FEBS Lett 582(16): 2402-2406.

Qiu, Y., C. Hoareau-Aveilla, S. Oltean, S. J. Harper and D. O. Bates (2009). "The anti-angiogenic isoforms of VEGF in health and disease." Biochem Soc Trans 37(Pt 6): 1207-1213.

Parsons, J. T. (2003). "Focal adhesion kinase: the first ten years." J Cell Sci 116(Pt 8): 1409-1416.

Parsons, J. T., J. Slack-Davis, R. Tilghman and W. G. Roberts (2008). "Focal adhesion kinase: targeting adhesion signaling pathways for therapeutic intervention." Clin Cancer Res 14(3): 627-632.

Paulsson, M. (1992). "Basement membrane proteins: structure, assembly, and cellular interactions." Crit Rev Biochem Mol Biol 27(1-2): 93-127.

Peng, X., H. Ueda, H. Zhou, T. Stokol, T. L. Shen, A. Alcaraz, T. Nagy, J. D. Vassalli and J. L. Guan (2004). "Overexpression of focal adhesion kinase in vascular endothelial cells promotes angiogenesis in transgenic mice." Cardiovasc Res 64(3): 421-430.

Petzold, T., A. W. Orr, C. Hahn, K. A. Jhaveri, J. T. Parsons and M. A. Schwartz (2009). "Focal adhesion kinase modulates activation of NF-kappaB by flow in endothelial cells." Am J Physiol Cell Physiol 297(4): C814-822.

Pozzi, A., P. E. Moberg, L. A. Miles, S. Wagner, P. Soloway and H. A. Gardner (2000). "Elevated matrix metalloprotease and angiostatin levels in integrin alpha 1 knockout mice cause reduced tumor vascularization." Proc Natl Acad Sci U S A 97(5): 2202-2207.

Qi, J. H. and L. Claesson-Welsh (2001). "VEGF-induced activation of phosphoinositide 3-kinase is dependent on focal adhesion kinase." Exp Cell Res 263(1): 173-182.

Rahman, S., Y. Patel, J. Murray, K. V. Patel, R. Sumathipala, M. Sobel and E. S. Wijelath (2005). "Novel hepatocyte growth factor (HGF) binding domains on fibronectin and vitronectin coordinate a distinct and amplified Met-integrin induced signalling pathway in endothelial cells." BMC Cell Biol 6(1): 8.

Reynolds, A. R., L. E. Reynolds, T. E. Nagel, J. C. Lively, S. D. Robinson, D. J. Hicklin, S. C. Bodary and K. M. Hodivala-Dilke (2004). "Elevated Flk1 (vascular endothelial growth factor receptor 2) signaling mediates enhanced angiogenesis in beta3-integrin-deficient mice." Cancer Res 64(23): 8643-8650.

Reynolds, L. E., L. Wyder, J. C. Lively, D. Taverna, S. D. Robinson, X. Huang, D. Sheppard, R. O. Hynes and K. M. Hodivala-Dilke (2002). "Enhanced pathological angiogenesis in mice lacking beta3 integrin or beta3 and beta5 integrins." Nat Med 8(1): 27-34.

Risau, W. (1997). "Mechanisms of angiogenesis." Nature 386(6626): 671-674.

Robinson, S. D., L. E. Reynolds, L. Wyder, D. J. Hicklin and K. M. Hodivala-Dilke (2004). "Beta3-integrin regulates vascular endothelial growth factor-A-dependent permeability." Arterioscler Thromb Vasc Biol 24(11): 2108-2114.

Romer, L. H., K. G. Birukov and J. G. Garcia (2006). "Focal adhesions: paradigm for a signaling nexus." Circ Res 98(5): 606-616.

Roy-Luzarraga, M. and K. Hodivala-Dilke (2016). "Molecular Pathways: Endothelial Cell FAK-A Target for Cancer Treatment." Clin Cancer Res 22(15): 3718-3724.

Schaller, M. D. (2010). "Cellular functions of FAK kinases: insight into molecular mechanisms and novel functions." J Cell Sci 123(Pt 7): 1007-1013.

Schaller, M. D., C. A. Borgman, B. S. Cobb, R. R. Vines, A. B. Reynolds and J. T. Parsons (1992). "pp125FAK a structurally distinctive protein-tyrosine kinase associated with focal adhesions." Proc Natl Acad Sci U S A 89(11): 5192-5196.

Schaller, M. D., J. D. Hildebrand, J. D. Shannon, J. W. Fox, R. R. Vines and J. T. Parsons (1994). "Autophosphorylation of the focal adhesion kinase, pp125FAK, directs SH2-dependent binding of pp60src." Mol Cell Biol 14(3): 1680-1688.

Schaller, M. D., C. A. Otey, J. D. Hildebrand and J. T. Parsons (1995). "Focal adhesion kinase and paxillin bind to peptides mimicking beta integrin cytoplasmic domains." J Cell Biol 130(5): 1181-1187.

Scheswohl, D. M., J. R. Harrell, Z. Rajfur, G. Gao, S. L. Campbell and M. D. Schaller (2008). "Multiple paxillin binding sites regulate FAK function." J Mol Signal 3: 1.

Schlaepfer, D. D. and S. K. Mitra (2004). "Multiple connections link FAK to cell motility and invasion." Curr Opin Genet Dev 14(1): 92-101.

Schmidt, T. T., M. Tauseef, L. Yue, M. G. Bonini, J. Gothert, T. L. Shen, J. L. Guan, S. Predescu, R. Sadikot and D. Mehta (2013). "Conditional deletion of FAK in mice endothelium disrupts lung vascular barrier function due to destabilization of RhoA and Rac1 activities." Am J Physiol Lung Cell Mol Physiol 305(4): L291-300.

Schultze, A., S. Decker, J. Otten, A. K. Horst, G. Vohwinkel, G. Schuch, C. Bokemeyer, S. Loges and W. Fiedler (2010). "TAE226-mediated inhibition of focal adhesion kinase interferes with tumor angiogenesis and vasculogenesis." Invest New Drugs 28(6): 825-833.

Senger, D. R., K. P. Claffey, J. E. Benes, C. A. Perruzzi, A. P. Sergiou and M. Detmar (1997). "Angiogenesis promoted by vascular endothelial growth factor: regulation through alpha1beta1 and alpha2beta1 integrins." Proc Natl Acad Sci U S A 94(25): 13612-13617.

Serini, G., L. Napione, M. Arese and F. Bussolino (2008). "Besides adhesion: new perspectives of integrin functions in angiogenesis." Cardiovasc Res 78(2): 213-222.

Serrels, A., K. McLeod, M. Canel, A. Kinnaird, K. Graham, M. C. Frame and V. G. Brunton (2012). "The role of focal adhesion kinase catalytic activity on the proliferation and migration of squamous cell carcinoma cells." Int J Cancer 131(2): 287-297.

Shalaby, F., J. Rossant, T. P. Yamaguchi, M. Gertsenstein, X. F. Wu, M. L. Breitman and A. C. Schuh (1995). "Failure of blood-island formation and vasculogenesis in Flk-1-deficient mice." Nature 376(6535): 62-66.

Shen, T. L., A. Y. Park, A. Alcaraz, X. Peng, I. Jang, P. Koni, R. A. Flavell, H. Gu and J. L. Guan (2005). "Conditional knockout of focal adhesion kinase in endothelial cells reveals its role in angiogenesis and vascular development in late embryogenesis." J Cell Biol 169(6): 941-952.

Shing, Y., J. Folkman, R. Sullivan, C. Butterfield, J. Murray and M. Klagsbrun (1984). "Heparin affinity: purification of a tumor-derived capillary endothelial cell growth factor." Science 223(4642): 1296-1299.

Sieg, D. J., C. R. Hauck, D. Ilic, C. K. Klingbeil, E. Schaefer, C. H. Damsky and D. D. Schlaepfer (2000). "FAK integrates growth-factor and integrin signals to promote cell migration." Nat Cell Biol 2(5): 249-256.

Somanath, P. R., O. V. Razorenova, J. Chen and T. V. Byzova (2006). "Akt1 in endothelial cell and angiogenesis." Cell Cycle 5(5): 512-518.

Steri, V., T. S. Ellison, A. M. Gontarczyk, K. Weilbaecher, J. G. Schneider, D. Edwards, M. Fruttiger, K. M. Hodivala-Dilke and S. D. Robinson (2014). "Acute depletion of endothelial beta3-integrin transiently inhibits tumor growth and angiogenesis in mice." Circ Res 114(1): 79-91.

Stromblad, S. and D. A. Cheresh (1996). "Integrins, angiogenesis and vascular cell survival." Chem Biol 3(11): 881-885.

Stuttfeld, E. and K. Ballmer-Hofer (2009). "Structure and function of VEGF receptors." IUBMB Life 61(9): 915-922.

Sulzmaier, F. J., C. Jean and D. D. Schlaepfer (2014). "FAK in cancer: mechanistic findings and clinical applications." Nat Rev Cancer 14(9): 598-610.

Sun, Y., J. Campisi, C. Higano, T. M. Beer, P. Porter, I. Coleman, L. True and P. S. Nelson (2012). "Treatment-induced damage to the tumor microenvironment promotes prostate cancer therapy resistance through WNT16B." Nat Med 18(9): 1359-1368.

Takahashi, Y., K. R. Cleary, M. Mai, Y. Kitadai, C. D. Bucana and L. M. Ellis (1996). "Significance of vessel count and vascular endothelial growth factor and its receptor (KDR) in intestinal-type gastric cancer." Clin Cancer Res 2(10): 1679-1684.

Takahashi, Y., Y. Kitadai, C. D. Bucana, K. R. Cleary and L. M. Ellis (1995). "Expression of vascular endothelial growth factor and its receptor, KDR, correlates with vascularity, metastasis, and proliferation of human colon cancer." Cancer Res 55(18): 3964-3968.

Tavora, B., S. Batista, A. N. Alexopoulou, V. Kostourou, I. Fernandez, S. D. Robinson, D. M. Lees, B. Serrels and K. Hodivala-Dilke (2014). "Generation of point-mutant FAK knockin mice." Genesis 52(11): 907-915.

Tavora, B., S. Batista, L. E. Reynolds, S. Jadeja, S. Robinson, V. Kostourou, I. Hart, M. Fruttiger, M. Parsons and K. M. Hodivala-Dilke (2010). "Endothelial FAK is required for tumour angiogenesis." EMBO Mol Med 2(12): 516-528.

Tavora, B., L. E. Reynolds, S. Batista, F. Demircioglu, I. Fernandez, T. Lechertier, D. M. Lees, P. P. Wong, A. Alexopoulou, G. Elia, A. Clear, A. Ledoux, J. Hunter, N. Perkins, J. G. Gribben and K. M. Hodivala-Dilke (2014). "Endothelial-cell FAK targeting sensitizes tumours to DNA-damaging therapy." Nature 514(7520): 112-116.

Toutant, M., A. Costa, J. M. Studler, G. Kadare, M. Carnaud and J. A. Girault (2002). "Alternative splicing controls the mechanisms of FAK autophosphorylation." Mol Cell Biol 22(22): 7731-7743.

Tseng, W. P., C. M. Su and C. H. Tang (2010). "FAK activation is required for TNF-alpha-induced IL-6 production in myoblasts." J Cell Physiol 223(2): 389-396.

Turner, N. and R. Grose (2010). "Fibroblast growth factor signalling: from development to cancer." Nat Rev Cancer 10(2): 116-129.

Vitale, S., E. Avizienyte, V. G. Brunton and M. C. Frame (2008). "Focal adhesion kinase is not required for Src-induced formation of invadopodia in KM12C colon cancer cells and can interfere with their assembly." Eur J Cell Biol 87(8-9): 569-579.

Wahl, M. L., D. J. Kenan, M. Gonzalez-Gronow and S. V. Pizzo (2005). "Angiostatin's molecular mechanism: aspects of specificity and regulation elucidated." J Cell Biochem 96(2): 242-261.

Wang, S. and M. D. Basson (2011). "Akt directly regulates focal adhesion kinase through association and serine phosphorylation: implication for pressure-induced colon cancer metastasis." Am J Physiol Cell Physiol 300(3): C657-670.

Wang, X., Q. Chen and D. Xing (2012). "Focal adhesion kinase activates NF-kappaB via the ERK1/2 and p38MAPK Pathways in amyloid-beta25-35-induced apoptosis in PC12 cells." J Alzheimers Dis 32(1): 77-94.

Ward, K. K., I. Tancioni, C. Lawson, N. L. Miller, C. Jean, X. L. Chen, S. Uryu, J. Kim, D. Tarin, D. G. Stupack, S. C. Plaxe and D. D. Schlaepfer (2012). "Inhibition of focal adhesion kinase (FAK) activity prevents anchorage-independent ovarian carcinoma cell growth and tumor progression." Clin Exp Metastasis.

Weis, S. M. and D. A. Cheresh (2011). "alphaV integrins in angiogenesis and cancer." Cold Spring Harb Perspect Med 1(1): a006478.

Weis, S. M., S. T. Lim, K. M. Lutu-Fuga, L. A. Barnes, X. L. Chen, J. R. Gothert, T. L. Shen, J. L. Guan, D. D. Schlaepfer and D. A. Cheresh (2008). "Compensatory role for Pyk2 during angiogenesis in adult mice lacking endothelial cell FAK." J Cell Biol 181(1): 43-50.

Wendt, M. K. and W. P. Schiemann (2009). "Therapeutic targeting of the focal adhesion complex prevents oncogenic TGF-beta signaling and metastasis." Breast Cancer Res 11(5): R68.

Xing, Z., H. C. Chen, J. K. Nowlen, S. J. Taylor, D. Shalloway and J. L. Guan (1994). "Direct interaction of v-Src with the focal adhesion kinase mediated by the Src SH2 domain." Mol Biol Cell 5(4): 413-421.

Yadav, L., N. Puri, V. Rastogi, P. Satpute and V. Sharma (2015). "Tumour Angiogenesis and Angiogenic Inhibitors: A Review." J Clin Diagn Res 9(6): XE01-XE05.

Yang, J. T., H. Rayburn and R. O. Hynes (1993). "Embryonic mesodermal defects in alpha 5 integrin-deficient mice." Development 119(4): 1093-1105.

Zhang, H. M., K. M. Keledjian, J. N. Rao, T. Zou, L. Liu, B. S. Marasa, S. R. Wang, L. Ru, E. D. Strauch and J. Y. Wang (2006). "Induced focal adhesion kinase expression suppresses apoptosis by activating NF-kappaB signaling in intestinal epithelial cells." Am J Physiol Cell Physiol 290(5): C1310-1320.

Zhang, M., G. Ye, J. Li and Y. Wang (2015). "Recent advance in molecular angiogenesis in glioblastoma: the challenge and hope for anti-angiogenic therapy." Brain Tumor Pathol 32(4): 229-236.

Zhang, Z., N. E. Ramirez, T. E. Yankeelov, Z. Li, L. E. Ford, Y. Qi, A. Pozzi and M. M. Zutter (2008). "alpha2beta1 integrin expression in the tumor microenvironment enhances tumor angiogenesis in a tumor cell-specific manner." Blood 111(4): 1980-1988.

Zhao, J. and J. L. Guan (2009). "Signal transduction by focal adhesion kinase in cancer." Cancer Metastasis Rev 28(1-2): 35-49.

Zhao, X., X. Peng, S. Sun, A. Y. Park and J. L. Guan (2010). "Role of kinase-independent and -dependent functions of FAK in endothelial cell survival and barrier function during embryonic development." J Cell Biol 189(6): 955-965.

Ziyad, S. and M. L. Iruela-Arispe (2011). "Molecular mechanisms of tumor angiogenesis." Genes Cancer 2(12): 1085-1096.